2017-05-31

Identification and Characterization of Rab39a and Its Role in Crosspresentation

Freidrich M. Cruz
University of Massachusetts Medical School

Let us know how access to this document benefits you.

Repository Citation

IDENTIFICATION AND CHARACTERIZATION OF RAB39A AND ITS ROLE IN CROSSPRESENTATION

A Dissertation Presented

By

FREIDRICH MAURICIO CRUZ

Submitted to the Faculty of the

University of Massachusetts Graduate School of Biomedical Sciences, Worcester

in partial fulfillment of the requirements for the degree of

DOCTOR OF PHILOSOPHY

May 31, 2017

IMMUNOLOGY AND MICROBIOLOGY

IDENTIFICATION AND CHARACTERIZATION OF RAB39A AND ITS ROLE IN CROSSPRESENTATION

A Dissertation Presented

By

FREIDRICH MAURICIO CRUZ

The signatures of the Dissertation Defense Committee signify completion and approval as to style and content of the Dissertation

Kenneth L. Rock, Ph.D., Thesis Advisor

Leslie J. Berg, Ph.D., Member of Committee

Evelyn A. Kurt-Jones, Ph.D., Member of Committee

Andrea Reboldi, Ph.D. Member of Committee

Peter Cresswell, Ph.D., FRS, Member of Committee

The signature of the Chair of the Committee signifies that the written dissertation meets the requirements of the Dissertation Committee

Lawrence J. Stern, Ph.D., Chair of Committee

The signature of the Dean of the Graduate School of Biomedical Sciences signifies that the student has met all graduation requirements of the school

Anthony Carruthers, Ph.D., Dean of the Graduate School of Biomedical Sciences

Program in Immunology and Microbiology

May 31, 2017

Acknowledgements

I would like to thank Dr. Kenneth L Rock. My years in the Rock lab have been the darkest and yet, probably the most fulfilling years in my life. I really appreciate the freedom, resources and guidance Ken gave me in exploring the science of my project. It was an arduous journey, and I have absolutely gone mad, but I must say my years in the Rock Lab have been the ones that forged me into being a real scientist. No textbook or lecture can compare to the training I had under this lab and this mentor.

I would like to thank my fellow lab members who have gone insane with me. Particularly, Lianjun Shen and Jeff Colbert for instilling in me the foundations of antigen presentation. Diego Farfan, for astounding me even to this day with his brilliant yet unconventional experiments. Dipti Karmarkar, my batchmate, for understanding exactly what it feels like to be a grad student in the Rock lab. To all Rock lab members past and present, I wish you all the success.

I would like to thank my committee members for giving me valuable insight on my experiments. I would also like to thank the Pathology Department, particularly the Stern Lab for sharing their ideas and resources. Dr. Stephen Baker of UMASS and the staff of ICCB-L at Harvard were very helpful in the siRNA screen.

I would like to thank Homer Pantua, Genevieve Hernandez, Rachel Madera, Jenny Babon, Arlene Lim, Inez Medado, Krista Serquina and Lucy Chao – the original gang I grew up with in the United States. I will forever cherish the moments we shared throughout the years.

Finally, I would like to thank my family for the love, sacrifice and understanding they have given me as I went through the years of graduate school.

Abstract

Crosspresentation allows antigen presenting cells to present peptides from exogenously derived antigens onto MHC Class I for presentation to CD8$^+$ T cells. Though this pathway shares key players with the Classical Class I and Class II pathways, several questions remain. A genomewide siRNA screen was performed to look for genes that selectively affected the crosspresentation or the Class II pathways. Among the genes identified in the screen was the Rab GTPase Rab39a. Rab39a was required for efficient crosspresentation but was dispensable for the presentation of endogenously expressed antigen. Both TAP-dependent and independent antigen required Rab39a for efficient presentation. Rab39a localized to late endosomes and phagosomes, though interestingly it was not required for the Class II pathway. Analysis of phagosomes from Rab39a KO or rescued cells has shown that in the presence of Rab39a, phagosomes were enriched for the open form of MHC Class I as well as TAP1, a member of the peptide loading complex. The enriched open form of MHC-I was peptide receptive, suggesting that it could contribute to crosspresentation. Phagosomes from Rab39a positive cells had reduced degradative capability and had increased levels of Sec22b, a SNARE protein reported to deliver ER-golgi sourced cargo to phagosomes. Furthermore, inhibition of ER-golgi transport via brefeldin A abolished the phenotype conferred by Rab39a. Thus, we hypothesize that Rab39a mediates the delivery of ER-golgi derived cargo to the antigen containing phagosome. This delivery allows peptide receptive MHC-I, as well as

the peptide loading complex to reach the antigen, thereby facilitating

crosspresentation.

Table of Contents

List of Tables

List of Figures

List of Publications

Cruz FM, Colbert JD, Merino E, Kriegsman BA, Rock KL. 2017. The Biology and Underlying Mechanisms of Cross-Presentation of Exogenous Antigens on MHC-I Molecules. *Annu Rev Immunol* 35: 149-76

The original research presented in this Dissertation is published in:

Cruz FM, Colbert JD, Rock KL: The GTPase Rab39a promotes phagosome maturation into MHC-I antigen-presenting compartments. EMBO J 2019:e102020.

doi: 10.15252/embj.2019102020

List of Third Party Copyrighted Material

The following figures were reproduced from journals: No permission required

Figure Number	Publisher
Figures 1-3	Annual Reviews

Preface

Experiments involving bacterial antigens and bead conjugated CSNENMETM peptide were done by Jeff Colbert (Figures 35 and 42).

Parts of this dissertation have appeared in the following publications:

Kincaid EZ, Che JW, York I, Escobar H, Reyes-Vargas E, Delgado JC, Welsh RM, Karow ML, Murphy AJ, Valenzuela DM, Yancopoulos GD, Rock KL. 2011. Mice completely lacking immunoproteasomes show major changes in antigen presentation. *Nat Immunol* 13: 129-35

Farfán Arribas, DJ. On the Source of Peptides for Major Histocompatibility Class I Antigen Presentation: A Dissertation. (2012). University of Massachusetts Medical School. GSBS Dissertations and Theses. Paper 589. http://escholarship.umassmed.edu/gsbs_diss/589

The above papers involved the use of the Luciferase Expressing T cell Reporters generated by the author for this Dissertation.

CHAPTER I: A Genomewide SiRNA Screen Identifies Genes Important For The Crosspresentation And Class II Presentation Pathways

I.   Introduction

A. Crosspresentation and its relevance

The initiation of an effective T cell response begins with the stimulation of naïve T cells by antigen presenting cells (APCs). This stimulation is primarily mediated by the interaction between the T cell receptor and its cognate peptide-MHC molecule presented on the APC surface. Peptide presented on MHC Class I stimulate CD8$^+$ T cells to become cytolytic (CTL) and produce cytokines. Meanwhile, peptides presented on MHC Class II stimulate CD4$^+$ T cells, which have a variety of functions including cytokine production and in some cases, cytolytic function as well.

Traditionally, it was thought that the presentation of peptides on MHC Class I vs Class II molecules was based solely on the source of antigen. MHC Class I was responsible for the presentation of endogenously expressed proteins, while MHC Class II was responsible for the presentation of peptides acquired from exogenous sources, i.e. those eaten by phagocytic macrophages and dendritic cells. This delineation was questioned however, when it was observed that antigens from transplanted tumors were somehow being presented

by host APCs for the generation of CTLs (1). This phenomenon was eventually discovered to be brought about through crosspresentation.

Crosspresentation (XPT) is the process wherein exogenous antigen is taken up by antigen presenting cells (APCs) to be processed and presented on MHC Class I molecules. *In vivo*, the main APCs that are capable of XPT are the dendritic cells (DC) (2-4) , though macrophages (5, 6) and more recently other cell types, have been demonstrated to have this ability (7-12).

Besides the original case of transplant rejection, it turns out that XPT has an important role to play in the adaptive immune response. Naïve T cells are mainly localized in the lymphoid tissues (13), and rely on incoming APCs for activation. XPT allows antigen in the peripheral tissues to reach these T cells via migrating APCs. DCs, through XPT, can present viral antigen to CD8$^+$ T cells, even though the DCs themselves are not infected (14). Presentation of tumor antigens is another important role (15). On the flipside, XPT has also been implicated in the initiation of autoimmunity, through the presentation of self antigens (16, 17). Islet dendritic cells are able acquire antigen from β-cells and initiate diabetogenic CD4$^+$ and CD8$^+$ T cell responses.

B. Specialized Antigen Presenting Cells

While many cells that are able to take up antigen has been shown to cross present, it is the dendritic cell that is the most efficient in this activity (3, 4). Of the various dendritic cell subtypes in the mouse, the CD8$^+$ dendritic cell is the most

capable of XPTing many antigens(18-20). These cells normally reside in the spleen and lymph nodes. Meanwhile, in the periphery, the CD8^{+} CD103^{+} migratory DCs share similar qualities. Why these DC subtypes are most specialized to crosspresent has been under intensive study.

One of the characteristics that CD8^{+} DCs have is their expression of Clec9A. Clec9A is a cell surface receptor that recognizes F-actin in dead and dying cells (21). This receptor allows the DC to engulf cellular debris more efficiently, and also directs engulfed material to endosomes that promote XPT (22). CD8^{+} DCs also express higher amounts of MHC-I related presentation genes, such as components of the peptide loading complex (TAP1, TAP2, Calnexin, Calreticulin, ERp57) as well as proteases known to trim MHC-I destined peptides (ERAP1) (23). CD8^{+} DCs can also regulate endosomal pH via Nox2 (24), which limits antigen degradation and preserves them for presentation. Conversely, CD8^{+} DCs also express lower amounts of genes that can compromise XPT. For instance, these cells express lower levels of Siglec-G, a lectin whose activation deactivates NOX2, thus promoting excessive antigen degradation (25).

C. Pathways of Crosspresentation

The ability of antigen presenting cells to XPT was soon discovered to be more complex than it seemed. XPT shared key players with the Classical Class I pathway, but it also shared key steps with the MHC Class II pathway. The degree

of contribution by the Classical Class I and the Class II pathways differed depending on the type of antigen given to cells. This section attempts to subdivide the pathways of crosspresentation into 3 general classes – the phagosome to cytosol to ER (P2C2E), the phagosome to cytosol to phagosome (P2C2P) and the vacuolar pathways. Recent advances in the field however, indicate that there might be novel pathways still waiting to be characterized.

i. The Classical MHC Class I pathway

Before discussing the pathways of XPT, it is important to detail the steps in the Classical Pathway of Class I presentation (26) (Figure 1). XPT shares numerous key players with the Classical Pathway such as the proteasome and TAP1. The known pathways of XPT can be roughly subdivided on how much they overlap with the Classical Pathway. Furthermore, for several antigens, the pathway of XPT that overlaps most with the Classical Pathway, particularly the requirement for proteasomal processing of antigen, seem to have the biggest contribution to the generated immune response (27).

Cellular proteins constantly undergo degradation as part of the normal catabolism of cells. These proteins are ubiquitinated and are hydrolyzed by the cytosolic proteasome to generate oligopeptides around 8-11 amino acids long (28). Most of these peptides are further degraded into amino acids by cytosolic peptidases (29). However, some peptides enter the endoplasmic reticulum (ER) through the transporter associated with antigen processing (TAP).

In the same compartment, newly synthesized MHC-I molecules associate with the peptide loading complex (PLC) which includes chaperone proteins such as Calnexin and Tapasin (30). These chaperones promote proper folding of free MHC heavy chains and facilitate β2m binding. Through association with the peptide loading complex (PLC), these now peptide receptive MHC Class I molecules are stabilized in the ER and can then accept peptides coming through the TAP transporter. In some cases, peptides that reach the ER are a bit too long – these peptides are trimmed by the ER resident protease ERAP1 prior to Class I loading (31, 32). Peptide-loaded MHC Class I molecules are freed from the PLC, and are shuttled to the cell surface for presentation.
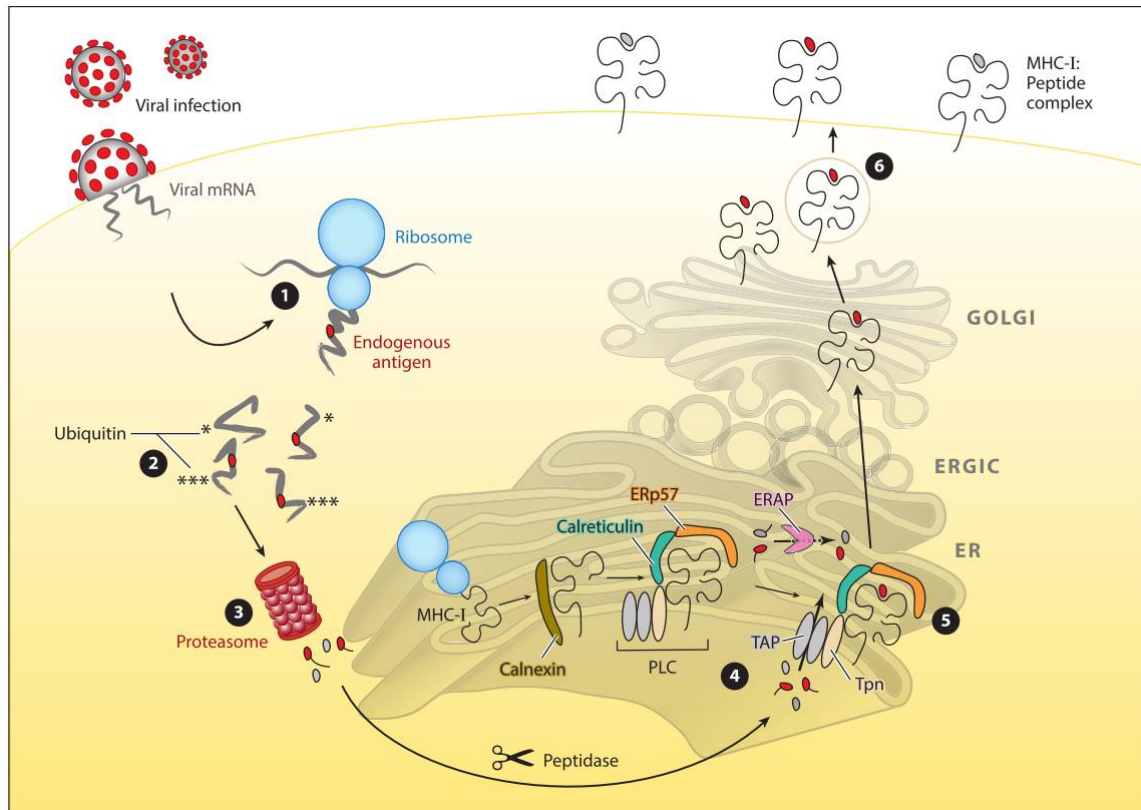
Figure 1. Classical class I antigen presentation. ❶ The classical pathway monitors the self-proteins and foreign proteins that are synthesized by cells. Expressed proteins destined for degradation are ❷ conjugated with ubiquitin and then ❸ degraded by proteasomes. Long peptides undergo trimming by cytosolic peptidases. ❹ A fraction of peptides are translocated into the lumen of the ER via TAP. Some long peptides undergo trimming in the ER by ERAP. Newly synthesized MHC-I molecules associate first with the chaperone calnexin and then, via Tpn, with TAP in the PLC. After ❺ binding TAP-transported peptide, the MHC class I:peptide complexes are ❻ transported through the secretory pathway to the plasma membrane, where they are presented to CD8^{+} cytotoxic T cells. Abbreviations: ER, endoplasmic reticulum; ERAP, ER aminopeptidase; ERGIC, ER-Golgi intermediate compartment; PLC, peptide loading complex; TAP, transporter associated with antigen processing, Tpn, tapasin. This figure was taken from a previous publication (Cruz, Colbert et al. 2017)

ii. The Phagosome – Cytosol - ER pathway

The intrinsic link between the Classical Class I and the XPT pathways can be traced to the observation that a number of exogenously derived antigens were dependent on cytosolic cellular components for presentation. The presentation of ovalbumin-coated beads for instance, could be disrupted using inhibitors of the proteasome (33). The absence of TAP also abrogated XPT (33). What these data implied was that exogenous antigen was being transferred to the cytosol, and thereafter can follow the same steps that occur in the Classical Pathway. Further experiments have confirmed this transfer. The ribosome inactivator Gelonin, when given to dendritic cells, was able to cause cell death (33, 34). The same occurred with exogenous cytochrome c (35). These proteins caused cell death through interactions with cytosolic cellular components. Exogenously given horse radish peroxidase has been found active in cytosolic fractions (36). Exogenous β-lactamase was able to cleave cytosolic fluorescent substrates when given to DCs (37). While still under intense study, the transport of phagosomal components into the cytosol has been attributed to translocation channels recruited to the phagosome such as Sec61 (38). Another hypothesized mechanism of transfer is phagosomal membrane disruption (39).

Thus, for a variety of antigens, the XPT pathway is no different to the Classical Pathway after a prior phagosome-to-cytosol step (Figure 2).
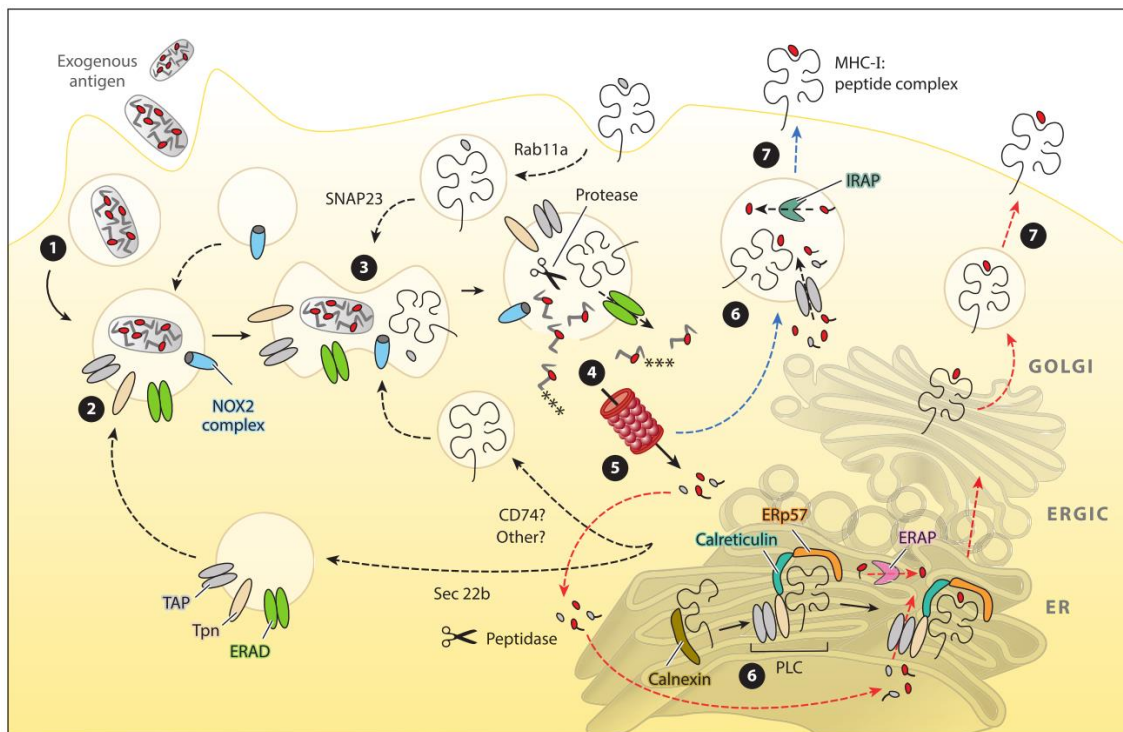
Figure 2. Cross-presentation, phagosome-to-cytosol pathway. ❶ For cross-presentation, exogenous antigen is internalized via pinocytosis, receptor-mediated endocytosis, or phagocytosis. ❷ Components of the PLC traffic to the endocytic compartment through a mechanism involving Sec 22b. ❸ MHC-I molecules may also traffic to endosomes from the plasma membrane (in part via a Rab11a and SNAP-23 mechanism) or from the ER (potentially by way of CD74 or another mechanism). ❹ Antigen within the phagosome escapes to the cytosol either by membrane disruption or through an ERAD-like translocation (green). ❺ Antigen is then conjugated with ubiquitin and degraded by the proteasome. ❻ Peptides are then transported by TAP into the ER (red lines) or back into the endocytic compartment (blue lines). ❼ Long peptides in the ER can be further trimmed by ERAP (pink), whereas those in the endosome can be trimmed by IRAP (blue-green) before binding MHC-I. The peptide-MHC I complexes are then exported to the plasma membrane. Dashed lines indicate steps in the pathway that are not fully understood. Abbreviations: ER, endoplasmic reticulum; ERAP, ER aminopeptidase; ERGIC, ER-Golgi intermediate compartment; IRAP, insulin-regulated aminopeptidase; NOX2, NADPH oxidase 2; PLC, peptide loading complex; TAP, transporter associated with antigen processing; Tpn, tapasin. This figure was taken from a previous publication (Cruz, Colbert et al. 2017).

iii. The Phagosome – Cytosol – Phagosome pathway

A layer of complexity was added to the phagosome to cytosol pathway when it was found that TAP was also recruited to some phagosomes (40). Phagosomal TAP was functional, and could mediate transport of peptides into purified phagosomes for Class I loading (41). Other novel transporters have also been reported to exist, as some peptides could be transported into phagosomes in the absence of TAP (42). When DCs were incubated with soluble US6, a viral inhibitor of TAP1, XPT of soluble ova was abrogated. This was due to the inactivation of TAP within the endosome itself, preventing re-entry of peptides (41). Moreover, members of the peptide loading complex (Tapasin, Calreticulin, Erp57) were found in the endosomes, providing the machinery required for Class I stabilization and loading.

Further evidence of this phagosome-cytosol-phagosome route has been shown by the finding that several antigens, such as ova coated beads, required the Insulin-Regulated Aminopeptidase (IRAP) for optimal XPT (43-45). IRAP was localized in endosomal compartments, and functioned similarly to ERAP – trimming peptides to the correct length. Knockout of IRAP caused around a 50% decrease in ova bead XPT, similar to ERAP deficiency, and double knockout cells had a more severe phenotype than single knockouts of either genes.

Collectively, these data suggested that phagosomes contained most if not all the necessary machinery to load MHC Class I. While the studied antigens still

required entry into the cytosol (presumably for proteasomal processing), the proteasomally generated antigen peptides could instead go back into the phagosome for Class I loading instead of heading through the ER. (Figure 2, blue lines)

iv. The Vacuolar pathway

This capability of certain phagosomes to recruit the Class I loading machinery became all the more apparent when it was observed that certain antigens, particularly bacteria (46, 47), did not require a cytosolic step in order to be presented. For some studies, XPT of this antigen was found to be brefeldin A and cycloheximide resistant, suggesting that presentation did not make use of newly synthesized MHC Class I molecules in the ER. Bacterial antigens were also presented in TAP knockout APCs, and were resistant to proteasome inhibitors – indicating that antigen processing was also occurring in a self-contained phagosomal environment. Since then, a variety of antigens, including polymer beads and cell associated antigen, have been found to at least be presented in part via this 'vacuolar pathway' (27).

In the vacuolar pathway, phagosomal proteases, particularly Cathepsin S, were responsible for generating the correct MHC-I peptide within the phagosome (27, 48-50). These proteases were able to generate the correct length of peptide, bypassing the need for the cytosolic proteasome and accessory trimming.

Phagosomal MHC Class I was then loaded with the peptides, and shuttled to the

surface (Figure 3).
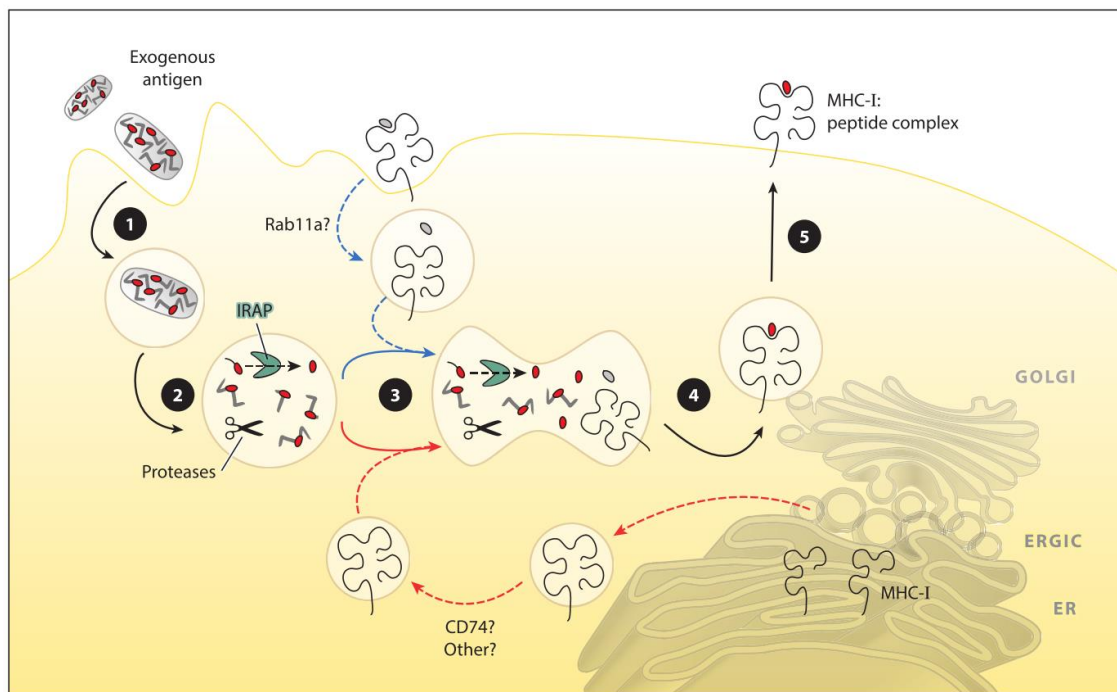
Figure 3. Cross-presentation, vacuolar pathway. ❶ Exogenous antigen is internalized via phagocytosis, pinocytosis, or receptor-mediated endocytosis. ❷ Antigen is cleaved by proteases within the endocytic compartment (primarily by cathepsins) and can be further trimmed by IRAP. ❸ MHC-I molecules are recruited either from the plasma membrane (*blue lines*) or from ER (*red lines*), presumably through similar mechanisms as in the P2C pathway. ❹ Peptide is loaded onto MHC-I in the endosome, ❺ and the complexes are then presented at the plasma membrane. Dashed lines indicate steps in the pathway that are not fully understood. Abbreviations: ERGIC, Endoplasmic reticulum--Golgi intermediate compartment; IRAP, insulin-regulated aminopeptidase. This figure was taken from a previous publication (Cruz, Colbert et al. 2017).

D. Unanswered questions

Throughout the years, a lot of progress has been made in characterizing XPT, though several questions remain. Dendritic cells have been shown to be specialized in preserving antigen and transferring it to the cytosol, but how this transfer occurs is unclear. Both XPT and the Class II pathway share the step of antigen internalization, but when or if these pathways diverge is still under study. While XPT and the Classical pathway share several key players such as the proteasome, new data suggest that the overlap between them is not as thorough as previously thought.

i. How is antigen transferred to the cytosol?

Notwithstanding the vacuolar pathway, the dependence of the majority of antigens on proteasomal processing implies that phagosome to cytosol transfer is a critical step in XPT. However, the mechanism of this transfer is poorly understood. Because phagosomes have been shown to acquire ER components, it has been proposed that antigens in the phagosome shuttle into the cytosol through an ER-associated degradation (ERAD)-like pathway (51). ERAD is the mechanism of how misfolded proteins escape the ER to be degraded by the cytosolic proteasome (52). These proteins are ubiquitinated and then transported by a complex including the ATPase p97 through an ER channel. The Sec61

translocon has been proposed to be this channel (38, 53), but other candidates such as Derlin or Hrd1 have also been put forward (52, 54, 55).

On the other hand, because several proteins have been shown to undergo phagosome to cytosol transfer intact (33-35), other mechanisms besides ERAD may play a role, as ERAD normally involves ubiquitination and denaturation of target proteins. Perhaps phagosome disruption might be one such mechanism. It has been shown that large particles like silica crystals can cause phagosomal membrane disruption in macrophages, releasing the vacuole's contents into the cytoplasm (39). Nevertheless, proteins in the phagosome may be denatured and chaperoned into the cytosol, where they can renature (56). This does not explain however, how non-proteins such as dextrans can also undergo cytosolic transfer (34).

ii. Which compartment does crosspresentation take place?

Another question is if there is a specialized phagosomal/endosomal compartment dedicated to XPT. In the MHC Class II pathway, antigen loading on Class II molecules occurs in the MHC Class II Compartment (MIIC), which contains antigen processing proteases, the Class II molecule, its associated Invariant Chain / Class II-associated invariant chain peptide (CLIP), and the peptide editing chaperones H2-DM and H2-DO (57, 58). Are there counter parts for XPT? Furthermore, the contrasting characteristics of the phagosome to

cytosol and vacuolar pathways adds another layer of complexity. What makes an antigen go through either?

The transport of intact, bioactive proteins from the phagosome to the cytosol suggests that this occurs in a relatively early phagosome, wherein the conditions for sufficient antigen degradation have not yet been met. This hypothesis is supported by the finding that Sec61, a proposed channel that mediates this transfer, colocalizes with the antigen in early endocytic (Rab5$^+$) compartments (38). Sec22b, proposed to transport the PLC from the ER to the phagosome, begins to be recruited to the phagosome within 15 minutes of phagocytosis (59). TAP1 and IRAP1 colocalize to these early vesicles as well (43, 60, 61). Several cell surface receptors implicated in XPT, such as Clec9a and the mannose receptor, directs antigen they bind to EEA1$^+$ / Rab5$^+$ vesicles (22, 62).

In contrast, antigens that go through the vacuolar pathway must be completely processed within the phagosome, suggesting that they are loaded onto MHC Class I in relatively late/mature phagosomes. Indeed, several studies show that targeting antigen to Dec205 or to TLR2 also promotes XPT (63, 64). These target the antigen to late endosomes (Lamp1$^+$ Rab7$^+$). In the case of TLR2, antigen presentation is shown to be TAP independent. When soluble ova is given to DCs for presentation, staining with the SIINFEKL – H2-K^b specific antibody 25D1.16 shows that peptide loading occurs in both early and late compartments (65) .Elucidating the requirements for a particular antigen to

undertake the P2C vs the vacuolar pathway is of increasing interest. As the two pathways make use of different proteases to process the antigen, it is conceivable that differences would arise in the MHC Class I peptides they generate. This in turn can lead to the development of different immunodominant epitopes and the corresponding CD8^{+} T cell hierarchy. In a viral infection situation for instance, infected cells would mostly generate Class I peptides through the Classical Pathway. This being the case, efficient vaccine design would probably require targeting the antigen to the P2C pathway in DCs, as opposed to the vacuolar pathway, to better match with the target cells the T cells will encounter.

iii. Where does phagosomal Class I come from?

While XPT along the P2C route is able to make use of newly synthesized MHC-I in the ER, the source of MHC-I for the phagosomal pathways of XPT is currently under intense study. Internalization of cell surface MHC-I along with the antigen is one proposed route (65-69). The cytoplasmic tail of MHC Class I contains a conserved tyrosine that controls its recycling, and mutation of this amino acid decreased localization of MHC-I in endolysosomal compartments (66). This mutation, as well as deletion of Class I exon 7, was subsequently shown to decrease MHC-I internalization in DCs as well as XPT of soluble ovalbumin (65).

Phagosomal MHC Class I has also been proposed to be sourced internally rather than from the cell surface. Invariant chain (CD74), responsible for trafficking MHC Class II from the ER-golgi to late endosomal compartments, has been also shown to traffic Class I (70). Splenic derived DCs from CD74 KO mice were defective in XPT of soluble ovalbumin. However, different forms of antigen, such as polymer bead ova, were shown to be independent of CD74 (27).

Recently, it has been proposed that APCs contain an internal pool of MHC Class I that is recruited to antigen containing phagosomes (71). The Rab GTPase Rab11a, implicated in MHC Class I recycling, supplies a specialized endosomal recycling compartment (ERC) with MHC from the surface. Once the APC internalizes antigen containing TLR ligands, MyD88 dependent signaling from the antigen containing phagosome triggers recruitment of MHC Class I containing vesicles from the ERC. Fusion of these vesicles with the phagosome brings the MHC in proximity of antigen derived peptides, for loading and XPT.

iv. What is the relationship between the XPT and Class II Pathways?

A big conundrum in the field of XPT is its relationship with the Class II pathway. While both pathways involve presentation of exogenous antigen, there are several divergences that occur even from the initial step of antigen acquisition. For instance, while both pathways are efficient in presenting particulate and cell associated antigens, soluble antigen is a particularly poor

source for XPT (5, 72). The phagosome to cytosol pathway of XPT involves the release of antigen into the cytosol. However, antigen processing for MHC Class II loading occurs in late endosomes/phagosomes. Thus, are the XPT and Class II pathways in competition for antigen? It has also been observed that dendritic cells have mechanisms to dampen endosomal degradative capability, allowing persistence of antigen for XPT. One example of which is the neutralization of endosomal pH by Nox2 (73). On the other hand, several endosomal proteases, such as Cathepsin B (74-78), are activated by low pH, and these same proteases have been shown to generate peptides destined for Class II presentation.

The vacuolar pathway of XPT is similar to the Class II pathway in that antigen processing and loading into MHC molecules occurs in a self-contained phagosome. They also share key proteases such as Cathepsin S, which processes antigen for XPT (27, 48-50) and degrades invariant chain for Class II presentation (74, 76). A still unanswered question is what makes an antigen go through the vacuolar vs the P2C (P2C2E/P2C2P) pathway. Cell associated antigen as well as polymer bead encapsulated ova undergo XPT using both P2C and vacuolar pathways (27) while iron oxide bound antigen seems to be restricted to P2C. Perhaps the presence of pathogen or damage associated molecular patterns (PAMPS or DAMPS) is the key. Bacterial antigens have been mostly associated with the vacuolar pathway (46, 47) . Moreover, the presence of TLR ligands on beads causes the recruitment of both MHC Class I and II to the bead containing phagosomes (71, 79). These PAMPS/DAMPS might be

triggering mechanisms that divert internalized antigen to degradative lysosomes (where pathogens are destroyed) rather than allow their release into the cytosol. Thus, the vacuolar pathway is utilized to allow XPT from these cytosol (more specifically, proteasome) inaccessible antigens.

E. The rationale for a genomewide siRNA screen for crosspresentation

Because of the several gaps in our understanding of the various XPT pathways, we have chosen to develop and utilize a forward genetic screen to identify genes involved in XPT. We hoped to do this by using a mouse genomewide siRNA library to look for such genes in an unbiased manner. The development of this screen as well as its results are discussed in this chapter.

II. Materials and Methods

A. Cell Lines and Culture Conditions

i. Media

Cells were maintained in Hybridoma Culture Media (HCM) composed of RPMI 1640, 10% FCS, 1X HEPES, 1X non-essential amino acids, 1X Antibiotic-antimycotic, 1X L-glutamine and 54 uM 2-mercaptoethanol (Sigma). All 100x reagents were purchased from Gibco (Invitrogen, Thermo Scientific).

For some experiments, complete DMEM (cDMEM) media was used. cDMEM is composed of all HCM supplements except 2-mercaptoethanol. The rationale for

the use of DMEM is its lack of glutathione, which is a reducing agent present in RPMI. Several experiments necessitated the need for reducing agent free environments.

ii. DC3.2

DC3.2 is one of the dendritic cell clones isolated from the work of Z.Shen & K.L.Rock (2). This clone was chosen as it has high levels of MHC Class I and Class II and gene silencing with siRNA worked well in this cell. In addition, these cells can be readily transduced with lentivirus harboring eukaryotic expression vectors.

iii. DC3.2R

DC3.2R is a variant of the DC3.2 cell line transduced with a lentiviral construct containing Renilla luciferase. The Thymidine Kinase – Renilla Luciferase insert from plasmid pRL-Tk (Promega) was PCR amplified and inserted into the lentiviral vector pCDH1-CMV-MCS-EF1-Puro (System Biosciences).

DC3.2R was chosen because it coincidentally had very good crosspresentation and Class II presentation abilities as compared to other DC clones.

iv. Luciferase expressing T cell Hybridomas (RF33-Luc, and MF2-Luc)

The RF33.70 cell line is a CD8$^+$ T cell hybridoma that recognizes the ova peptide SIINFEKL on H2-K^b (80). MF2.2D9 is a CD4$^+$ T cell hybridoma that recognizes the ova peptide Ova$_{258-276}$ on I-A^b (2).

The T cell hybridomas were transduced with lentivirus containing NFAT-Luciferase. The NFAT-Luciferase insert from plasmid pGL3-NFAT luciferase (A gift from Jerry Crabtree, Addgene plasmid #17870) (81) was PCR amplified and inserted into pCDH1-CMV-SV40-Bsd. This backbone vector is a modification of pCDH1-CMV-MCS-EF1-Puro (System Biosciences) wherein the EF1-Puro region was replaced with the blasticidin resistance gene under the SV40 promoter. Lentiviral infection was performed according to listed protocol below.

B. Lentiviral transduction of Dendritic Cell Lines

Lentivirus was produced by transfecting HEK-293T (ATCC) cells with the viral construct along with equimolar amounts of the plasmids Delta8.9 and VSVg (gifts from Dr. Eicke Latz, UMASS Medical School). Transfection conditions were done according to Lipofectamine 2000 protocol (Invitrogen). After 24 hours post transfection, cell culture media was replaced. The viral supernatant at 48 hours was collected and filtered through a 0.45 µm syringe filter. 1x10^5 DC3.2 cells were seeded in 6 well plates. The next day, media was removed and replaced with 1:1 mix of viral supernatant and HCM with 5 µg/ml polybrene (Sigma-Aldrich). After 24 hours, cell media was replaced and after 48 hours post infection, 5 µg/ml puromycin/blasticidin (depending on vector) was added. Cells

were maintained in antibiotic media for at least two weeks, replacing media with fresh antibiotic every 2 days.

C. siRNA transfections

The siRNA used were SiGenome smartpools purchased from Dharmacon/GE. To transfect dendritic cell lines, the protocol for Lipofectamine RNAiMax (Invitrogen) was followed with the following conditions. Each well of a 384 well plate was seeded with a mixture containing 0.2 µl of RNAiMax, 6.8 µl of 1X siRNA buffer (Dharmacon/GE) and 3 µl of 0.5 µM siRNA. The mixture was incubated for 20 mins at room temperature. Then, 20 µl of dendritic cells (total of $2.5x10^3$) in RPMI 1640 with 15% FCS were added. The plate was spun down at 200xg for 1 minute and incubated for 48 hours prior to assays.

D. Antigen Presentation Assay

i. Biomag-ova beads

Biomag-ova beads are magnetic particles (Iron oxide) covalently conjugated to ovalbumin.

BioMag Amine and BioMagPlus Amine Protein Coupling Kit were purchased from Bangs Laboratories. Chicken ovalbumin was purchased from Sigma-Aldrich. Protein conjugation was performed using the glutaraldehyde method according to bead manufacturer instructions. Briefly, beads were washed

in pyridine buffer and activated with 5% glutaraldehyde for 4 hours. The beads were then washed and incubated with 5 mg/ml ovalbumin dissolved in pyridine buffer overnight. Beads were extensively washed and resuspended in PBS. Ova concentration on the beads were measured using absorbance at 280 nm of pre and post coupling solutions.

ii. Protocol for XPT and Class II Presentation assays

To the transfected dendritic cells, biomag-ova was added along with a 1:1 (DC:T cell) number of luciferase expressing reporter T cells. We assumed 1×10^4 DCs were on the wells after 48 hours of transfection. For the genomewide siRNA screen, the concentration used for the XPT assay was 20 µg/ml ova (1 µg of ova in 50 µl total volume of the well). For the Class II assay, the concentration was 2 µg/ml ova. After overnight incubation, luciferase expression by the T cells was measured using Oneglo reagent (Promega) according to manufacturer instructions. The luminometer used was an Envision (Perkin Elmer) equipped with ultra-sensitive luminescence module.

III. Results

A. The Dharmacon Mouse Genome siRNA Library

We performed the screen in collaboration with the Institute for Chemistry and Cell Biology Screening Facility (ICCB-L) at Harvard Medical School. We utilized Dharmacon siGenome siRNA library plates containing 20,552 siRNA wells. Of these, 719 were targeted against mouse Kinases and phosphatases, 474 against GPCRs and the remainder for the rest of the genome. The library was composed of siRNA pools, with 4 different siRNA sequences targeting the same gene mixed in a single well. This increased the likelihood of gene knockdown, by targeting different regions of the mRNA.

The siRNA library was reverse transfected into dendritic cells in 384 well plates. Each plate also contained controls containing H2-Ab or β2m siRNA using lipofectamine RNAiMax.

B. DC3.2R as antigen presenting cells

Before proceeding with the siRNA screen, our first task was to choose the appropriate antigen presenting cell for our assay. For this we chose a variant of the dendritic cell line DC3.2 (2). We have chosen to go through the cell line route as opposed to using primary cells as isolation of dendritic cells from mice is technically difficult and results in poor yields. Moreover, the isolated cells are of a mixed population, and various dendritic cell subsets have been reported to have differing crosspresentation abilities (23). Generation of large amounts of DCs

from the bone marrow is possible through GM-CSF or Flt3 ligand (82), though these only last for a week (requiring multiple preps that can increase variability) and are not amenable to siRNA transfection (Cruz F, Rock K, unpublished data).

DC3.2 was chosen among the various clones generated in the previous work because this clone retained high amounts of MHC Class II, which we would be using as a counter screen for XPT.

DC3.2 was lentivirally transduced to express Renilla luciferase under a thymidine kinase promoter to create a new cell called DC3.2R. This was initially done in order to incorporate a viability assay along our siRNA screen. The rationale was that healthy, living cells would express Renilla luciferase commensurate to cell number and viability, and this can be correlated with T cell activity (discussed below). This would have allowed us to screen out genes that affected XPT nonspecifically, by disrupting normal cellular metabolism.

However, during the optimization of the siRNA screen, we found that incorporation of this viability screen was not technically feasible. First, the siRNA screen was designed to have a 48 hour knockout period. When siRNA against several housekeeping genes was tested as positive controls, the knockdowns did not alter renilla luciferase signal significantly at 48 hours (Cruz F, Rock K, unpublished data). Moreover, the screen was to be done in 384 well plates, which greatly limited the volumes we could manipulate. Adding in the viability screen necessitated the dilution of reagents to keep the same volumes, and this

compromised the integrity of the T cell assay due to signal variability. Thus, we decided to drop this assay.

Nevertheless, we proceeded to use the DC3.2R cells in the screen because it was found to have better XPT and Class II presentation abilities than its parental cell.

C. Biomag-ova as particulate antigen

We chose to use biomag-ova (ovalbumin covalently conjugated iron-oxide particles) as the antigen for the screen. This antigen was found to be TAP and proteasome dependent (33), suggesting that it goes through the phagosome to cytosol pathway. We chose to use this antigen as it was readily crosspresented by our various dendritic cell lines, that led to strong and consistent signals from the reporter T cells.

Other antigens exist that are able to go through the vacuolar pathway as well (27). These include polymer encapsulated ova (PLGA-ova) and cell associated antigen. One concern in using this form of antigen was that if the P2C and vacuolar pathways had redundancy, then knockdown of genes that only affected one pathway would be missed by the screen. Furthermore, we were beset with technical difficulties in using them. *In vitro*, these forms of antigen were not crosspresented well by our cell lines and required steps not compatible with 384 well plates such as washing. These issues prevented us from utilizing them in a screen that required reproducibility and data reliability.

D. Reporter T cells (RF33-Luc and MF2-Luc) Compatible With High Throughput Assays

The XPT ability of dendritic cells in vitro can be read in a number of ways. It can be read through the use of specific peptide-MHC antibodies such as 25-D1 (83). A similar method was employed in a genome wide siRNA screen for Class II presentation, wherein antibodies against MHC II – peptide and MHC II-CLIP were employed (84). However, XPT in vitro is very inefficient as compared to the Class II and Classical Class I pathways, making surface detection of peptide-MHC even from high amounts of antigen nearly undetectable (Cruz F, Rock K, unpublished data). For better sensitivity, readouts using T cell activity have been employed (2, 85).

CD8^{+} T cell hybridomas exist for the detection of peptide-MHC I complexes in vitro (85, 86). Traditionally, target cell lysis, or T cell IL-2 production have been used to correlate with APC XPT. The level of sensitivity by these T cells far exceed that of peptide-MHC antibodies (83), making them ideal for detecting slight changes in surface peptide MHC levels.

Nevertheless, due to the high throughput nature of siRNA screens, we had to modify these cell lines to make them feasible for use in our assays, typically done in bulk and contained within the confines of a 384 well plate. These limitations prevented the use of IL-2 detection and target killing (which require

washing steps for ELISA and reagent additions) as well as the use of IL-2

dependent cell lines (85), which require radiometric analysis.

Thus, we modified CD8 [+] (RF33.70) and CD4^{+} (MF2-2D9) T cell

hybridomas (2, 85) by transducing them with a luciferase construct under the

control of a minimal IL-2 promoter and 3x NFAT binding sites (now called Rf33-

Luc and MF2-Luc). T cell activation upon interaction with the appropriate peptide-

MHC activates NFAT, allowing expression of luciferase at levels that correspond

to T cell signal. While reporter CD8^{+} T cells employing the same design but

expressing β-galactosidase have been constructed (87), putting in luciferase in

our reporter cells allowed us to take advantage of the greater speed and high

throughput compatibility of luciferase's luminescent read out as compared to

other assays that employ colorimetry.

As shown in (Figure 4), the generated reporter T cells were able to detect

XPT and Class II presentation by APCs, and expressed luciferase in proportion

to the amount of peptide MHC presented on the APC surface.
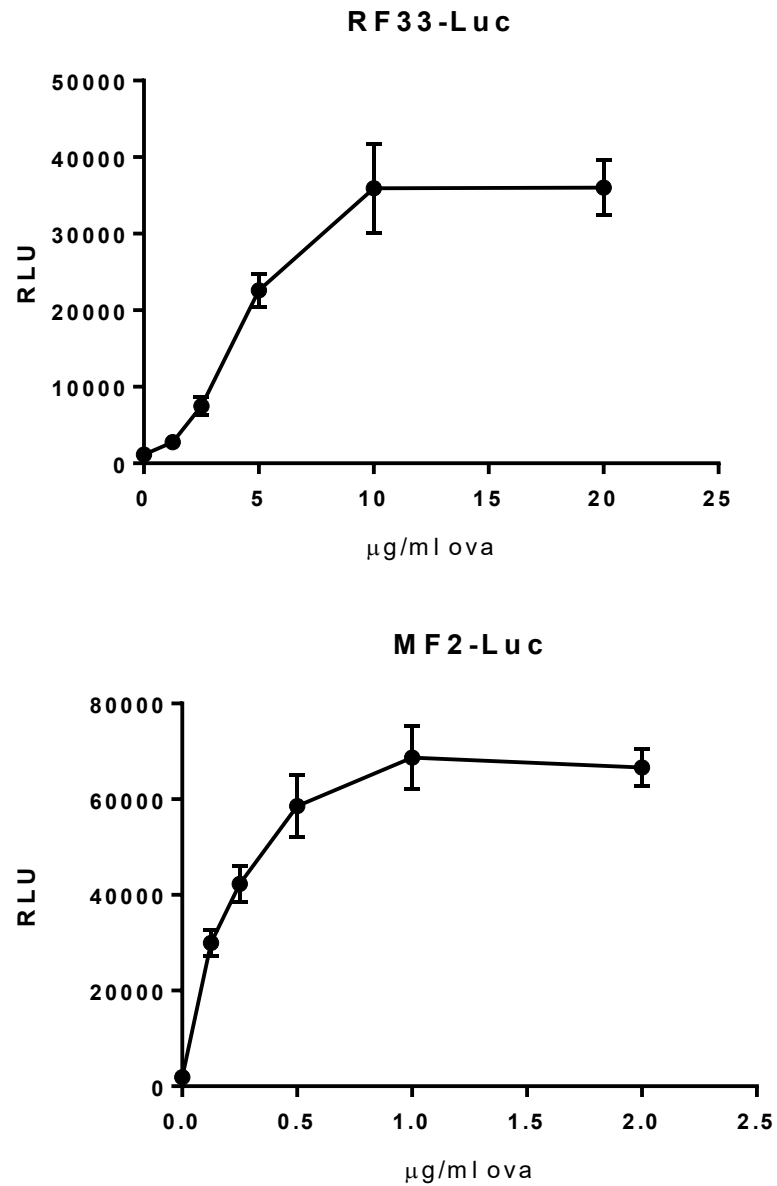
RF33-Luc

MF2-Luc

Figure 4. **Reporter T cells express luciferase upon interaction with cognate MHC peptides.**

5×10^4 RF33-Luc or MF2-Luc were incubated with the same number of APCs (DC2.4 cell line) as well as the indicated amounts of biomag-ova overnight. T cell luciferase activity was measured using Promega Oneglo reagent. Error bars indicate the standard deviation between triplicate wells. Data shown represents one experiment of ≥ 3.

E. Developing a Class II Counter Screen

In designing a genome-wide siRNA screen, it was important to be able to determine if the phenotype observed was due to a gene specifically involved in the pathway studied, or was due to a pleiotropic effect commonly associated with housekeeping genes. For our assay, we have chosen to run a counter screen for the Class II pathway.

In parallel to the XPT screen, we also screened the Class II pathway. The same transfected cells were instead exposed to reporter $CD4^+$ T cells. If a gene being silenced was a housekeeping gene, and its knockdown caused cell death, then both XPT and Class II pathways would drop. This scheme also allowed us to determine if a particular gene was involved in a process shared by both XPT and the Class II pathway. Antigen internalization, as well as phagosomal degradation of proteins are among these shared processes. This permitted us to not only reduce the screen background but also uncover potential Class II specific genes.

F. siRNA knockdowns effectively reduce XPT or Class II presentation

When known MHC Class I related genes (β2m, TAP1) were knocked down with siRNA, XPT by DC3.2R of biomag-ova was selectively reduced (Figure 5). Conversely, when Class II related genes (I-Ab, H2-DMα) were silenced with siRNA, only Class II presentation was decreased. The decrease in

presentation was effectively measured by the luciferase expressing reporter T cells. Thus, we now had all the components necessary for the siRNA screen.

We then performed the screen in following the workflow shown in (Figure 6).
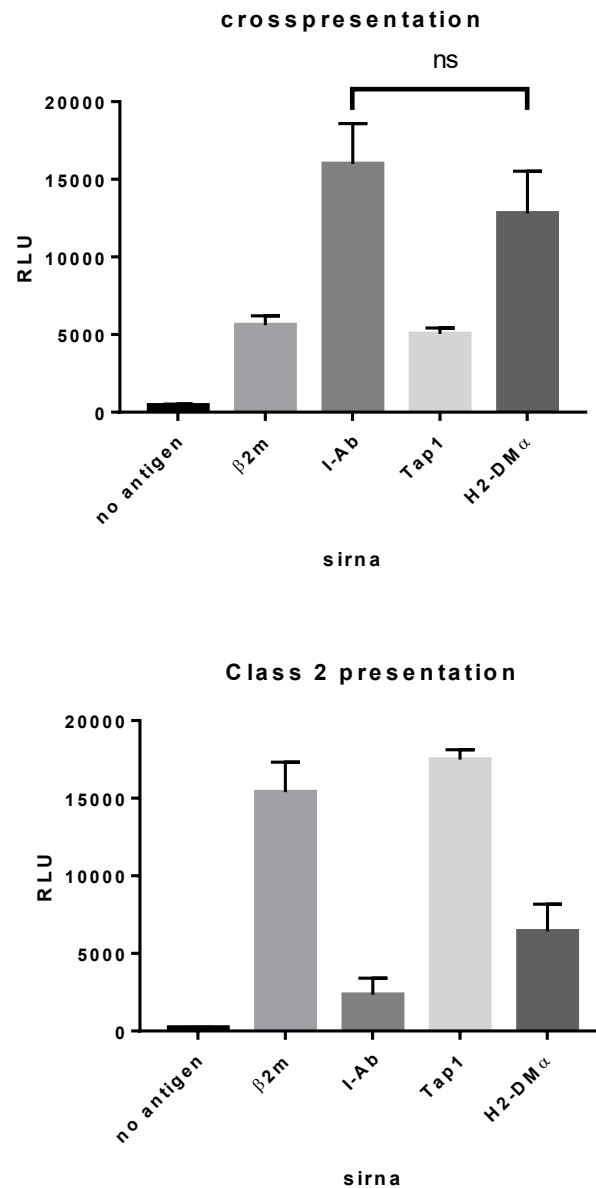
Figure 5. **Knockdown of antigen presentation using sirna.**

2.5 x10^3 DC3.2R cells were transfected with 50 nM sirna using Lipofectamine RNAiMax. After 48 hours, 1 x 10^4 Rf33-Luc or Mf2-Luc cells were added along with 20 µg/ml (XPT) or 2 µg/ml (Class II) of biomag ova. After overnight incubation (~18 hours), Luciferase activity of the T cells were read using Oneglo reagent (Promega). Error bars indicate the standard deviation between triplicate wells. Data shown represents one experiment of $\geq$3. ns indicates p >0.05 in ANOVA. For xpt, all siRNA treatments except H2-DM have p$\leq$ 0.05 against I-Ab. For Class 2, all siRNA treatments except Tap1 have p$\leq$ 0.05 against β2m.

Transfect two sets of dendritic cells
(3 replicates each)
(~320 gene targets / plate)

48 hours later:
Add antigen and reporter T
cells

+18 hours: luciferase assay
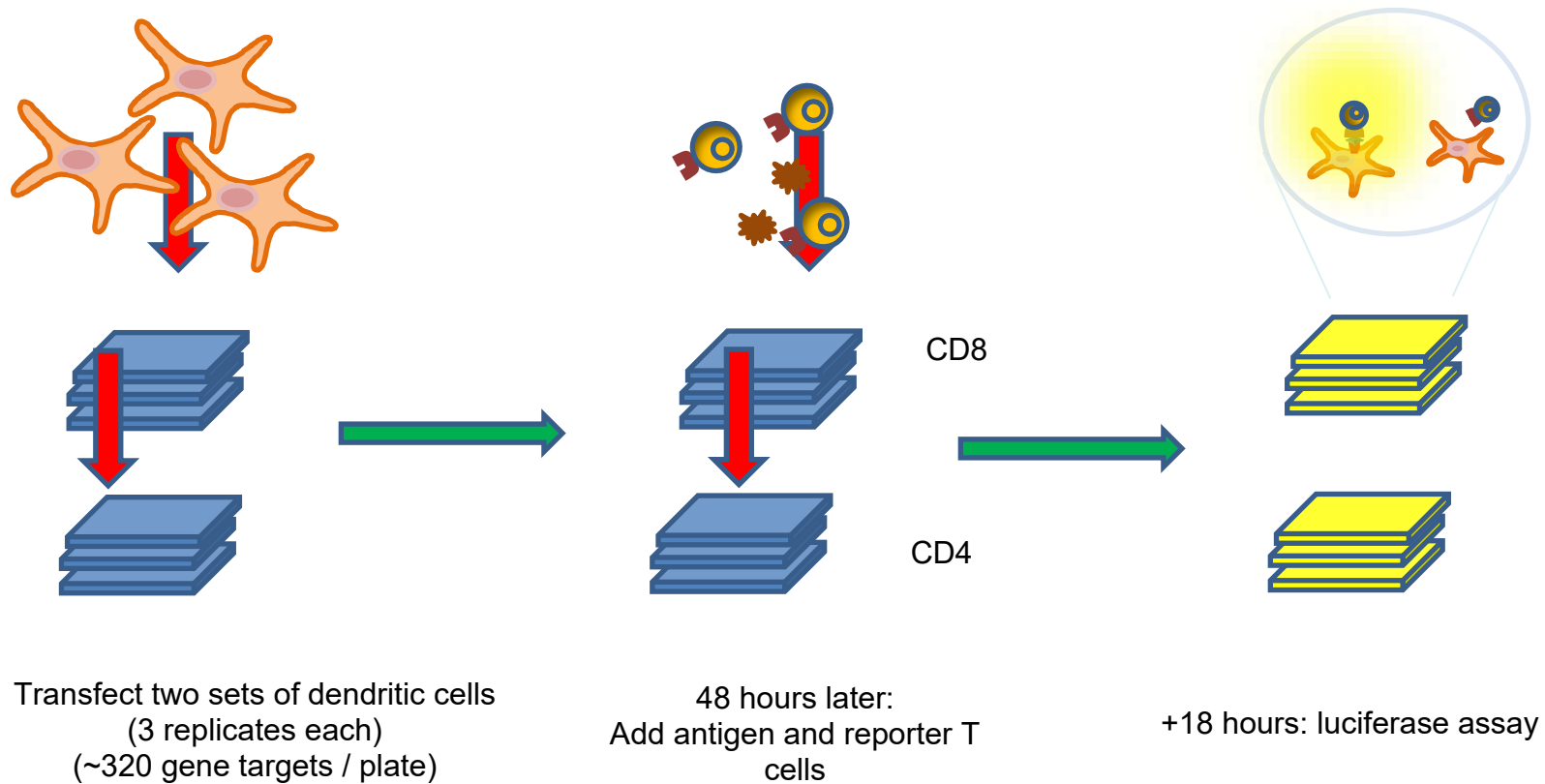
Figure 6. **Screen Workflow**

In each well of a 384 well plate, 2.5 x10^3 DC3.2R cells were transfected with 50 nM sirna using Lipofectamine RNAiMax. This was done for 2 sets of triplicate plates. After 48 hours, 1 x 10^4 Rf33-Luc or Mf2-Luc cells were added along with 20 µg/ml (XPT) or 2 µg/ml (Class II) of biomag ova. After overnight incubation (~18 hours), Luciferase activity of the T cells was read using Oneglo reagent (Promega).

G. Statistical Analysis for the Genome Wide Primary Screen

To interpret the primary screen results, we have performed the statistical analysis as described below. All statistical analyses were performed in collaboration with Dr. Stephen Baker of UMASS Medical School.

The entire mouse genome siRNA library consisted of 69 (384 well) plates and these were screened across several months. In order to account for experimental variation between library plates, we normalized plate values against internal controls.

Each library plate (done in triplicate) contained siRNA wells against H2-Ab1 (beta chain of the Class II molecule I-A) and β2m. For each plate, the average T cell readouts from these controls were taken and were set to 100 (percent signal from negative control) and 0 (positive control) respectively by generating a scaling factor using the equation:

$$scaling\ factor = \frac{100}{negative\ control - positive\ control}$$

For the XPT screen this translates to:

$$scaling\ factor = \frac{100}{IAb - \beta 2m}$$

* the controls are reversed during analysis of the Class II screen

The T cell readout from each siRNA well in a particular plate was then normalized to both positive and negative controls in the same plate. For the XPT screen, this was done in the equation:

$$scaled\ value = (IAb - sirna) * scaling\ factor$$

This generated values that represent each siRNA's position in relation to the negative and positive controls. Thus, when a variation in the experiment caused an increase or decrease in overall plate signal (which can be due to cell condition, plate reader variability, transfection and knockdown efficiency, etc), the relative value of the siRNA wells was preserved. This allowed comparison of values generated from multiple plates read over several days.

All 69 plates of a single replicate were then merged, and z-scores for each gene were calculated:

$$z\ score = \frac{s - M}{MAD}$$

where:

s = scaled value of individual siRNA

M = median of all experimental siRNA scaled values

MAD = median absolute deviation

where:

$$MAD = \frac{median(s - M)}{0.6745}$$

*0.6745 constant assuming a normal distribution

The z score transformed the raw luminescence values into their distance to the genomic median. It was expected that majority of the genes would not hit XPT and would have z scores close to 0. Very low (negative values) represented genes that caused a huge knockdown in XPT, while very high values represented an augmentation in XPT. In genomewide screens, a threshold z-score is chosen to limit the number of hits. Before that however, we needed to take into account experimental variability.

The siRNA plates were done in triplicate plates. To take into account variability among the plates, the following equation was applied:

$$t_{stat} = \frac{Z_{ave}}{\sqrt{(Z_{sd}^2/3)}}$$

where:

$Z_{ave} = average\ z\ score\ of\ an\ sirna\ (triplicates)$

$Z_{sd} = standard\ deviation\ of\ the\ z\ scores\ of\ an\ sirna$

To determine the confidence level that a particular gene has of being a real hit, a T-distribution was then generated using the EXCEL equation:

$$p = TDIST(ABS(t_{stat}), 2, 1)$$

* 2 degrees of freedom, 1 tailed

If a given gene had a good z score (in this case, very negative meaning a huge average knockdown in T cell signal), but was extremely variable between its triplicates (due to technical/human error), the variability brought down the t_{stat}. This would have brought down its p value lowering the confidence that it was a real screen hit.

For selecting primary screen crosspresentation hits, the following criteria was chosen:

$$CD8\ scaled\ knockdown \geq 50\%$$

This corresponds to a CD8 z-score = 0.5

$$CD4\ scaled\ knockdown \leq 0$$

and

$$p \leq 0.02$$

H. Association of genes with available databases

497 of the 20,552 screened genes (2.4%) passed the thresholds we set for the primary XPT screen. In order to limit the number of candidates for further study, a number of genes were selected for siRNA deconvolution (discussed below). Before this however, we screened the hits against publicly available literature and databases in order to determine which genes would be suitable for this analysis.

i. Clustering and enrichment of hits via General Ontology

One method used to analyze large scale gene datasets is to cluster them via functional annotation. Genes that clustered around the same pathways or had conserved domains/structures would likely have similar or complementary roles in XPT, therefore aiding in their characterization. Several tools such as DAVID (The Database for Annotation, Visualization and Integrated Discovery)(88) and the Panther (Protein Analysis Through Evolutionary Relationships) Classification System (89, 90) exist that allow clustering of genes via common properties, such as involvement in the same cellular pathway. Once clustered, we wanted to see if certain gene subsets were being enriched by the screen. This was calculated by the above listed tools by comparing the proportion of the generated clusters within our gene set to their natural proportion in the whole mouse genome.

When genes selectively affecting XPT were clustered according to cellular component / localization, significant enrichment of golgi and cilum localized

genes was observed (Table 1). When looked at more closely, these genes seemed to be involved in cytoskeleton and membrane/trafficking processes (Rab GTPases, EHD1, dynein, etc) (Table 2, Table 3).

Concordant to this finding, when XPT selective genes were clustered according to their involvement with specific biological processes, we observed significant enrichment in genes involved in vesicle organization and organelle fusion (Table 4, Table 5, Table 6).

Despite not being a category particularly enriched in the clustering/annotation process, we also looked for genes that were specifically localized in the endosomes and lysosomes, where the XPT and Class II pathways were likely to diverge. Several endo-lysosomal and vesicular components have been recently published to affect XPT. Among these were several Rab GTPases (discussed in later chapters), usually implicated in controlling vesicular transport (44, 67, 71, 91). While the Class II pathway was not specifically addressed in these studies, most of the proposed models seemed to indicate a role of these proteins in the specific trafficking of MHC Class I. Our primary screen also identified genes localized in the vesicles / endo-lysosomes (Table 7). How these affect XPT but not Class II would be an interesting field to study.

Category	Term	Count	%	P-Value
GOTERM_CC_ALL	Golgi membrane	23	4.7	0.0027
GOTERM_CC_ALL	bounding membrane of organelle	48	9.8	0.0067
GOTERM_CC_ALL	ciliary membrane	6	1.2	0.0069
GOTERM_CC_ALL	organelle membrane	69	14.1	0.0073
GOTERM_CC_ALL	cilium	21	4.3	0.013
GOTERM_CC_ALL	ciliary part	15	3.1	0.014
GOTERM_CC_ALL	Golgi apparatus part	26	5.3	0.017
GOTERM_CC_ALL	primary cilium	10	2	0.029
GOTERM_CC_ALL	ciliary transition zone	4	0.8	0.03
GOTERM_CC_ALL	myelin sheath	10	2	0.046

Table 1. Clustering of XPT selective hits via cellular component/localization
XPT selective hits were annotated using DAVID (https://david.ncifcrf.gov) using the specified categories. Count represents the number of genes that fall in each term and percentage represents its proportion in comparison to the whole gene list. P-values represent the probability that the given term is enriched within the gene list when compared to the whole mouse genome. Shown are categories with p values $\leq$ 0.05.

Entrez Gene ID	Gene Name
56350	ADP-ribosylation factor-like 3(Arl3)
232237	FYVE, RhoGEF and PH domain containing 5(Fgd5)
226075	GLIS family zinc finger 3(Glis3)
15461	Harvey rat sarcoma virus oncogene(Hras)
80877	LPS-responsive beige-like anchor(Lrba)
226407	RAB3 GTPase activating protein subunit 1(Rab3gap1)
270160	RAB39, member RAS oncogene family(Rab39)
54613	ST3 beta-galactoside alpha-2,3-sialyltransferase 6(St3gal6)
20447	ST6 (alpha-N-acetyl-neuraminyl-2,3-beta-galactosyl-1,3)-N-acetylgalactosaminide alpha-2,6-sialyltransferase 3(St6galnac3)
20449	ST8 alpha-N-acetyl-neuraminide alpha-2,8-sialyltransferase 1(St8sia1)
207839	UDP-N-acetyl-alpha-D-galactosamine:polypeptide N-acetylgalactosaminyltransferase 6(Galnt6)
56041	USO1 vesicle docking factor(Uso1)
77590	carbohydrate (N-acetylgalactosamine 4-sulfate 6-O) sulfotransferase 15(Chst15)
56773	carbohydrate (N-acetylglucosamine 6-O) sulfotransferase 5(Chst5)
12922	corticotropin releasing hormone receptor 2(Crhr2)
107522	endothelin converting enzyme 2(Ece2)
14317	formiminotransferase cyclodeaminase(Ftcd)
14419	galanin(Gal)
72077	glucosaminyl (N-acetyl) transferase 3, mucin type(Gcnt3)
230101	glucosidase beta 2(Gba2)
14594	glycoprotein galactosyltransferase alpha 1, 3(Ggta1)
70231	golgi reassembly stacking protein 2(Gorasp2)
15478	heparan sulfate (glucosamine) 3-O-sulfotransferase 3A1(Hs3st3a1)
54710	heparan sulfate (glucosamine) 3-O-sulfotransferase 3B1(Hs3st3b1)
268510	mannoside acetylglucosaminyltransferase 5, isoenzyme B(Mgat5b)
17480	myeloproliferative leukemia virus oncogene(Mpl)
18176	neuroblastoma ras oncogene(Nras)
18197	neuron specific gene family member 2(Nsg2)
18576	phosphodiesterase 3B, cGMP-inhibited(Pde3b)
66889	ring finger protein 128(Rnf128)
114679	selenoprotein M(Selm)
236727	solute carrier family 9 (sodium/hydrogen exchanger), member 7(Slc9a7)
319613	syntabulin (syntaxin-interacting)(Sybu)
66682	trafficking protein particle complex 5(Trappc5)

Table 2. Golgi localized genes involved in XPT
Genes associated with the golgi apparatus, a subset of Table 1

Entrez Gene ID	Gene Name
68146	ADP-ribosylation factor-like 13B(Arl13b)
56350	ADP-ribosylation factor-like 3(Arl3)
102774	Bardet-Biedl syndrome 4 (human)(Bbs4)
319845	Bardet-Biedl syndrome 9 (human)(Bbs9)
66573	DAZ interacting protein 1(Dzip1)
13660	EH-domain containing 1(Ehd1)
71820	WD repeat domain 34(Wdr34)
231214	coiled-coil and C2 domain containing 2A(Cc2d2a)
433956	dynein, axonemal assembly factor 5(Dnaaf5)
13417	dynein, axonemal, heavy chain 8(Dnah8)
76568	intraflagellar transport 46(Ift46)
21821	intraflagellar transport 88(Ift88)
27276	pleckstrin homology domain containing, family B (evectins) member 1(Plekhb1)
192190	polycystic kidney and hepatic disease 1-like 1(Pkhd1l1)
74362	sperm associated antigen 17(Spag17)
24069	suppressor of fused homolog (Drosophila)(Sufu)
57253	taste receptor, type 2, member 108(Tas2r108)
654470	tectonic family member 1(Tctn1)
620631	tetratricopeptide repeat domain 30A2(Ttc30a2)
330010	tubulin tyrosine ligase-like family, member 10(Ttll10)
237930	tubulin tyrosine ligase-like family, member 6(Ttll6)

Table 3. Cilium localized genes involved in XPT
Genes associated with the golgi apparatus, a subset of Table 1.

Category	Term	Count	%	P-Value
GOTERM_BP_ALL	dorsal/ventral pattern formation	10	2	0.00047
GOTERM_BP_ALL	organelle fusion	11	2.3	0.0015
GOTERM_BP_ALL	organelle membrane fusion	9	1.8	0.0022
GOTERM_BP_ALL	regulation of calcium ion-dependent exocytosis	7	1.4	0.0023
GOTERM_BP_ALL	vesicle organization	13	2.7	0.0027
GOTERM_BP_ALL	endothelial cell morphogenesis	4	0.8	0.0028
GOTERM_BP_ALL	membrane fusion	11	2.3	0.0031
GOTERM_BP_ALL	smoothened signaling pathway	9	1.8	0.0034
GOTERM_BP_ALL	embryonic epithelial tube formation	10	2	0.0042
GOTERM_BP_ALL	single-organism membrane fusion	10	2	0.0043
GOTERM_BP_ALL	epithelial tube formation	10	2	0.0043

Table 4. Clustering of XPT selective hits via involvement with specific biological processes
XPT selective hits were annotated using DAVID (https://david.ncifcrf.gov) using the specified categories. Count represents the number of genes that fall in each term and percentage represents its proportion in comparison to the whole gene list. P-values represent the probability that the given term is enriched within the gene list when compared to the whole mouse genome. Shown are categories with p values $\leq$ 0.005.

Entrez Gene ID	Gene Name
270160	RAB39, member RAS oncogene family(Rab39)
67231	TBC1 domain family, member 20(Tbc1d20)
210789	TBC1 domain family, member 4(Tbc1d4)
56041	USO1 vesicle docking factor(Uso1)
76959	charged multivesicular body protein 5(Chmp5)
50518	nonagouti(a)
72287	pleckstrin homology domain containing, family F (with FYVE domain) member 1(Plekhf1)
55925	synaptotagmin VIII(Syt8)
319508	synaptotagmin XV(Syt15)
236643	synaptotagmin-like 5(Sytl5)
68159	syntaxin 19(Stx19)
57394	transmembrane protein 27(Tmem27)
330192	vacuolar protein sorting 37B(Vps37b)

Table 5. Genes associated with vesicle organization
List of genes associated with vesicle organization, a subset of Table 4.

Entrez Gene ID	Gene Name
114896	AFG3-like AAA ATPase 1(Afg3l1)
270160	RAB39, member RAS oncogene family(Rab39)
210789	TBC1 domain family, member 4(Tbc1d4)
56041	USO1 vesicle docking factor(Uso1)
76959	charged multivesicular body protein 5(Chmp5)
55925	synaptotagmin VIII(Syt8)
319508	synaptotagmin XV(Syt15)
236643	synaptotagmin-like 5(Sytl5)
68159	syntaxin 19(Stx19)
70381	tectonin beta-propeller repeat containing 1(Tecpr1)
57394	transmembrane protein 27(Tmem27)

Table 6. Genes associated with organelle fusion
List of genes associated with organelle fusion, a subset of Table 4.

endosomes	
Gene	**Name**
Ehd1	EH-domain containing 1
Fgd5	FYVE, RhoGEF and PH domain containing 5
L1CAM	L1 cell adhesion molecule
Arhgap27	Rho GTPase activating protein 27
Galntl5	UDP-N-acetyl-alpha-D-galactosamine:polypeptide N-acetylgalactosaminyltransferase-like 5
Chmp5	charged multivesicular body protein 5
Mvb12a	multivesicular body subunit 12A
Nsg2	neuron specific gene family member 2
Plekhf1	pleckstrin homology domain containing, family F (with FYVE domain) member 1
Slc38a9	solute carrier family 38, member 9
Slc9a7	solute carrier family 9 (sodium/hydrogen exchanger), member 7
Vps37b	vacuolar protein sorting 37B

lysosomes	
Gene	**Name**
LRBA	LPS-responsive beige-like anchor
Rab39	RAB39, member RAS oncogene family
9530002B09Rik	RIKEN cDNA 9530002B09 gene
Epdr1	ependymin related protein 1 (zebrafish)
Hpse	heparanase
Plekhf1	pleckstrin homology domain containing, family F (with FYVE domain) member 1
Slc38a9	solute carrier family 38, member 9
Tecpr1	tectonin beta-propeller repeat containing 1

Table 7. Screen Hits enriched in endosomes and lysosomes.
Primary screen hits selective for crosspresentation were functionally annotated with DAVID (https://david.ncifcrf.gov). Tabulated are genes found in endosomes and lysosomes as characterized under the GOTERM_CC_DIRECT database (Gene Ontology Consortium, cellular component).

ii. Expression in immune cell subsets

Another criterion we used to determine gene candidates was their expression in specific immune subsets. Dendritic cells have been shown to be specialized for XPT, and among the DCs, the CD8α^{+} (and CD103^{+}) subsets were the ones with the most XPT potential. Studies have shown that CD8α^{+} DCs highly expressed genes involved in the Classical Class I Pathway such as ERAP and the members of the PLC (TAP1/2, Calnexin, Erp57, etc) (23). This subset also expressesed high amounts of Clec9a (92) and Nox2 complex components (24). Because of this, screen hits that were highly enriched in CD8α[+] DCs were taken for further study.

We matched our database with that of Immgen (93), which contained probe-based (Affymetrix) gene expression profiles of specific immune subsets. (Table 8) shows crosspresentation selective genes that were enriched in CD8α[+] DCs from various tissues.

Symbol	THY	MLN	SLN	SPL	Gene Name
Got2	0.0340	0.1366	0.1151	0.1739	glutamatic-oxaloacetic transaminase 2, mitochondrial(Got2)
HTR7	0.0138	0.0497	0.0667	0.0324	5-hydroxytryptamine (serotonin) receptor 7(Htr7)
Ppfibp2	0.0405	0.0359	0.0597	0.0214	PTPRF interacting protein, binding protein 2 (liprin beta 2)(Ppfibp2)
Tmem27	0.0080	0.0783	0.0910	0.0483	transmembrane protein 27(Tmem27)
2610034N03RIK	0.0421	0.2057	0.1861	0.1660	isochorismatase domain containing 1(Isoc1)
Lcorl	0.0387	0.2443	0.1448	0.1282	ligand dependent nuclear receptor corepressor-like(Lcorl)
Rab39	0.0408	0.0268	0.0410	0.0149	RAB39, member RAS oncogene family(Rab39)
1700110A09RIK	0.4997	0.2840	0.0496	0.0359	ADP-ribosylation factor-like 9(Arl9)

Table 8. Screen Hits enriched in CD8α+ Dendritic Cells.
Primary screen hits for crosspresentation were matched with the Immgen database (Immgen.org). Standard z scores of the entire Immgen database were calculated using the database mean and standard deviation. P values from the generated T distribution of z scores were obtained and the gene list was filtered for genes that were positively enriched ($z > 0$) in any of the listed CD8α DC subsets. Tabulated are p values and highlighted are $p \leq 0.05$. *THY, thymic; MLN, mesenteric lymph node; SLN, skin draining lymph node; SPL, splenic

iii. Comparison with a published MHC Class II screen

Neefjes et. al. has published a genomewide siRNA screen for human genes affecting Class II presentation (84). In their screen, they utilized antibodies specific for MHCII-CLIP peptide (CerCLIP antibody) as well as peptide bound MHCII (L243 antibody).

In the Class II pathway, MHC Class II is trafficked by the invariant chain to late endosomes, wherein invariant chain is degraded into a remnant CLIP peptide that caps the MHC Class II molecule. Through the function of low pH as well as chaperones such as H2-DM and H2-DO, this CLIP peptide is replaced by peptides that derive from exogenous antigen taken up by the APC.

The multidimensional approach employed in their screen allowed them to differentiate genes that affected general MHC Class II trafficking (which would decrease staining of cells by both antibodies) or those that had more specific effects, such as peptide loading and/or invariant chain processing (would likely increase staining of CerClip).

We compared Class II pathway hits in our screen to the mouse orthologs of the published screen hits. Of the 262 candidate genes in the published work, 43 of them were also hits in our Class II screen (with at least 50% knockdown in Class II presentation and a p value of ≤ 0.05 for Class II presentation). These common hits are shown in (Table 9).

Symbol	Mouse Name
Sh3bp5l	SH3 binding domain protein 5 like
Sucnr1	succinate receptor 1
Arg2	arginase type II
Stk32c	serine/threonine kinase 32C
Tollip	toll interacting protein
Dyrk1a	dual-specificity tyrosine-(Y)-phosphorylation regulated kinase 1a
Chchd10	coiled-coil-helix-coiled-coil-helix domain containing 10
Map3k10	mitogen-activated protein kinase kinase kinase 10
Efhd2	EF hand domain containing 2
Map3k8	mitogen-activated protein kinase kinase kinase 8
Fam63a	family with sequence similarity 63, member A
Pik3ip1	phosphoinositide-3-kinase interacting protein 1
Nek3	NIMA (never in mitosis gene a)-related expressed kinase 3
Ropn1l	ropporin 1-like
Dapk3	death-associated protein kinase 3
Reep6	receptor accessory protein 6
Cx3cr1	chemokine (C-X3-C) receptor 1
Zfp462	zinc finger protein 462
Camk1	calcium/calmodulin-dependent protein kinase I
Abca3	ATP-binding cassette, sub-family A (ABC1), member 3
Vps28	vacuolar protein sorting 28 (yeast)
Snapc4	small nuclear RNA activating complex, polypeptide 4
Atp2b2	ATPase, Ca++ transporting, plasma membrane 2
Creb3l2	cAMP responsive element binding protein 3-like 2
Gnaz	guanine nucleotide binding protein, alpha z subunit
Zc3h10	zinc finger CCCH type containing 10
Dapk1	death associated protein kinase 1
Fam53b	family with sequence similarity 53, member B
Naca	nascent polypeptide-associated complex alpha polypeptide
Ap2a1	adaptor protein complex AP-2, alpha 1 subunit
Thrb	thyroid hormone receptor beta
Map3k9	mitogen-activated protein kinase kinase kinase 9
Npr2	natriuretic peptide receptor 2
Ulk2	Unc-51 like kinase 2 (C. elegans)
Trip13	thyroid hormone receptor interactor 13
Chek1	checkpoint kinase 1
Csk	c-src tyrosine kinase
Tas2r119	taste receptor, type 2, member 119
Srsf1	serine/arginine-rich splicing factor 1
Gigyf2	GRB10 interacting GYF protein 2
Araf	v-raf murine sarcoma 3611 viral oncogene homolog
H2-DMb1	histocompatibility 2, class II, locus Mb1
Cdk13	cyclin-dependent kinase 13

Table 9. Common hits with a previously published screen for Class II presentation

Shown are hits in our screen that had $\geq$ 50% knockdown in Class II presentation as well as $p \leq 0.05$ for the Class II pathway. These genes are mouse orthologs of genes that were previously published to affect Class II presentation in a human sirna screen (Paul, van den Hoorn et al. 2011).

However, several of these common hits also affected crosspresentation in our primary screen. This was expected as XPT and the Class II pathways shared the steps of phagocytosis as well as endosome/phagosome maturation. Of these hits, 7 genes were reliably selective for the Class II pathway and did not hit the crosspresentation pathway (with $p \leq 0.05$ for both pathways). These genes are shown in (Table 10). Many genes were not considered selective primarily due to the fact that they did not pass the statistical test for variability (p value). Thus, these 7 genes were probably an underestimation of the real hits. How these genes only selectively affect the Class II pathway would be interesting to study.

Symbol	Mouse Name
Wdr37	WD repeat domain 37
Gnaz	guanine nucleotide binding protein, alpha z subunit
Trip13	thyroid hormone receptor interactor 13
Thrb	thyroid hormone receptor beta
Vps28	vacuolar protein sorting 28 (yeast)
Eftud2	elongation factor Tu GTP binding domain containing 2
Zfp462	zinc finger protein 462

Table 10. Class II selective hits that are common with a previously published screen for Class II presentation.
Shown are hits in our screen that had $\geq$ 50% knockdown in Class II presentation as well as $p \leq 0.05$ for the Class II pathway. The genes also did not affect the crosspresentation pathway with $p \leq 0.05$.
The human orthologs of these genes were previously published to affect Class II presentation in a human sirna screen (Paul, van den Hoorn et al. 2011).

I. siRNA Deconvolution

Before proceeding with the characterization of the primary screen hits, we performed siRNA deconvolution. This process allowed us to determine if our primary screen phenotype was due to the knockout of the particular gene or was due to siRNA off target effects.

A particular siRNA can have sequence specific off target effects. The siRNA pathway generally requires a perfect match between the guide siRNA and its target to initiate Argonaute mediated mRNA cleavage (94), and siRNA libraries are constructed to generate guide sequences unique to target genes. However, a parallel pathway in the cell - the miRNA pathway, mediates a similar knockdown of genes but do not require exact miRNA-target complementarity. In this pathway, complementarity between an inner "seed" sequence of the miRNA and its target is sufficient to mediate knockdown, while the miRNA flanking sequences are allowed some variability. Because of this, particular regions of an siRNA introduced into cells have a chance of mimicking miRNAs, thereby causing unintended knockdowns. Besides mimicking miRNAs, partial siRNA complementarity to nonspecific mRNA can decrease gene expression by blocking translation initiation.

Furthermore, siRNAs can also demonstrate sequence independent off-target effects (94). Rather than binding to nonspecific mRNA, siRNA, particularly in high concentrations, can instead disrupt normal miRNA processes occurring

within cells. High concentrations of siRNA can displace miRNA from the RISC complex, or compete with miRNA trafficking and export factors (95) . The disruption of miRNA can have global effects on the cell, as they are utilized to regulate gene expression. Other sequence independent siRNA effects include the activation of immune sensors and increased cell stress.

In order to account for siRNA off-target effects, a selection of genes was subjected to siRNA deconvolution. The siRNA smartpool used in the primary screen (composed of a mixture of 4 different siRNA oligos) was separated into its individual components. Cells were transfected separately with each of the individual oligos. Genes that had at least 2 different siRNAs recapitulating the phenotype (affected XPT but not Class II presentation) were picked for further study (Table 11).

Gene Symbol	Gene Name
Slc39a3	solute carrier family 39 (zinc transporter), member 3
KDELC1	KDEL (Lys-Asp-Glu-Leu) containing 1
Ccdc141	coiled-coil domain containing 141
Psg27	pregnancy-specific glycoprotein 27
Prl7a2	prolactin family 7, subfamily a, member 2
Glul	glutamate-ammonia ligase (glutamine synthetase)
Tmem81	transmembrane protein 81
Gal	galanin
P2rxl1	purinergic receptor P2X, ligand-gated ion channel, 6
Glrp1	glutamine repeat protein 1
Slc24a2	solute carrier family 24 (sodium/potassium/calcium exchanger), member 2
CPNE4	copine IV
Rab39	RAB39, member RAS oncogene family
Senp3	SUMO/sentrin specific peptidase 3
Prpmp5	proline-rich protein MP5
Slc24a4	solute carrier family 24 (sodium/potassium/calcium exchanger), member 4
Pde1a	phosphodiesterase 1A, calmodulin-dependent

Table 11. A selection of genes that passed siRNA deconvolution.
Listed are genes with at least 2 individual sirna oligos causing a knockdown in crosspresentation but not Class II presentation.

IV.   Discussion

In this work, we have successfully developed and utilized a genomewide siRNA screen for genes that affected crosspresentation or the Class II pathway. A number of genes are currently undergoing characterization.

From the entire annotated mouse genome, our primary screen has identified 472 genes to be selectively involved in XPT based on the thresholds we have set. This was not an absolute number, as one can loosen the thresholds to identify additional genes. We had set the threshold to only pick genes that caused a large decrease ($\geq$ 50%) in XPT. This was done to limit the number of genes to a more manageable number. Certainly, there could be genes relevant to XPT that do not cause such huge defects. Examples of these are certain proteases/peptidases that can have important but redundant effects. The specialized proteasome subunits (immunoproteasome & thymoproteasome) are an example. These subunits have been shown to critically influence antigen presentation and T cell development (96-98) but their lack or deficiency can be rescued by components of the constitutive proteasome.

Several limitations affected the number of hits and the nature of the genes that we got from the screen. One of these was the nature of the antigen used for screening. XPT *in vitro* is a very inefficient process, as compared to Classical presentation *in vitro* or XPT *in vivo*. This inefficiency limited us to using magnetic bead conjugated ova, as this form of antigen was the most consistent in *in vitro*

experiments. Because of this, the screen was limited to the P2C pathway of XPT. On the other hand, this might have been a benefit as well, as using antigens that routed through multiple pathways (like cell associated antigen), might encounter redundancy. For instance, knockdown of cytosolic proteases (proteasome) might not greatly affect XPT of cell associated antigen if this antigen can alternatively be processed in the endosomes by Cathepsins.

Besides limiting the nature of the antigen, the assay had to be constrained in 384 well plates with a relatively short assay duration. The use of 384 well plates prevented media exchange or excessive additions of reagents. Thus, we could only work within 48 to 72 hours post siRNA transfection, to prevent media exhaustion or cell overgrowth. This meant that we could not extend the knockdown periods. Therefore, we could expect that genes important to XPT, but had long enough protein half lives might have been missed by the screen.

The very small volumes in 384 well plates also meant that small variations in pipetting volume or even temperature could produce huge effects in well to well variability. In fact, we have experienced this as we observed a significant edge effect while optimizing the screen. We observed decreased XPT from wells near the edges of the 384 well plate regardless of siRNA. Edge effects in high throughput screens have been reported, and these effects were primarily brought about by temperature changes occurring on plate edges (99). The edges of the plate changed temperature more rapidly than the center, and this had effects on cell growth and settling distribution. We did our best to combat these pitfalls

through the use of robotics for pipetting as well as the use of special humidified plate chambers to normalize temperature. However, other factors could have affected our screen, causing several potential candidate genes to fail our threshold tests due to variability between its triplicate wells.

Nevertheless, the candidate genes that did pass our strict thresholds that we chose to follow up on all recapitulated the phenotype when we repeated the experiments in our laboratory, using less constrained methods. These genes only affected XPT and not the Class II pathway, showing that our screen and method of picking gene candidates were robust. These genes are now being characterized by several members of our group.

One cannot truly say that a particular gene is important to XPT based on an siRNA screen alone. In order to do so, the candidate genes need to be further characterized and their mechanism in relation to XPT established. One such gene, the Rab GTPase Rab39a, has been identified by the screen to affect XPT. The characterization of this gene – its nature, mechanism and relevance to XPT is the focus of the next chapter of this dissertation.

CHAPTER II: Rab39a Promotes Crosspresentation Through The Delivery Of ER-Golgi Components To The Nascent Phagosome

I.   Introduction

A. Rationale for Rab39a

Using a genome-wide siRNA screen for genes affecting the XPT and Class II pathways, we have identified Rab39a as having a potential and specific role. We were particularly interested in this candidate because the screen showed that its knockdown only affected XPT, but left Class II presentation intact. Published data (discussed in later sections) showed that Rab39a is localized in endosomes and phagosomes. XPT and the Class II pathway both acquire exogenous antigen similarly, and Rab39a might be able to shed light on how and when these pathways diverge. Another interesting observation was that this gene is primarily expressed in the professional APCs, with the highest expressers being the CD8α⁺ dendritic cells (Immgen) (93).

B. Role of vesicular trafficking and Rab GTPases

The apparent divergence of antigen into the XPT and Class II pathways is still a mystery. The notion of phagosome to cytosol transfer of antigen, which is a requirement for several XPT antigens due to their requirement for proteasome

processing, seems detrimental to the Class II pathway. This is because Class II antigen processing and MHC Class II loading occurs within the phagosomes. Are some antigens routed to XPT while others are sent to the Class II pathway? If so, how and when? Are phagosomes segregated based on what internalization receptor is utilized for entry? Does kinetics and maturation state of the phagosome play a role, wherein early phagosomes are more suitable for XPT while later, more mature ones are used for Class II?

The discovery of Rab39a as a selective hit for XPT led us to look into the role of Rab GTPases and vesicular trafficking. Rab proteins (ras gene from rat brain) are monomeric GTPases that serve as molecular switches that regulate trafficking, fusion and organization of membranes in eukaryotic cells (100). They exist in two forms, a GDP-bound 'inactive' form, and an 'active' form bound to GTP. Upon synthesis Rabs are in the inactive form, and are chaperoned by Rab escort proteins (REP) to geranylgeranyl transferase (GGT). This enzyme modifies the cytosolic tail of the Rab protein, allowing it to be membrane bound. Targeting to their cognate membranes is then mediated by Rab GDP dissociation inhibitors (GDI) and GDI displacement factors (GDF). Membrane bound inactive Rabs are then activated by guanine nucleotide exchange factors (GEF), switching the bound GDP for GTP. This activation causes a conformational change on the Rab protein, allowing it to bind specific effectors to mediate its function. Examples of these effectors include motor adaptors, that permit trafficking of Rab bound vesicles along the cytoskeletal track. Other effectors are

tethering proteins, that stabilize opposing membranes with t- and v- SNARES (SNAP (soluble NSF attachment protein) receptor) and prepare them for fusion. Once its work is done, Rab proteins are inactivated by GTPase activating proteins (GAP) – returning the Rab to its original GDP bound state for recycling.

Recently, a variety of Rabs have been implicated in the regulation of XPT. Rab11a, first implicated in the recycling of MHC-I (69), has been shown to cause accumulation of Class I molecules in a distinct intracellular compartment (71). These Class I molecules are then shuttled to phagosomes containing TLR4 ligands. It has been proposed that this intracellular pool can be the source of Class I molecules utilized by XPT, particularly during phagosomal loading in the phagosome-cytosol-phagosome and vacuolar pathways. A similar phenotype has been observed with Rab22a, wherein its knockdown caused a decrease in the recycling and intracellular pool of Class I (68). Rab3b/3c, identified in an siRNA screen of Rabs affecting XPT by DCs, has been proposed to be involved in exocytosis of recycled Class I (67). Rab14 positive endosomes have been associated with Insulin Responsive Aminopeptidase (IRAP), which trims peptides in the phagosomes. Rab27a regulates recruitment of NADPH oxidase (NOX2), to dendritic cell phagosomes. NOX2 modulates phagosomal pH and prevents extensive antigen degradation and loss, thereby increasing DC XPT capability (101). In Rab43 knockout mice, XPT of cell associated antigen is defective specifically in CD8α^+ dendritic cells (91). This might be due to its role in Cathepsin D delivery, which can aid in peptide generation (102).

C. Background on Rab39a

Rab39 was first described after having been isolated from a human dendritic cell cDNA library (103). It was found to colocalize with the golgi apparatus, and overexpression increased endocytosis by HeLa cells.

Further advances in the field has shown that while Rab39 is conserved in most metazoans, there are in fact 2 isoforms (in this case, a Rab of similar protein sequence) of the gene in mouse and humans (104). Rab39a localizes at the periphery of Lamp2 positive vesicles, while Rab39b is golgi localized (105). Rab39a has been reported to bind Caspase-1 and mediate IL-1β release in thymocytes (106). It has also been shown to downregulate LPS-mediated autophagy by macrophages (105). Rab39b on the other hand, is involved in neurite morphology and has been linked to X-linked mental retardation (107).

In the field of immunology, Rab39a has been shown to be utilized by the immune response against pathogens (102) as well as being utilized by the pathogens themselves (108). In macrophages fed with *S.aureus* or *M.tuberculosis*, Rab39a is recruited to late phagosomes (peaking at 1 hour post phagocytosis). Overexpression of the dominant negative form of Rab39a led to a decrease in phagosome staining by Lysotracker dye, implying that it plays a role in host defence through phagosome acidification. *Chlamydia* has been shown to recruit Rab39a to its inclusions (108). It has been proposed to mediate delivery of

multivesicular bodies and sphingolipids to the parasite inclusion to facilitate its growth.

Our work sheds light on a new role of Rab39a in the immune response. Here we show that Rab39a specifically promotes XPT, while having no effect on both the Classical Class I and the Class II pathways. We propose that Rab39a achieves this by facilitating transport of ER-golgi derived cargo to phagosomes. This cargo includes Sec22b, as well as components of the peptide-loading complex such as TAP and open forms of MHC-I. In accordance to published reports on Sec22b, this delivery also facilitates a downregulation in phagosomal antigen degradation (59), which can possibly aid in antigen persistence. An interesting finding of this work shows that Rab39a expression leads to an accumulation of peptide receptive MHC Class I molecules in the phagosome – possibly shedding a light on the source and nature of the Class I molecule used for XPT.

II. Materials and Methods

A. Chapter I Protocols

Parts of Chapter 2 utilized the same experiments as those in Chapter I. The detailed protocols for them can be found in that Chapter. Modifications of the protocols are detailed below. For reference, the protocols that can be found in Chapter 1 are:

Cell lines and culture conditions

Lentiviral transduction of Dendritic Cell
Lines

SiRNA transfections

Antigen presentation assay

B. Cell terminology

Various cell lines have been used in this study. Cell creation and detailed cell properties are discussed in other sections of Materials and Methods. Here is a list of cells and a summary of their properties:

Cell name	Property
DC2.4	Dendritic cell line
DC3.2	Dendritic cell line similar to DC2.4 but with high levels of MHC Class II
DC3.2R	DC3.2 cell line expressing Renilla Luciferase. Cloned for high XPT and Class II ability
DC3.2-Rab39aKO	DC3.2 cells where Rab39a was knocked out with CRISPR
DC3.2-Rab39aKO-Rab39a	A doxycycline inducible Rab39a construct was transduced into the knockout cells
DC3.2-Rab39aKO-Rab39a-L^d	H2-L^d was transduced in the above cell
DC3.2-Rab39aKO-Rab39a(DN)	A doxycycline inducible Rab39a dominant negative construct was transduced into the knockout cells

DC3.2-Rab39aKO-Rab39a(CA)	A doxycycline inducible Rab39a constitutively active construct was transduced into the knockout cells
RF33.70	CD8$^+$ T cell hybridoma recognizing SIINFEKL on H2-K^b
RF33-Luc	RF33.70 that expresses Firefly luciferase upon activation via TCR
MF2-2D9	CD4$^+$ T cell hybridoma recognizing ISQAVHAAHAEINEAGR on I-A^b
MF2-Luc	MF2-2D9 that expresses Firefly luciferase upon activation via TCR
12.64-Luc	CD8$^+$ T cell hybridoma recognizing the ASNENMETM peptide of the influenza peptide NP366. Expresses Firefly luciferase upon activation via TCR
DC3.2 NSova	DC3.2 cells transduced with a doxycycline inducible cytosolic ovalbumin
DC3.2 UbS8L	DC3.2 cells transduced with a doxycycline inducible SIINFEKL

conjugated to the C-terminus of

Ubiquitin

C. Additional cell lines used in this study

i. DC3.2 NSova and DC3.2 UbS8L

DC3.2 NSova is a variant of DC3.2 (see Chapter I) that expresses a non-secreted form of ovalbumin upon induction with doxycycline. The gene for chicken ovalbumin (109) was amplified without the first 50 amino acids, replacing it with a methionine. The insert was put into the Age-I Mlu-I sites of pTRIPZ (Open Biosystems) for lentiviral production and transduction of DC3.2. pTRIPZ contains the tet on promoter system allowing dox inducible expression of cloned genes.

DC3.2 UbS8L is another doxycycline inducible cell line. This line expresses the SIINFEKL peptide fused to the C-terminus of Ubiquitin. The Ubiquitin-S8L construct (110, 111) was PCR amplified and inserted into the above listed lentiviral vector.

ii. 12.64-Luc T cell Hybridoma

12.64 is a CD8$^+$ T cell hybridoma recognizing the ASNENMETM peptide of the influenza peptide NP366 (86). This hybridoma was also transduced with the NFAT-Luciferase construct similarly to RF33-Luc and MF2-Luc (see Chapter I). The 12.64-luc cell was made by D. Farfan (96).

D. Antibodies

The following antibodies were used: H2-K^b (Af6-88.5, BD biosciences) I-A/I-E (M5/114.15.2, BD biosciences), Lamp1 (1d4B, Bd biosciences), Lamp2 (abl-93, abcam) ovalbumin (ova-14, Sigma-Aldrich), mouse IgG1 anti HA-tag (6E2, Cell Signaling), rabbit anti HA-tag (C29F4, Cell Signaling), H2-L^d closed conformer (30-5-7s, Thermo Scientific) Sec22b (rabbit polyclonal, Synaptic Systems), TAP1 (B-8, Santa Cruz Biotech), Mouse anti actin (C-4, Santa Cruz) . The antibody for H2-L^d open conformers (64-3-7) was generated by Dr. Clifford Harding (Case Western Reserve University) and is a gift from Dr. Xiaoli Wang (Washington University, St Louis MO). Fluorescently labelled secondary antibodies (goat anti mouse IgG2a, goat anti mouse IgG2b, goat anti mouse IgG1, goat anti mouse IgG, Donkey anti rabbit IgG) were purchased from Thermo Scientific. HRP conjugated secondary antibodies were purchased from Jackson Immunoresearch.

E. Quantitative PCR

After siRNA treatment of cells, total RNA was extracted using RNeasy Mini Kit (Qiagen) according to manufacturer instructions. Quantitative PCR was performed using Luna Universal One-Step RT-qPCR kit in a Bio-Rad CFX96 cycler. HPRT was used as housekeeping control and relative expression were calculated using $\Delta\Delta C_T$ method. The primers used were HPRT (5'-AGGGATTTGAATCACGTTTG-3' and 5'-TTTACTGGCAACATCAACAG-3'),

Rab39a (5'-CGCTTCAGATCAATAACTCG-3' and 5'-

TGTCCCACCAGTAGAAATAC-3') Rab39b (5'-

GGATACAGCGGGTCAAGAGAGG -3' and 5'-

GTTGGTAATGTCAAATAAGAGAAGAC -3'). Primers for Rab39b were derived

from a previous work (107).

F. Antigen presentation assay

The protocol antigen presentation can be found in Chapter I. Some

experiments in this Chapter make use of different antigen concentrations and

different forms of antigen. These are detailed within the figures. Detailed below

are new forms of antigen we used in this Chapter, not found in Chapter I.

i. Peptide beads

Peptide beads are biomag beads conjugated to various peptides via a

disulfide bond.

All peptides were custom made to >98% purity (Genscript). For bead

conjugation, biomag Amine beads were reacted with SPDP (succinimidyl 3-(2-

pyridyldithio)propionate) (Thermo Scientific) according to manufacturer

instructions. 1 mg of lyophilized cysteine containing peptides were dissolved in

DMSO and added 1:1 with PBS to SPDP-activated beads for overnight

incubation at room temperature. Peptide-bound beads were extensively washed with PBS.

As a control, full length ovalbumin (Sigma-Aldrich) was also conjugated to biomag beads via a disulfide bond rather than the previously used glutaraldehyde method. To do this, 1 mg/ml ova was prepared in PBS with 2 mM EDTA (Thermo Scientific). In a separate tube, 2 mg/ml of Traut's reagent (Thermo Scientific) was prepared in PBS-EDTA. 10 µl of Traut's solution were added to 1 ml of ova, and the solution was rotated for 1 hour at room temperature to convert some of the ova amine groups to sulfydryls. After incubation, the ova solution was mixed with SPDP-modified biomag beads, rotated overnight and extensively washed.

ii. Latex-ova beads

Latex-ova beads are polystyrene beads covalently conjugated to ovalbumin.

1 µm polystyrene latex (amine group modified) beads were purchased from Bangs Laboratories. Beads were washed with PBS and incubated with 10% glutaraldehyde (Thermo Scientific) for 2 hours. Beads were washed twice with PBS and incubated with 5 mg/ml of ovalbumin in PBS overnight. Beads were then washed and resuspended in PBS.

iii. Antigen-expressing Bacteria

*This protocol was designed and performed by Jeff Colbert, UMASS Medical School.

E.Coli (BL21 strain) expressing GST-peptide fusion proteins (GST-ASNENMETM or GST-SIINFEKL cloned into vector pGEX-6P) were cultured in LB+ampilicillin medium overnight. OD_{600} was adjusted to 0.1 in new LB medium containing 0.5mM IPTG. Cultures were then grown from 4-6 hrs at 30°C to an OD_{600} of 1.0. Bacteria were washed 3x by centrifugation in PBS and resuspended in 1ml PBS following the last wash. E.coli expressing GST-fusion proteins were heat inactivated by incubating cells at 70°C for 50 min vortexing bacteria every 15 min. Inactivation of bacteria was confirmed by plating cells on LB-agar plates overnight. Heat inactivated bacteria was resuspended in PBS at $1X10^8$ cfu/ml. Bacterial cell numbers were determined on live bacteria by counting colonies of serially diluted bacteria grown overnight on LB agar plates with amplicillin. Colony numbers were calculated from the OD_{600} of the original stock culture. E.coli expressing GST-fusion proteins grown to an OD_{600} of 1.0 were shown to correlate to $12.5X10^6$ bacteria/ml. Heat inactivated bacteria were cultured with DCs and peptide-specific T cell hybridoma overnight at 37°C. T cell activation was determined based the luciferase reporter assay as described.

G. Assaying the Classical Pathway with NSova and UbS8L

In a 384 well plate, 30 µl of DC3.2 NSova and DC3.2 UbS8L cells were plated at the indicated cell numbers in media with the indicated amount of doxycline. After a period of time (depending on the experiment), 20 µl of reporter T cells (corresponding to 1:1 ratio with DCs) were added along with a final concentration of 1:1000 brefeldin A (Golgiplug, BD). Brefeldin A stops further egress of H2-K^b – SIINFEKL to the surface, thereby allowing titration of peptide-MHC expression. The cells were incubated overnight and luciferase expression of the T cells was measured.

H. Creation of Rab39a CRISPR knockout cells (DC3.2-Rab39aKO)

Rab39a was knocked out at the genomic level using CRISPR. The target sequence was elucidated using an algorithm as presented (112). The guide sequence of gtgatcggagactccacggt was chosen because it had an endogenous restriction site (BtgI) within the CRISPR cutting site. This allowed screening of clones via restriction enzyme digestion. Guide sequence was inserted into CRISPR plasmid pX330-U6-Chimeric_BB-CBh-hSpCas9 (Addgene plasmid #42230) (113). A gfp construct was PCR amplified from pEGFP-N1 (Clontech) and inserted within the Nar1 site of the CRISPR plasmid.

$2x10^6$ DC3.2 were electroporated with 2 µg of the CRISPR construct using Amaxa nucleofector II with program T-030 and Cell Line Nucleofector Kit V. Cells

were allowed to recover overnight in HCM. GFP expressing cells were flow sorted into 96-well plates at 1 cell per well (UMASS Medical School Flow Cytometry Core Facility).

The sorted DC clones were screened by DNA sequencing. DNA from clones were extracted using DNeasy Blood and Tissue Kit (Qiagen). A region of Rab39a containing the CRISPR target site was PCR amplified using primers 5'AGGTGCTGAAGGGACAGTTC3' and 5'AAACTGCGGAGGAGGAAGTC3'. PCR products were screened by cutting with BtgI (New England Biolabs). Successful mutations generated by CRISPR would have destroyed this cutting site. PCR clones that resisted digestion were cloned into PCR2.1-TOPO (Invitrogen) according to manufacturer instructions. For every dendritic cell clone, 10 bacterial clones were sequenced to check mutations in the CRISPR target site. Clones that showed exactly 2 different mutations (which indicated that both alleles of the gene were mutated) were chosen.

The generated cell was called DC3.2-Rab39aKO.

I. **Rab39a rescue on knockout cells (DC3.2-Rab39KO-Rab39a)**

For Rab39a rescue experiments, a Rab39a CRISPR clone of DC3.2 was transduced with a lentiviral vector containing doxycycline inducible Rab39a. The cDNA for Rab39a was amplified from C57BL/6 cDNA, with an HA tag added on the N-terminus. This construct was inserted within the Age1 – Mlu1 sites of the

plasmid pTRIPZ (GE Dharmacon). Lentivirus production and DC transduction was performed as described. Selection was done at 5 µg/ml puromycin. Knockout cells were rescued with Rab39a by adding 1 µg/ml doxycycline (Sigma Aldrich).

Western blot was performed to determine expression levels and inducibility of the transduced Rab39a (HA-tag).

The generated cell was called DC3.2-Rab39aKO-Rab39a.

Some experiments necessitated the need for the Class I molecule H2-L^d. H2-L^d was PCR cloned and inserted into the lentiviral vector pCDH1-CMV-SV40-Bsd. DC3.2-Rab39aKO-Rab39a was transduced using this lentiviral construct.

These cells were called DC3.2-Rab39aKO-Rab39a-L^d

To generate GDP (DN) and GTP-locked (CA) Rab39a mutants, mutations were generated via pcr using primers as described (102). The DN form of Rab39a has an S22N mutation while the CA form has Q72L.The mutant constructs were cloned into lentivirus vectors and transduced into DC3.2-Rab39KO cells.

The generated cells were called DC3.2-Rab39aKO-Rab39a(DN) and DC3.2-Rab39aKO-Rab39a(CA).

J. pH and DQ ova assay

i. Beads for assaying protein degradation and pH

DQ-ovalbumin (Thermo Scientific) was conjugated to Compel 6 μm COOH modified beads (Bangs Laboratories) using 1-ethyl-3-[3-dimethylaminopropyl]carbodiimide hydrochloride (EDC) (Thermo Scientific) following manufacturer instructions. 1 mg of DQ-ovalbumin was conjugated to 200 μl stock beads.

To make pH sensor beads, the pH sensor dye pHrodo (Thermo Scientific) was conjugated to 1 μm latex or Compel 6 μm COOH modified beads. For latex beads, 500 μg of pHrodo Green STP Ester was mixed with 100 μl of stock beads to make a final volume of 500 μl in PBS. The mixture was rotated overnight and washed extensively with PBS. For 6 μm COOH beads, Lysine was conjugated to 200 μl Compel beads using EDC. After extensive washing with PBS, 500 μg of pHrodo Green STP Ester was bound following manufacturer instructions.

ii. Ova degradation and pH assay

To assay for overall ova degradation, dendritic cells were fed with DQ-ova beads at 1 bead per cell for the listed number of hours. Uneaten beads were washed off with PBS and the cells were detached with Versene (Thermo Scientific). Cells were resuspended in 1% FCS in PBS for flow cytometric analysis.

To assay for overall phagosomal pH, dendritic cells were fed with pHrodo beads at 1 bead per cell for the listed number of hours. Uneaten beads were washed off with PBS and the cells were detached with Versene (Thermo Scientific). Cells were resuspended in 1% FCS in PBS for flow cytometric analysis. In some cases, cells were treated with 25 nM bafilomycin A1 (Sigma-Aldrich) during the feeding period.

K. Staining and Confocal microscopy

i. Fixed cell microscopy

For fixed cell imaging, cells were grown in coverslips overnight. The next day, cells were washed and fixed with 4% PFA for 10 minutes. Cells were permeabilized and stained in 0.25% saponin, 1% BSA in PBS and mounted in ProLong Antifade (Thermo Scientific). Cells were imaged under a Leica TCS SP5 confocal microscope. Image analysis and processing were done in ImageJ software.

ii. Live cell microscopy

For live cell imaging, DC3.2-Rab39aKO cells were transduced with lentivirus containing inducible Rab39a (see previous protocol) fused with an N-terminal mcherry construct. Cells were grown to 70% confluency in 7mm glass bottom dishes (MatTek Corporation) with 1 µg/ml doxycycline overnight. The next day, cells were fed with 3 µm polystyrene beads (Bangs Laboratories) for 2

hours. Cells were imaged live under a Leica TCS SP5 confocal microscope. Image analysis and processing were done in ImageJ software.

L. Phagosome Flow Cytometry (PhagoFACS)

i. C6-biotin

To make biotinylated 6 µm magnetic beads, COMPEL COOH (Bangs Laboratories) were conjugated to Biotin Hydrazide (Covachem) using EDC (Thermo Scientfic).

ii. C6-ova biotin

To make biotinylated ova beads, COMPEL COOH beads were conjugated with ovalbumin (Sigma Aldrich) using EDC. After extensive washing, beads were conjugated to Biotin-NHS (Thermo Scientific) using manufacturer instructions.

iii. Phagosome Preparation and Flow Cytometry (PhagoFACS)

Dendritic cells were plated with or without 1µg/ml doxycycline for 24 or 48 hours in tissue culture plates (12 well or 6 well). After 1-2 days, cells were about 75% confluent. Media was replaced and dendritic cells were fed with the appropriate number and type of biotinylated beads depending on the experiment. Phagocytosis was done at 37ºC in a 10% CO_2 incubator at the listed time point. Cells were then washed with PBS and detached with room temperature Versene

for 5 minutes. Cells were spun down at 180xg using a swinging bucket centrifuge and resuspended in 1% FCS in ice cold PBS.

Uneaten or surface-bound beads were first stained by incubating cells in 6.4 µg/ml of Streptavidin Pacific Blue or Orange (Thermo Scientific) in 1% FCS-PBS for 10 mins on ice. Cells were then washed in 1% FCS-PBS. Cells were then resuspended in ice cold homogenization buffer (HB) containing 250 mM sucrose, 10 mM $CaCl_2$ with 1X HALT EDTA free protease inhibitor (Thermo Scientific). Cell disruption was performed in a 0.3 ml dounce homogenizer (Kimble Chase) using the tight fitting "B" pestle. The extent of homogenization was observed under a microscope and cells were dounced to at least 50% lysis while minimizing disruption of the nucleus. Phagosomes were extracted magnetically.

To stain ruptured phagosomes, phagosomes were washed in Wash Buffer (1% BSA in PBS) and stained once again with streptavidin pacific blue/orange for 10 minutes. After extensive washing, phagosomes were fixed in 2% paraformaldehyde for 20 minutes or directly permeabilized and stained.

For staining, the isolated magnetic bead phagosomes were incubated for 10 minutes in Perm Buffer (1% BSA in PBS with 0.25% saponin). Phagosomes were stained with the indicated antibodies. For FACS analysis, phagosomes were resuspended in wash buffer.

For flow cytometric analysis of phagosomes, events were gated according to the FSC and SSC of plain magnetic beads as well as the lack of Pacific Blue/Orange staining.

iv. Peptide loading of phagosomes

Isolated, unfixed phagosomes were permeabilized in ice cold Perm Buffer supplemented with 1X HALT protease inhibitor (Thermo Scientific). Peptide was added (nature and concertation was dependent on the experiment) and the mixture was rotated at room temperature for 3-4 hours. The phagosomes were washed extensively in Perm Buffer before staining for FACS analysis.

III. Results

A. Lack of Rab39a inhibits crosspresentation

Before characterizing the role of Rab39a in XPT, we sought to validate the primary screen and siRNA deconvolution phenotype observed for Rab39a.

To do this, we transfected DC3.2R with either the smartpool (mixtures of 4 different oligos against the same gene) or individual siRNA sequences targeting Rab39a. The transfected cells were then fed with biomag-ova (ova conjugated to magnetic iron oxide beads) and exposed to reporter CD8$^+$ T cells (RF33-Luc). The use of smartpool and individual oligos was done to determine if the phenotype previously observed in the siRNA screen was due to siRNA artifacts

or to a specific requirement for Rab39a in XPT. Smartpool siRNA is primarily

used to mitigate the off-target effects of each individual oligo through dilution (1/4

of final concentration), while keeping their effects on the intended target intact.

However, we also tested the effects of the individual oligos, to make sure that the

majority of the smartpool components were able to produce the phenotype. Both

the smartpool (Figure 7), and all individual siRNAs (Figure 8) against Rab39a

decreased XPT.

crosspresentation of biomag-ova

Figure caption:

Figure 7. **Rab39a sirna reduces crosspresentation of biomag-ova.**

2.5 x10^3 DC3.2R cells were transfected with 50 nM sirna pools using Lipofectamine RNAiMax. After 48 hours, 1 x 10^4 Rf33-Luc cells were added along with the indicated amounts of biomag ova. After overnight incubation (~18 hours), Luciferase activity of the T cells were read using Oneglo reagent (Promega). Error bars indicate the standard deviation between triplicate wells. Data shown represents one experiment of $\geq$3. For all wells with antigen, all p-values (ANOVA) between Rab39a or β2m vs that of I-Ab are $\leq$0.05.

Figure 8. **The effects of individual Rab39a sirna on crosspresentation.**
2.5 x10^3 DC3.2R cells were transfected with 50 nM sirna pools or individual oligos using Lipofectamine RNAiMax. After 48 hours, 1 x 10^4 RF33-Luc cells were added along with biomag beads (4 µg of ova). After overnight incubation (~18 hours), Luciferase activity of the T cells was read using Oneglo reagent (Promega). *Rab39a-01 to 04 are the individual oligos that comprise the smartpool. Error bars indicate the standard deviation between triplicate wells. Data shown represents one experiment of $\geq$3. Using I-Ab as negative control, all siRNA treatments are p$\leq$0.05 using ANOVA.

Similar to magnetic bead particles, Rab39a knockdown also inhibited XPT from OVA-latex beads, another form of antigen substrate that utilizes the P2C2E and P2C2P pathways (Figure 9). Though inherently less efficient than XPT of particulate antigen, the cell lines we used were also capable of presenting soluble ova, though only at very high protein concentrations. Nevertheless, Rab39a was still required for efficient XPT of this form of antigen (Figure 10).
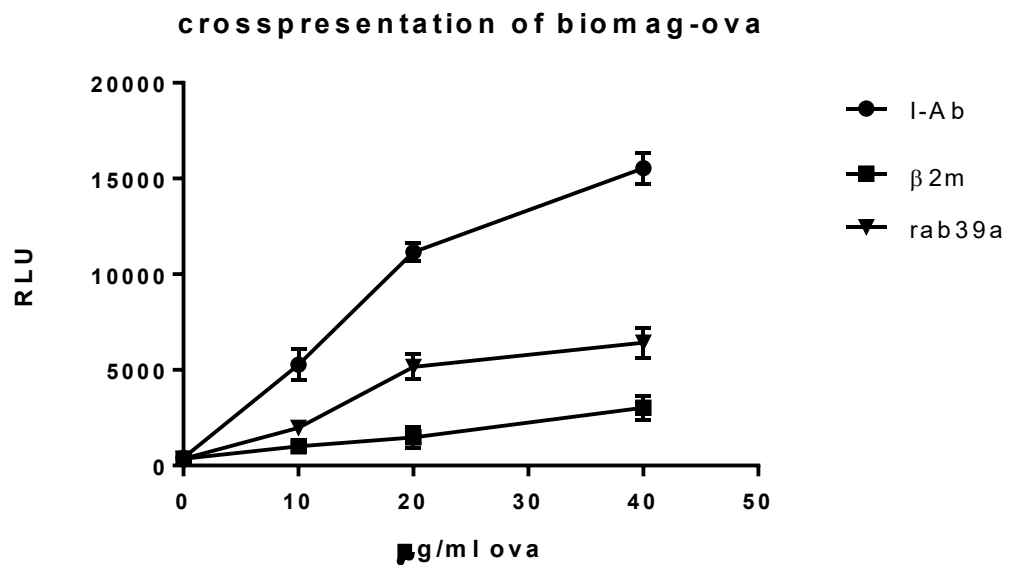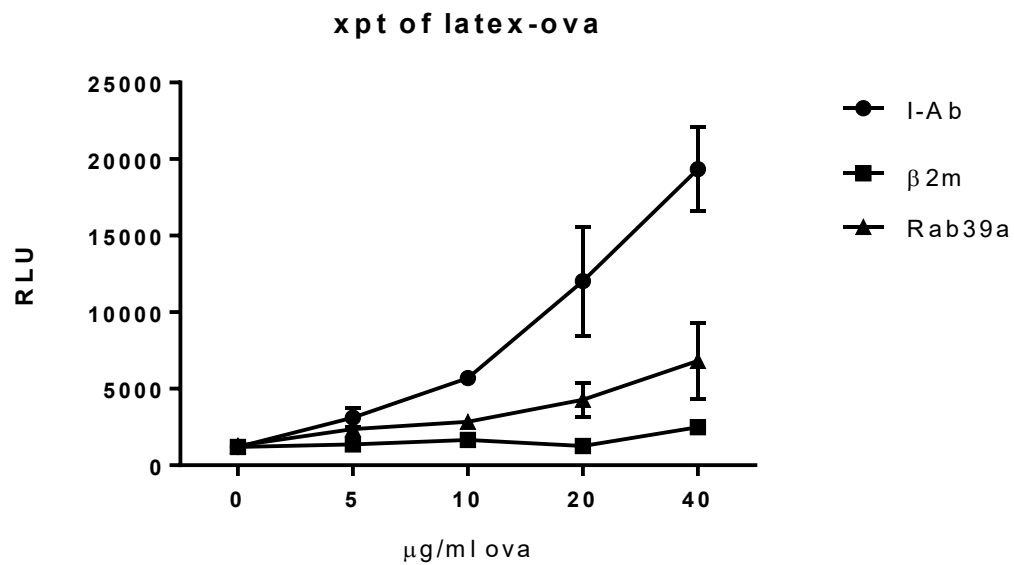
Figure 9. **Rab39a affects crosspresentation of latex ova.**

2.5 x10³ DC3.2R cells were transfected with 50 nM sirna pools using Lipofectamine RNAiMax. After 48 hours, 1 x 10⁴ Rf33-Luc cells were added along with the indicated amounts of latex ova. After overnight incubation (~18 hours), Luciferase activity of the T cells were read using Oneglo reagent (Promega). Error bars indicate the standard deviation between triplicate wells. Data shown represents one experiment of $\geq$ 3. For all wells with $\geq$ 5 µg/ml antigen, all p-values (ANOVA) between Rab39a or β2m vs that of I-Ab are $\leq$0.05.
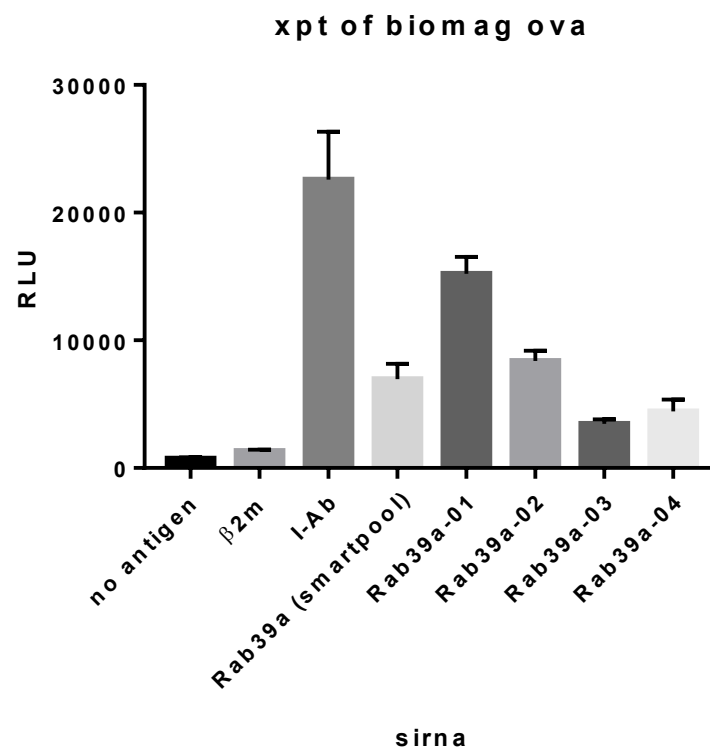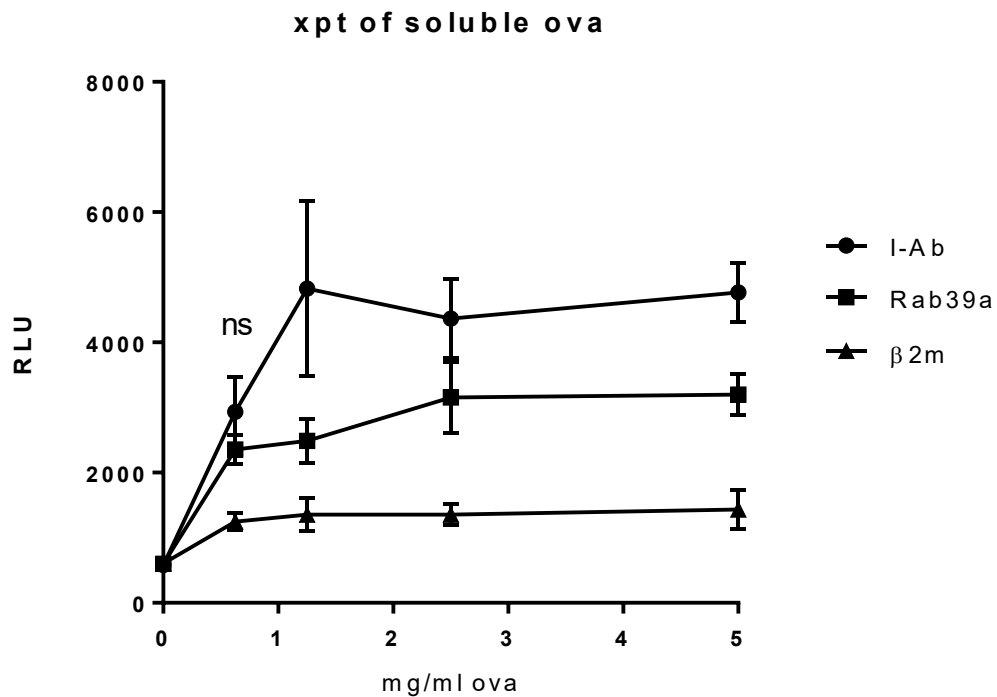
xpt of soluble ova

Figure 10. **Rab39a sirna affects crosspresentation of soluble ova.**
2.5 x10³ DC3.2R cells were transfected with 50 nM sirna using Lipofectamine
RNAiMax. After 48 hours, 1 x 10⁴ Rf33-Luc cells were added along with the
indicated concentrations of ova. After overnight incubation (~18 hours),
Luciferase activity of the T cells were read using Oneglo reagent (Promega).
For all wells with ≥ 1.25 mg/ml antigen, all p-values (ANOVA) between Rab39a
or β2m vs that of I-Ab are ≤0.05.

We also confirmed the necessity of Rab39a for XPT by generating a conditional Rab39a knockout dendritic cell. Rab39a was knocked out at the genetic level using CRISPR. This was done to further confirm that the phenotype observed in the siRNA experiments was not due to siRNA off-target effects. The generated cell line showed that both alleles of the Rab39a gene were mutated, thereby causing frameshifts that prevented the proper expression of full length Rab39a (Figure 11). To this knockout cell, we transduced in an HA-tagged doxycycline inducible Rab39a construct. Thus, we were able to "rescue" expression of Rab39a in knockout cells through the addition of doxycycline (Figure 12). XPT of biomag-ova was enhanced upon rescue with Rab39a, confirming our previous siRNA knockdown experiments (Figure 13). Interestingly, the knockout cells were still capable of XPT, which suggested that either Rab39a was not absolutely essential for XPT of this form of antigen or there were compensation mechanisms that occurred in long term Rab39a knockouts (as opposed to short term knockdowns with siRNA).

Through two different assays – that of siRNA knockdown and a full knockout with CRISPR, we were able to show that efficiency of XPT was enhanced by the presence of Rab39a, and this phenotype was not due to artifact that might arise from siRNA experiments.

Figure 11. **DNA sequence of DC3.2 Rab39a CRISPR cells.**
Rab39a was knocked out using CRISPR and a DC clone was isolated (DC3.2-Rab39aKO). A region of DNA corresponding to the CRISPR target site for Rab39a was amplified through PCR, cloned into TOPO vector and transformed into *E.coli*. Several bacterial clones were sequenced and compared to wt Rab39a. The figure shows two different mutations (1 base and 2 base deletion) corresponding to both alleles of the Rab39a gene. Alignment done with Multalin (http://multalin.toulouse.inra.fr/multalin/)

No dox   1 µg/ml dox

24 h   48 h   72 h   time

HA-tag

β-actin
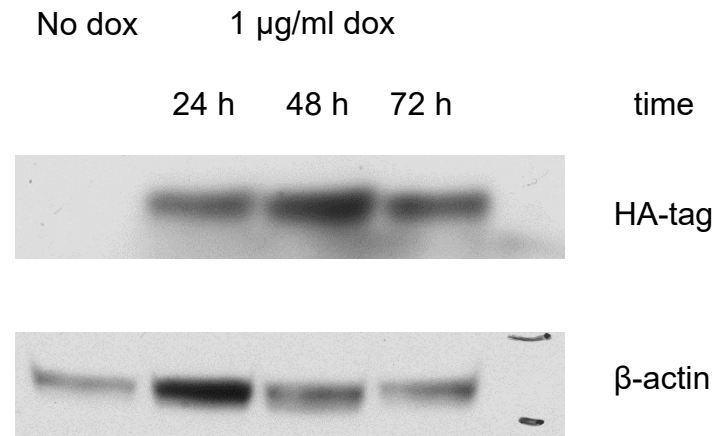
Figure 12. HA-tagged Rab39a is used to rescue Rab39a CRISPR DCs.
A doxycycline inducible construct of Rab39a (N-terminal HA-tagged) was lentivirally transduced into the generated Rab39a knockout DC (DC3.2-Rab39aKO) to generate rescuable cells (DC3.2-Rab39aKO-Rab39a). After puromycin selection, $5x10^5$ cells were plated in 6 well plates with the indicated amount of doxycycline at the indicated amounts of time. Cells were harvested and lysed with RIPA buffer then run in a Western Blot. Data shown represents one experiment of 2.
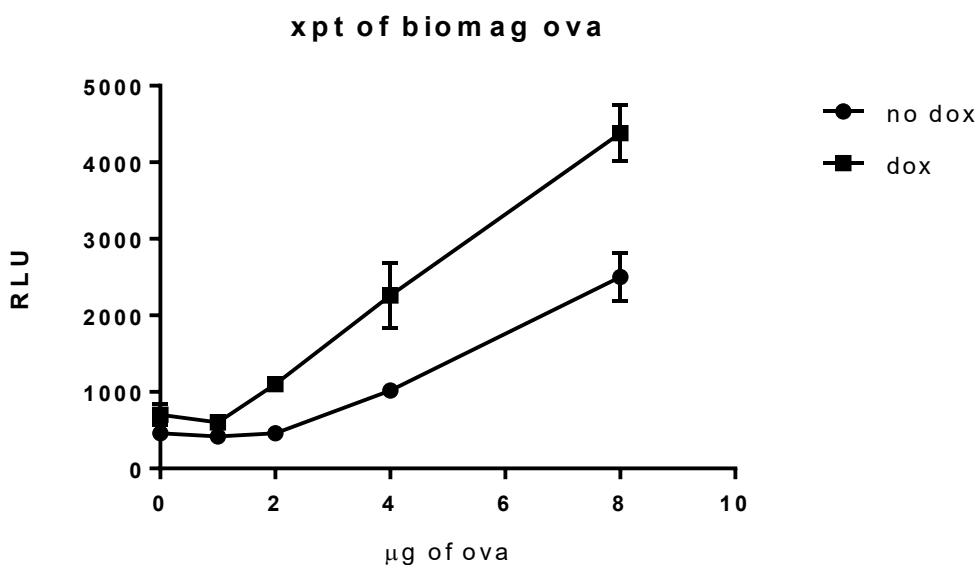
Figure 13. Rab39a rescue of knockout DCs increases crosspresentation.
1.25×10^4 DC3.2-Rab39aKO-Rab39a cells were incubated with 1 µg/ml dox for 48 hours in a 96 well plate. Then, the indicated amounts of biomag-ova beads were added along with 5×10^4 Rf33-Luc. After overnight incubation, luciferase activity from the T cells were quantified using Oneglo reagent (Promega). Error bars indicate the standard deviation between triplicate wells. Data shown represents one experiment of ≥ 3. P-values (ANOVA) at 2 µg ova and beyond are ≤ 0.05.

B. Silencing Rab39a does not inhibit Class II presentation

Next, we sought to confirm the selectivity of Rab39a for XPT by assaying for its effect on Class II presentation. The siRNA experiment was performed as discussed above but this time, the DCs were exposed to reporter CD4$^+$ T cells (MF2-Luc).

Treatment of cells with Rab39a smartpool siRNA did not inhibit the Class II pathway when using biomag-ova (Figure 14), latex -ova (Figure 15) or soluble ova (Figure 16). In some cases, a slight increase in Class II presentation was observed (data not shown). Rab39a knockdown did not affect Class II presentation across the entire antigen dose range. This showed that the lack of inhibition of Class II presentation was not due to antigen saturation.

For the individual oligos, 2 out of 4 caused a decrease in Class II presentation (Figure 17). It is in this case that the smartpool data proved important. Because dilution of the individual oligos to a 4th of their original concentration (in a smartpool) abolished their Class II effect, the observed phenotype was probably due to off-target effects of these particular oligos.

This off-target effect on the Class II pathway was confirmed using Rab39a knockout cells. When these knockout cells were rescued through doxycycline induction of Rab39a, there was little to no effect on Class II presentation (Figure 18).
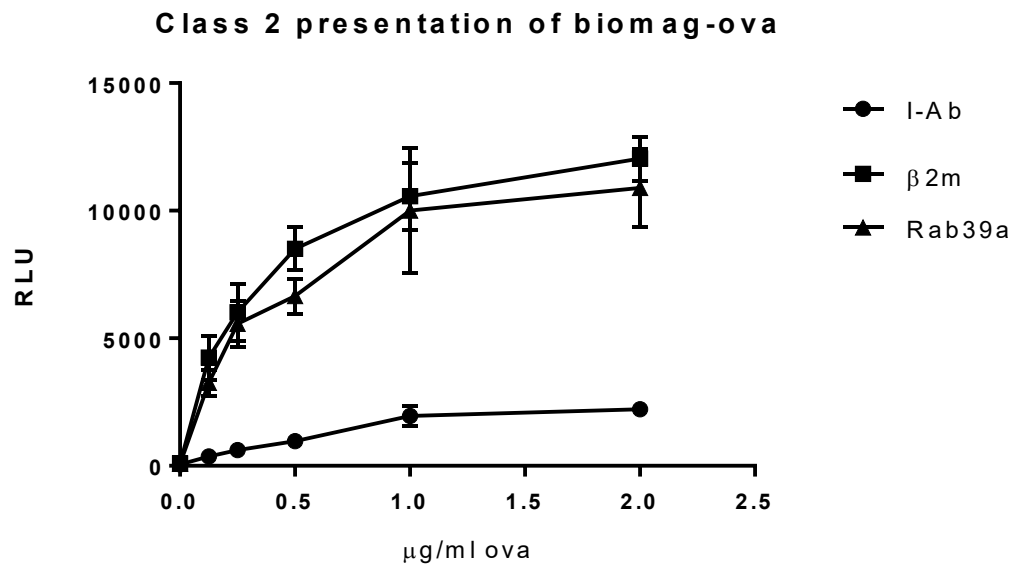
Figure 14. **Rab39a sirna does not reduce Class II presentation of biomag-ova.**

2.5 x10^3 DC3.2R cells were transfected with 50 nM sirna pools using Lipofectamine RNAiMax. After 48 hours, 1 x 10^4 MF2-Luc cells were added along with the indicated amounts of biomag ova. After overnight incubation (~18 hours), Luciferase activity of the T cells were read using Oneglo reagent (Promega). Error bars indicate the standard deviation between triplicate wells. Data shown represents one experiment of $\geq$ 3. For all wells with antigen, all p-values (ANOVA) between Rab39a vs that of β2m are > 0.05. For I-Ab vs β2m, all are p $\leq$ 0.05 for wells with antigen.
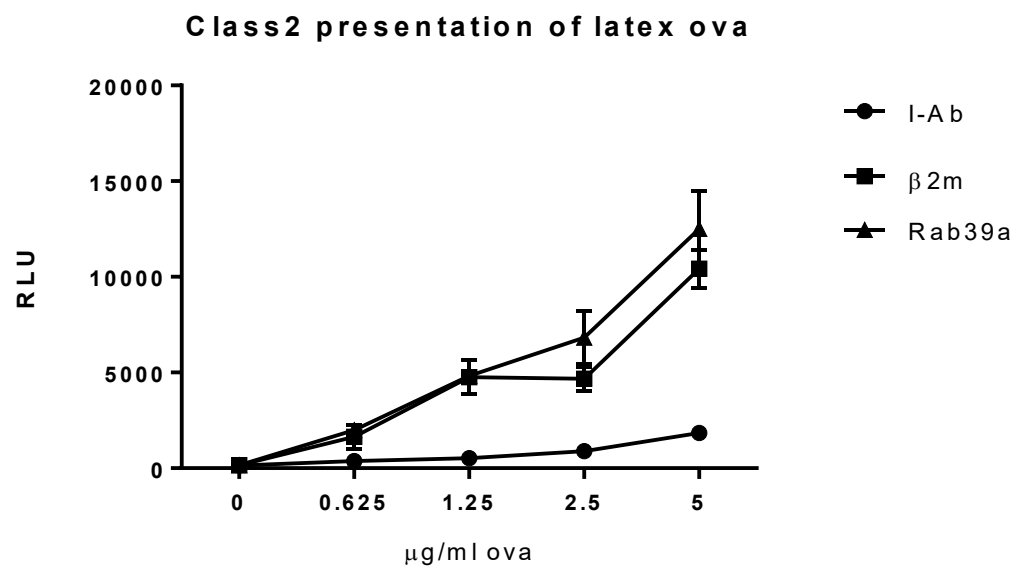
Figure 15. **Rab39a does not affect Class II presentation of latex ova.**
2.5 x10^3 DC3.2R cells were transfected with 50 nM sirna pools using
Lipofectamine RNAiMax. After 48 hours, 1 x 10^4 Mf2-Luc cells were added along
with the indicated amounts of latex ova. After overnight incubation (~18 hours),
Luciferase activity of the T cells were read using Oneglo reagent (Promega).
Error bars indicate the standard deviation between triplicate wells. Data shown
represents one experiment of $\geq$ 3. For all wells with antigen, all p-values
(ANOVA) between Rab39a vs that of β2m are > 0.05. For I-Ab vs β2m, all are
p $\leq$ 0.05 for wells with antigen.

Class 2 presentation of soluble ova
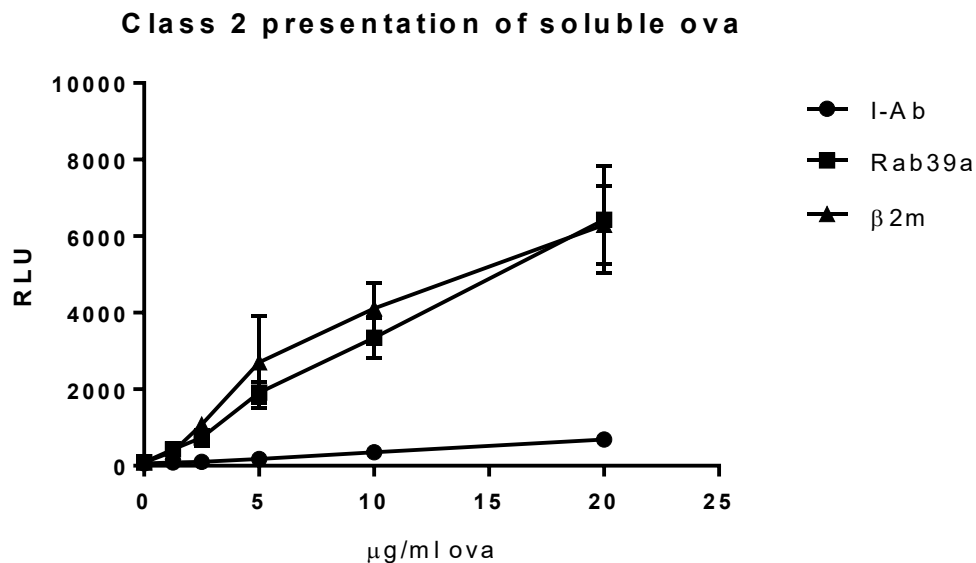
Figure 16. **Rab39a sirna does not affect Class II presentation of soluble ova.**

2.5 x10^3 DC3.2R cells were transfected with 50 nM sirna using Lipofectamine RNAiMax. After 48 hours, 1 x 10^4 MF2-Luc cells were added along with the indicated concentrations of ova. After overnight incubation (~18 hours), Luciferase activity of the T cells were read using Oneglo reagent (Promega). Error bars indicate the standard deviation between triplicate wells. Data shown represents one experiment of $\geq$ 3. For all wells with antigen, all p-values (ANOVA) between Rab39a vs that of β2m are > 0.05. For I-Ab vs β2m, all are p $\leq$ 0.05 for wells with antigen.
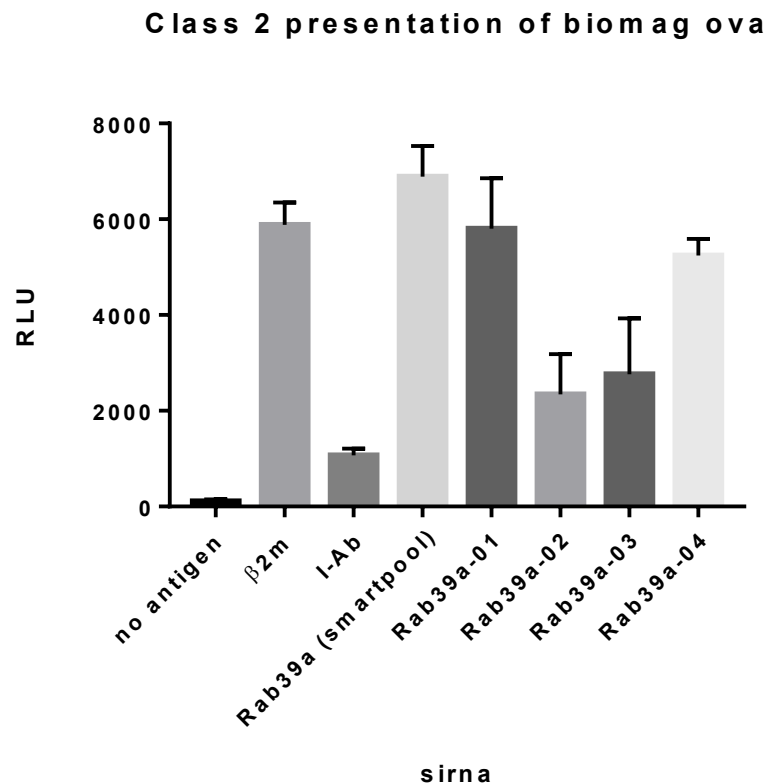
Figure 17. **The effects of individual rab39a sirna on Class II presentation.**
2.5 x10^3 DC3.2R cells were transfected with 50 nM sirna pools or individual oligos using Lipofectamine RNAiMax. After 48 hours, 1 x 10^4 Mf2-Luc cells were added along with biomag beads (0.4 µg of ova). After overnight incubation (~18 hours), Luciferase activity of the T cells was read using Oneglo reagent (Promega). *Rab39a-01 to 04 are the individual oligos that comprise the smartpool. Error bars indicate the standard deviation between triplicate wells. Data shown represents one experiment of $\geq$ 3. Using β2m as negative control, p-values (ANOVA) of smartpool, -01 and -04 oligos are not significant. P values for -02 and -03 $\leq$ 0.05.
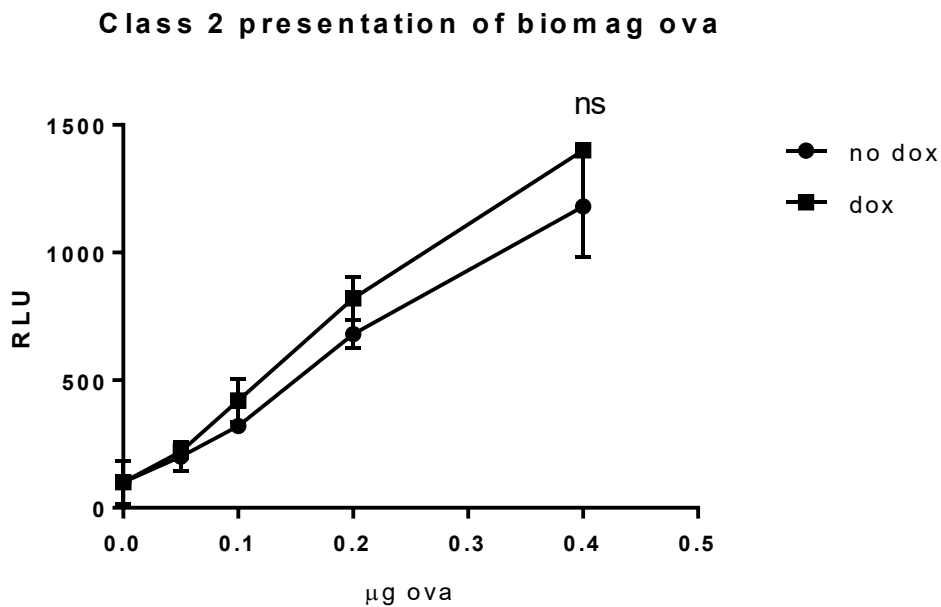
Figure 18. Rab39a rescue of knockout DCs does not affect Class II presentation.

1.25×10^4 DC3.2-Rab39aKO-Rab39a cells were incubated with 1 μg/ml dox for 48 hours in a 96 well plate. Then, the indicated amounts of biomag-ova beads were added along with 5×10^4 MF2-Luc. After overnight incubation, luciferase activity from the T cells were quantified using Oneglo reagent (Promega). Error bars indicate the standard deviation between triplicate wells. Data shown represents one experiment of $\geq$ 3. P-values for all wells between samples are not significant based on ANOVA (p>0.05)

C. Rab39a knockdown does not affect overall phagosomal pH in dendritic cells

The observation that Rab39a caused a defect in XPT but not Class II showed that the gene was playing a selective role in the XPT pathway. If Rab39a was necessary for normal cell homeostasis, then its loss would have affected the Class II pathway as well (due to cell death or other defects). The lack of effect on the Class II pathway also meant that Rab39a was probably not playing a role in the common steps between XPT and Class II presentation. These steps include antigen acquisition and internalization. This was an interesting finding as Rab39 was first described as promoting endocytosis when expressed in HeLa cells (103).

Another common step between XPT and the Class II pathway is endosome/phagosome maturation. These steps include a decrease in phagosomal pH as well as the acquisition and activation of various phagosomal proteases. Previously, Rab39a was described to promote phagosome acidification (102). In that study, overexpression of the dominant negative form of Rab39a (a non functional competitor to the endogenous form's binding partners) decreased the number of phagosomes that colocalized with lysotracker dye (a dye that stains acidic compartments). We however, hypothesized that the effect of Rab39a on XPT was not due to a change in phagosomal acidification, at least in dendritic cells. This was because the MHC Class II pathway relied on acidification and subsequent activation of various phagosomal proteases to

generate Class II peptides (74, 76). Furthermore, it has been shown that the deliberate blocking of endosomal acidification using agents such as chloroquine and bafilomycin inhibited Class II presentation (114) (also our unpublished data). Thus, if Rab39a promoted phagosomal acidification, then its knockdown would have also decreased presentation via the Class II pathway.

On the other hand, some extent of phagosomal acidification could conceivably influence XPT. It could influence vacuolar proteolysis to generate MHC I peptides, particularly for the XPT of vacuolar pathway antigens. It could destabilize MHC I molecules and in theory possibly promote exchange of MHC I-bound peptides with ones derived from internalized antigen.

In order to directly determine the role of Rab39a on phagosomal acidification, we fed dendritic cells with pH sensing beads. Beads conjugated to a pH sensor dye (pHrodo, Thermo Scientific) were fed to siRNA treated dendritic cells. This dye increased fluorescence as the environment pH became more acidic. If Rab39a was necessary for acidification, then its knockdown should have caused a decrease in bead fluorescence. As shown in (Figure 19), we did not see significant changes in fluorescence by cells that were treated with Rab39a siRNA as compared to cells treated with control siRNA. In contrast, the vacuolar ATPase inhibitor Bafilomycin A1 effectively prevented phagosomes from acidifying as expected, and served as a positive control that the assay was working.

The same lack of phenotype was observed when pH sensing beads were fed to either Rab39a knockout cells or doxycycline induced / rescued cells (Figure 20). Thus, it appears that for the cell lines we are using, phagosome acidification proceeded normally despite the lack of Rab39a.

The discrepancy between our results and that of previously published data (102) can be attributed to several factors. First, we utilized dendritic cell lines while the previous study used macrophages. It has been shown that dendritic cells, unlike macrophages, have specialized pathways to neutralize phagosomal pH (73). Second, the method of Rab39a disruption was different between our and the published experiments. In our experiments, we reduced Rab39a via siRNA, or eliminated it completely via CRISPR. In the published work, Rab39a was disrupted through the overexpression of the dominant negative form (GDP locked form) of Rab39a. While the dominant negative forms of Rab GTPases are usually used to compete out the wildtype forms from their natural binding partners, there are some cases where the GDP bound form of a Rab protein has a unique function as compared to its GTP bound form (discussed further in later sections) (69, 115-117). In addition, dominant negative forms of proteins have the potential to block other interacting proteins and thereby cause broader inhibitory effects that selective depletion of the wild type protein.

Workspace Annotation	Geometric Mean : FL1-H
☐ I-Ab	12.9
☐ b2m	10.1
☐ rab39a	13.9
☐ 100nM bafilomycin	4.43
cells alone	3.49
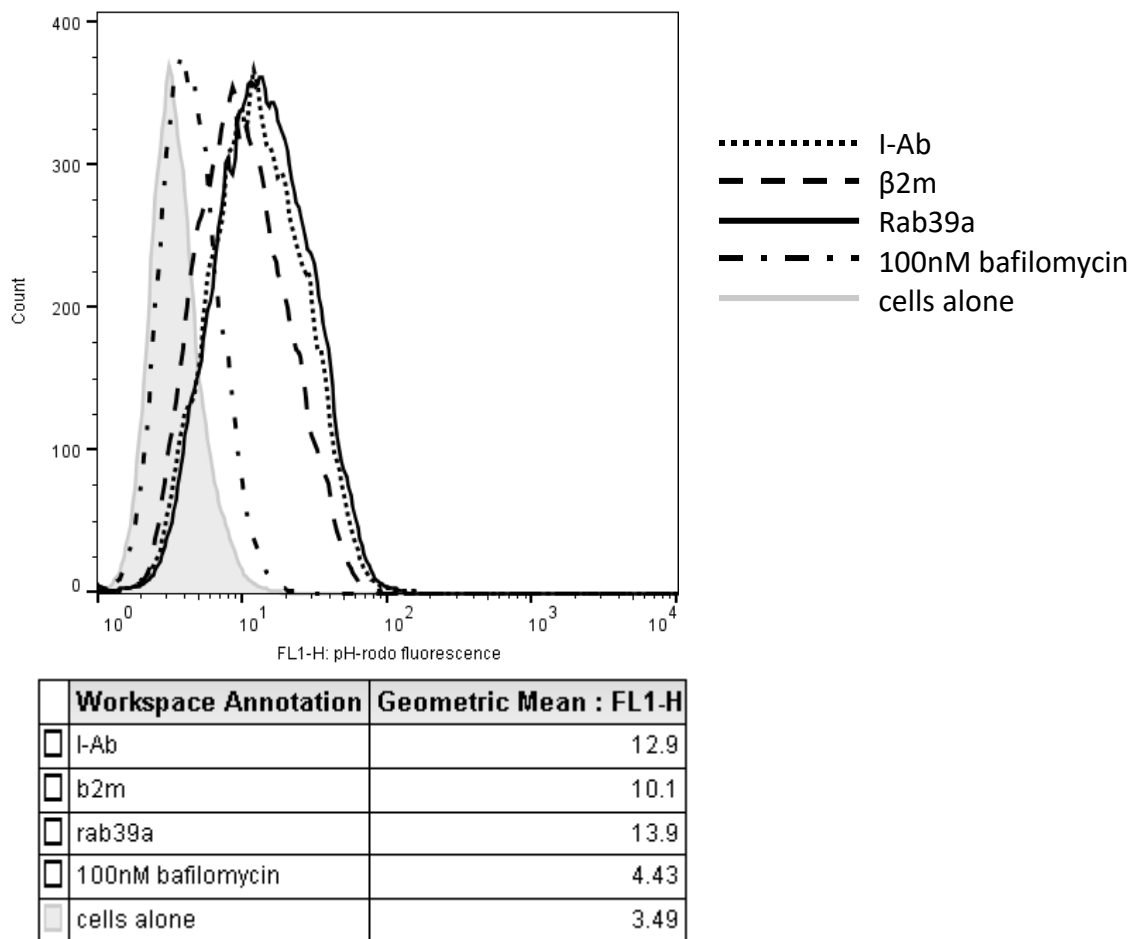
Figure 19. **Rab39a does not affect overall phagosome pH.**

8×10^4 DC3.2R cells were transfected with 50 nM sirna using lipofectamine RNAiMax in a 24 well plate. 48 hours later, cells were fed at 10 beads / cell of 1 μm pHrodo latex beads for 2 hours at 37°C. Wells were washed and the cells were detached with trypsin, washed in 1%FCS-PBS then run for facs analysis. For control, untransfected cells were treated with 100 nM bafilomycin during phagocytosis. Shown are gMFI of indicated fluors. Data shown represents one experiment of ≥ 3.
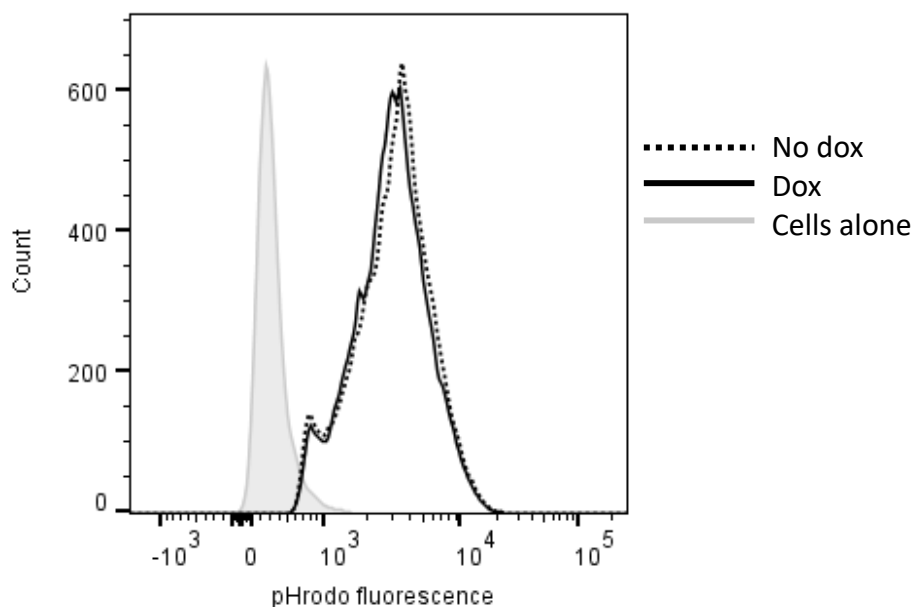
	Workspace Annotation	Geometric Mean : Alexa Fluor 488-A
☐	dox	2882
☐	no dox	2981
▨	cells alone	328

Figure 20. Rab39a rescue does not affect overall phagosome pH.

1.25×10^5 DC3.2-Rab39aKO-Rab39a cells were incubated with 1 µg/ml dox for 48 hours in a 12 well plate. Cells were fed at 1 bead / cell of 6 µm magnetic beads conjugated with pHrodo for 4 hours at 37°C. Wells were washed and the cells were detached with versene, washed in 1%FCS-PBS then run for facs analysis. Shown are gMFI of cells that have eaten beads. Data shown represents one experiment of ≥ 3.

D.   GDP and GTP locked Rab39a as well as Rab39b do not affect XPT

To further characterize role of Rab39a in the XPT pathway as well as address the previously discussed discrepancy in data, we utilized the dominant negative (DN, GDP-locked) and constitutively active (CA,GTP-locked) forms of Rab39a in our CRISPR rescue experiments.

Rab proteins, being GTPases, can either be in a guanosine diphosphate (GDP)-bound or guanosine triphosphate (GTP)-bound form (118). The activation state of the Rab determines its function, with many Rabs only being active when gtp is bound. Because of this, several studies on Rab GTPases have made use of Rab mutants, wherein the GTPase is permanently bound to GDP or GTP. Dominant negative mutants can be overexpressed to compete out endogenous Rabs from their interaction partners, thereby inhibiting their function. The reverse is true for constitutively active mutants, which when overexpressed, have no need for prior activation.

To test the effect of the Rab39a DN and CA forms in XPT, we transduced the Rab39a knockout cells with doxycycline inducible forms of these Rab39a mutants. Interestingly, only the wildtype form of Rab39a, and not DN or CA, could enhance crosspresentation of bead bound antigen (Figure 21). While this was expected for the DN, the lack of phenotype even with the CA form was

surprising. These data suggest that the proper cycling of Rab39a from the GDP to the GTP bound form (and back) was important for conveying the XPT phenotype.

It is important to note that the wt, DN and CA rescue cell lines used in this experiment arose from separate transductions of lentivirus constructs. The random integration of the constructs in the genome, as well as the time needed for proper antibiotic selection of transduced clones caused these three cell lines (wt, DN and CA) to diverge in their characteristics. These characteristics included cell size, division time, culture plate adherence properties, Class I and 2 levels, as well as crosspresentation and Class 2 presentation abilities. As such, in figure 21, one cannot compare the reporter T cell signals (RLU) of the three cell lines against each other (eg. Wt vs DN baseline xpt). What this figure shows, is the effect of dox (Rab39a rescue) on each of the independent cell lines.

The requirement for a fully functional Rab GTPase on-off cycle was also described with Rab3a (116). In mouse chromaffin cells, only the wt form of Rab3a was able to regulate secretory vesicle docking, while both DN and CA forms failed to do so. In a large scale screen for *Drosophila* Rab effectors, it was shown that while majority of effector proteins bound to the GTP-bound form of Rab GTPases, there are indeed some that prefer the GDP bound form (117). Rab22a, involved in recycling of cell surface molecules including MHC Class-I, has also been shown to require both GDP and GTP bound forms for full activity (69). Knockdown of Rab22a or overexpression of its DN form blocked MHC-I

recycling and depleted recycling tubules in human cell lines. When the CA form was overexpressed however, there was an increase in recycling tubules and peripheral vesicles, but MHC-I recycling was still defective. The data suggested that while the active form of Rab22a was required to initiate the formation of recycling tubules and vesicles, its inactivation is required for fusion of these vesicles to the cell surface. Our data show that Rab39a is similar in that it requires active GDP/GTP cycling to confer its phenotype on XPT.
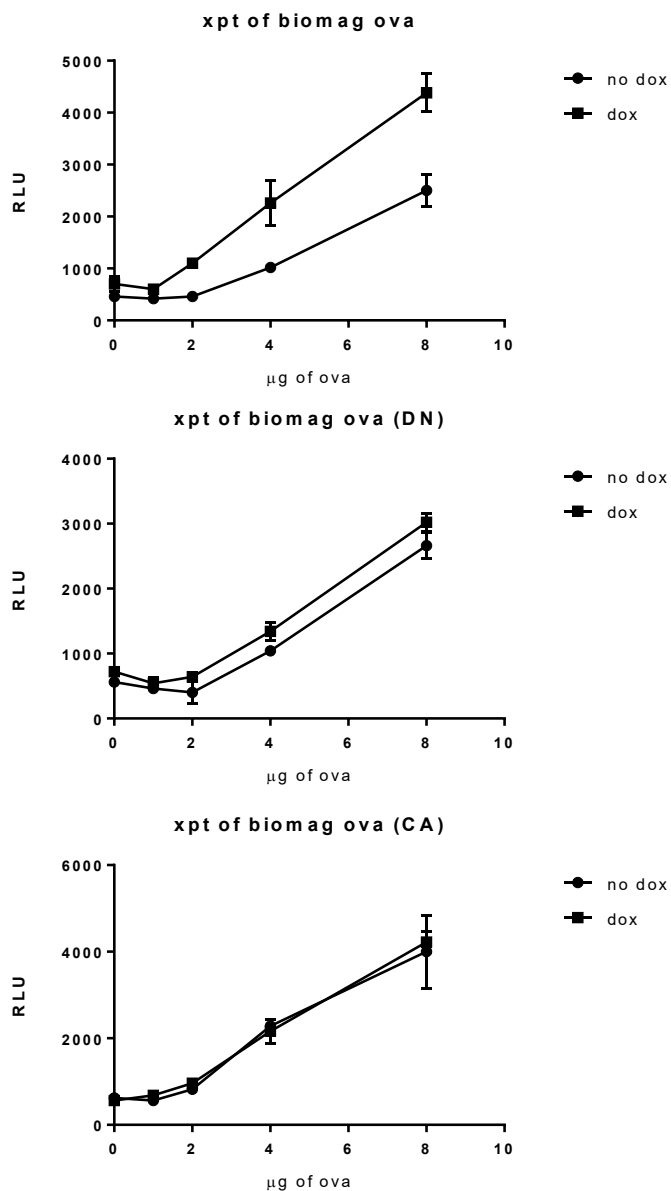
Figure 21. Mutants of Rab39a cannot rescue of crosspresentation of knockout DCs.
DC3.2-Rab39aKO cells were transduced with doxycycline inducible constructs containing the wt sequence of Rab39a, or its DN (S22N), or CA (Q72L) mutants and selected with puromycin. 1.25×10^4 cells were incubated with 1 μg/ml dox for 48 hours in a 96 well plate. Then, the indicated amounts of biomag-ova beads were added along with 5×10^4 Rf33-Luc. After overnight incubation, luciferase activity from the T cells were quantified using Oneglo reagent (Promega). Error bars indicate the standard deviation between triplicate wells. Data shown represents one experiment of ≥ 3. For Rab39a (wt), all wells with antigen at and beyond 2 μg ova have p-values (ANOVA) ≤ 0.05. P-values for all wells in both DN and CA setups are not significant (p > 0.05)

Further investigation of the Rab39a mutants showed that while both Rab39a wt and CA forms were stable in the cell, the DN form had a short half life. As shown in (Figure 22), cells expressing the DN form had very low levels of Rab39a unless rescued by addition of the proteasome inhibitor MG132. This might indicate a difference in Rab39a regulation between dendritic cells (our data) and macrophages (102), where overexpression of the DN form decreased phagosome acidification. Why the stable CA form did not cause an increase in XPT would be interesting to study.
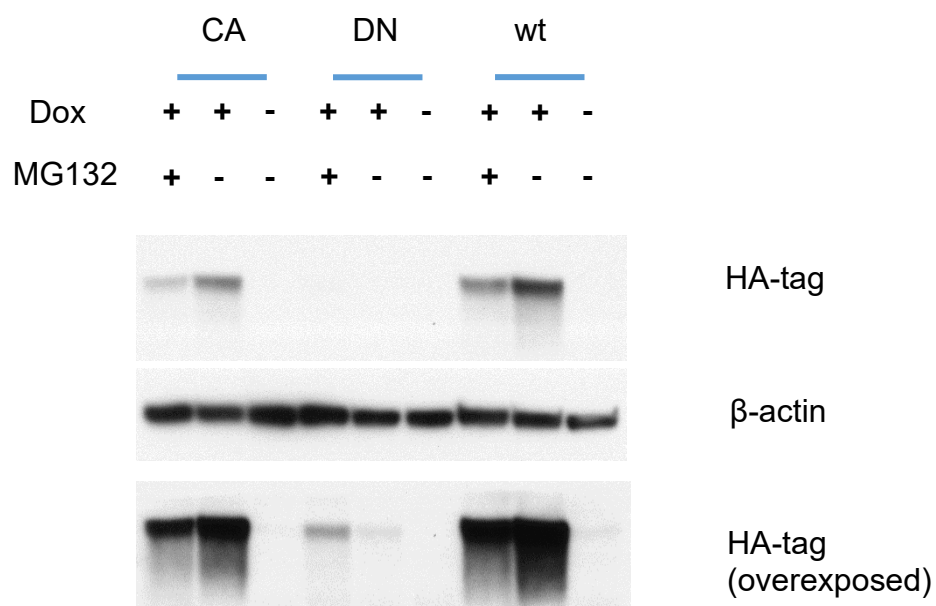
Figure 22. Mutants of Rab39a have differing protein stabilities.
DC3.2-Rab39aKO cells were transduced with Doxycycline inducible constructs containing the wt sequence of Rab39a, or its DN (S22N), or CA (Q72L) mutants and selected with puromycin. 1 x 10^6 cells were incubated with or without 1 μg/ml dox for 24 hours in a 6 well plate. A set of cells preincubated with dox were further incubated with 10 μM MG132 for 4 hours. Cells were harvested, lysed in RIPA buffer and run in a Western Blot. Data shown represents one experiment of $\geq$3.

Rab39b is another isoform (different gene with high homology of protein sequence) of Rab39 that shares 78% amino acid similarity with Rab39a (104). This difference in amino acid sequence completely changed Rab39a and b localization. While Rab39a was present on late endosomes, Rab39b was golgi-localized (105). Nevertheless, we tested whether Rab39b also affected XPT.

Silencing of Rab39b with siRNA did not affect XPT of biomag-ova (Figure 23). Thus, despite high sequence homology, Rab39a was distinct enough from Rab39b to affect XPT. We hypothesized that the endosomal localization of Rab39a was the reason and this is discussed in the later sections.

A.

x p t o f b i o m a g - o v a

B.
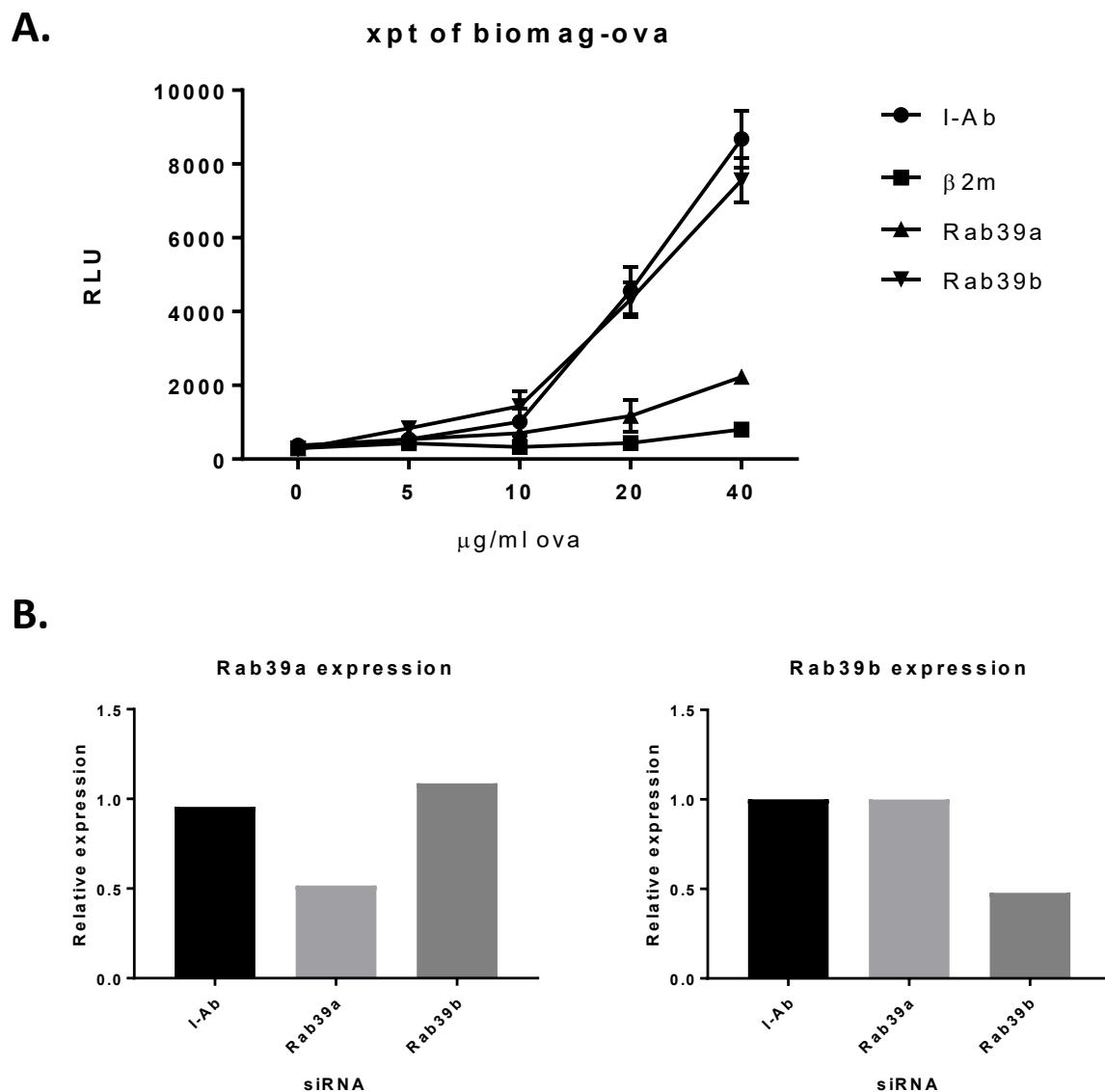
Figure 23. **Rab39b does not affect crosspresentation.**

A. 2.5 x10^3 DC3.2R cells were transfected with 50 nM sirna pools using Lipofectamine RNAiMax. After 48 hours, 1 x 10^4 Rf33-Luc cells were added along with the indicated amounts of biomag ova. After overnight incubation (~18 hours), Luciferase activity of the T cells were read using Oneglo reagent (Promega). Error bars indicate the standard deviation between triplicate wells. For all wells, p-values (ANOVA) between Rab39b vs that of β2m are not significant ($\geq$ 0.05). **B.** qPCR of Rab39a and Rab39b following siRNA treatments. Expression was normalized to that of siRNA control (I-Ab). Data shown represents one experiment of $\geq$ 3.

E. Silencing Rab39a does not inhibit the Classical Pathway

Given that inhibition or lack of Rab39a affected XPT but not the Class II pathway, we next determined whether or not Rab39a affected the Classical MHC Class I pathway. The XPT and Classical pathways are intricately linked by several key molecules.

The phagosome to cytosol pathways (P2C2E and P2C2P) of XPT shared with the Classical pathway genes such as TAP1, the proteasome, and in some cases, other peptidases like ERAP1 (28, 29, 31, 32) (33). Moreover, for XPT antigens that route through the ER for Class I loading, pathways that allow MHC-I egress and trafficking to the cell surface are also shared.

A XPT antigen that routed through the vacuolar pathway could also be potentially affected by components of the Classical pathway. The source of MHC-I utilized for phagosomal loading has been proposed to come from the cell surface, the endpoint of the Classical pathway (65-69). Class I stability and peptide loading in the ER could also be important, as several models proposed that MHC-I loaded with low affinity peptides in the ER were the ones primarily being loaded with peptides derived from phagosomally processed antigens (119, 120). Thus, genes that encoded proteins that altered the MHC peptide repertoire (chaperones, peptidases, etc) could be important for both pathways.

In order to determine the role of Rab39a in the Classical Class I pathway, we transfected siRNA into two different ova expressing cell lines.

First, we generated a dendritic cell line that could inducibly express a cytosolic form of ovalbumin (DC3.2 NS-ova) upon addition of doxycycline. The expressed ovalbumin protein underwent all the steps involved in the Classical pathway – proteasomal processing, import into the ER through TAP1, trimming by ERAP and finally Class I loading in the ER and egress toward the surface.

We also generated a second DC line (DC3.2 Ub-S8L) that instead inducibly expressed the SIINFEKL peptide conjugated to the C-terminus of Ubiquitin (110). In this cell, deubiquitinases free the S8L peptide, thereby bypassing proteasomal processing and peptidase trimming (121). The S8L peptide however, still required transport through TAP1 and ER loading onto Class I.

We utilized both cell lines to be able to distinguish between the antigen processing and Class I-loading steps of the Classical pathway. A defect in NSova presentation but not UbS8L would probably mean a defect in a cytosolic (or ER) antigen processing step (protein unfolding, chaperoning to proteasome, trimming, etc). A defect in both NSova and UbS8L would likely point to a defect in peptide transport (through TAP1) or MHC-I trafficking (from the ER to the cell surface).

Knocking down Rab39a in these cell lines showed no defect in Class I presentation of S8L (Figure 24). Because the Classical pathway is much more efficient that XPT, there was a danger of oversaturating the system with MHC-

peptide. Titration of doxycycline allowed for the expression of minute amounts of

antigen, and even in these cases, Rab39a did not have an effect.

Classical Presentation of NSova

Classical Presentation of UbS8L
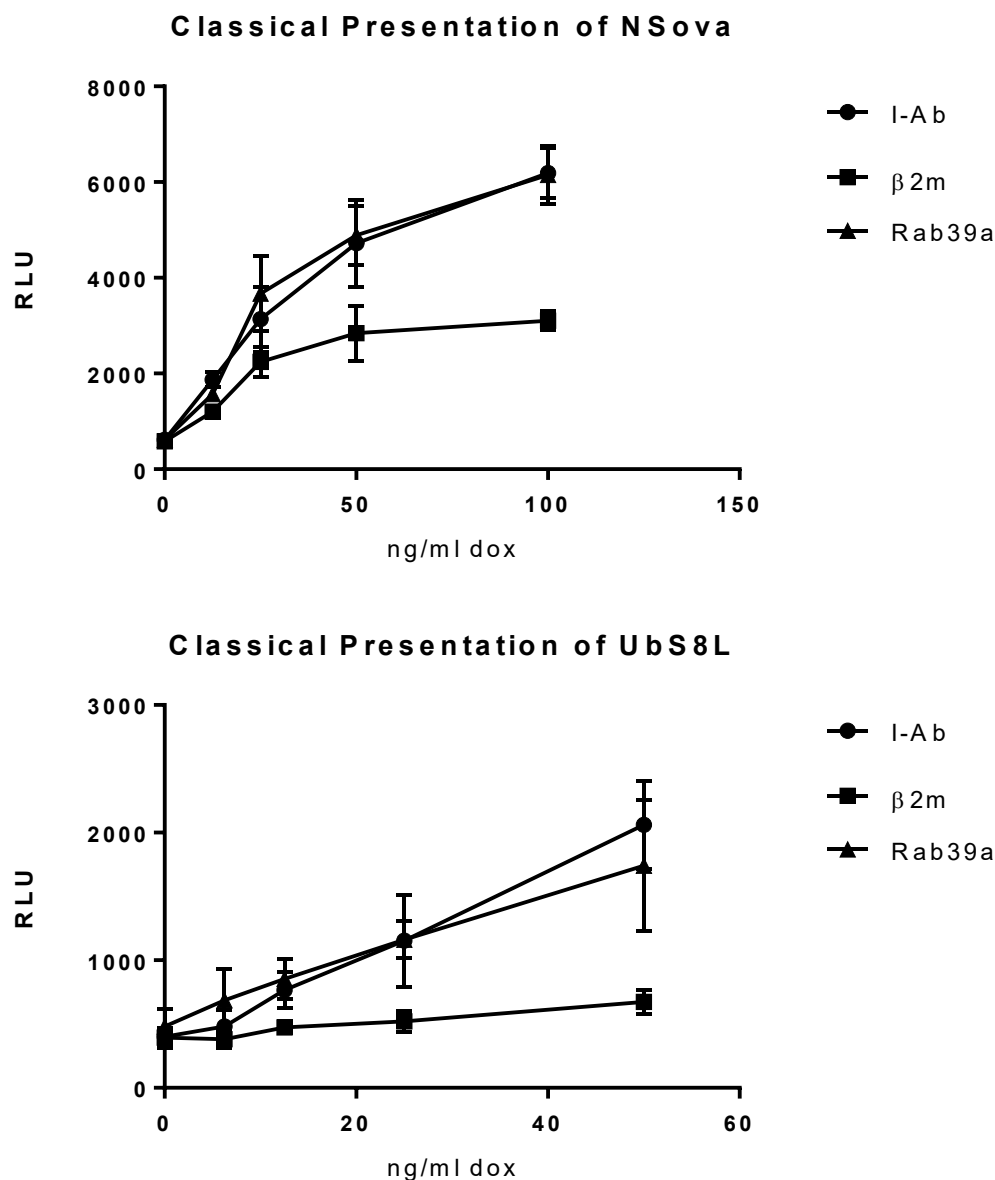
Figure 24. **Rab39a does not affect the Classical Class I pathway.**
2.5×10^3 DC3.2 NS-ova or DC3.2 UbS8L cells were transfected with 50 nM sirna pools using Lipofectamine RNAiMax. After 48 hours, the listed concentrations of doxycycline were added. After 6 hours (NS-ova) or 2 hours (UbS8l) incubation at 37°C, Classical presentation was stopped by the addition of 1:1000 Brefeldin A (Golgiplug, BD). 1×10^4 Rf33-Luc cells were added and luciferase activity measured after overnight incubation. Error bars indicate standard deviation of triplicate wells. Data represents one experiment of $\geq$ 3. Using I-Ab as negative control, for all wells with dox, p-values of β2m are $\leq$ 0.05 (ANOVA). None of the wells for Rab39a show significant difference compared to the control.

We also looked at the effect of Rab39a on surface MHC Class I levels via flow cytometric analysis of siRNA treated cells. This allowed determination of overall peptide supply because peptide-binding is required for MHC I molecules to exit the ER and therefore reduction in peptide supply reduces steady state surface Class I levels. Defects in MHC-I trafficking could also be observed using this assay. The steady state levels of MHC Class I were unchanged despite Rab39a knockdown (Figure 25). The same phenotype was observed when we rescued knockout cells with Rab39a (Figure 26).

These data indicated that Rab39a affected XPT in a process distinct from those shared with the Classical pathway. Because of this, and Rab39a's published endosomal localization (102, 105), we then focused on the phagosomal processes that occur during XPT.

	Workspace Annotation	Geometric Mean : FL4-H
☐	I-Ab	583
☐	b2m	56.1
☐	rab39a	522
☐	unstained cells	10.4
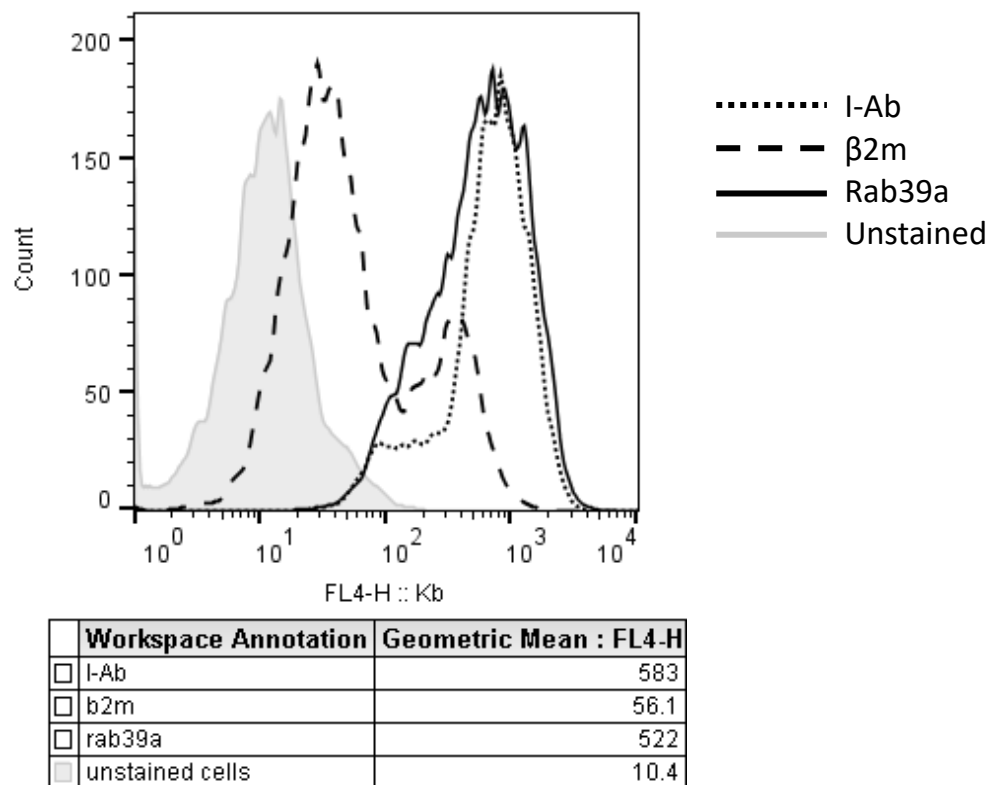
Figure 25. **Rab39a sirna does not affect surface MHC Class I levels.**
8×10^4 DC3.2R cells were transfected with 50 nM sirna using lipofectamine RNAiMax in a 24 well plate. 48 hours later, cells were detached and stained for MHC Class I (H2-K^b). Shown are gMFI of indicated stains
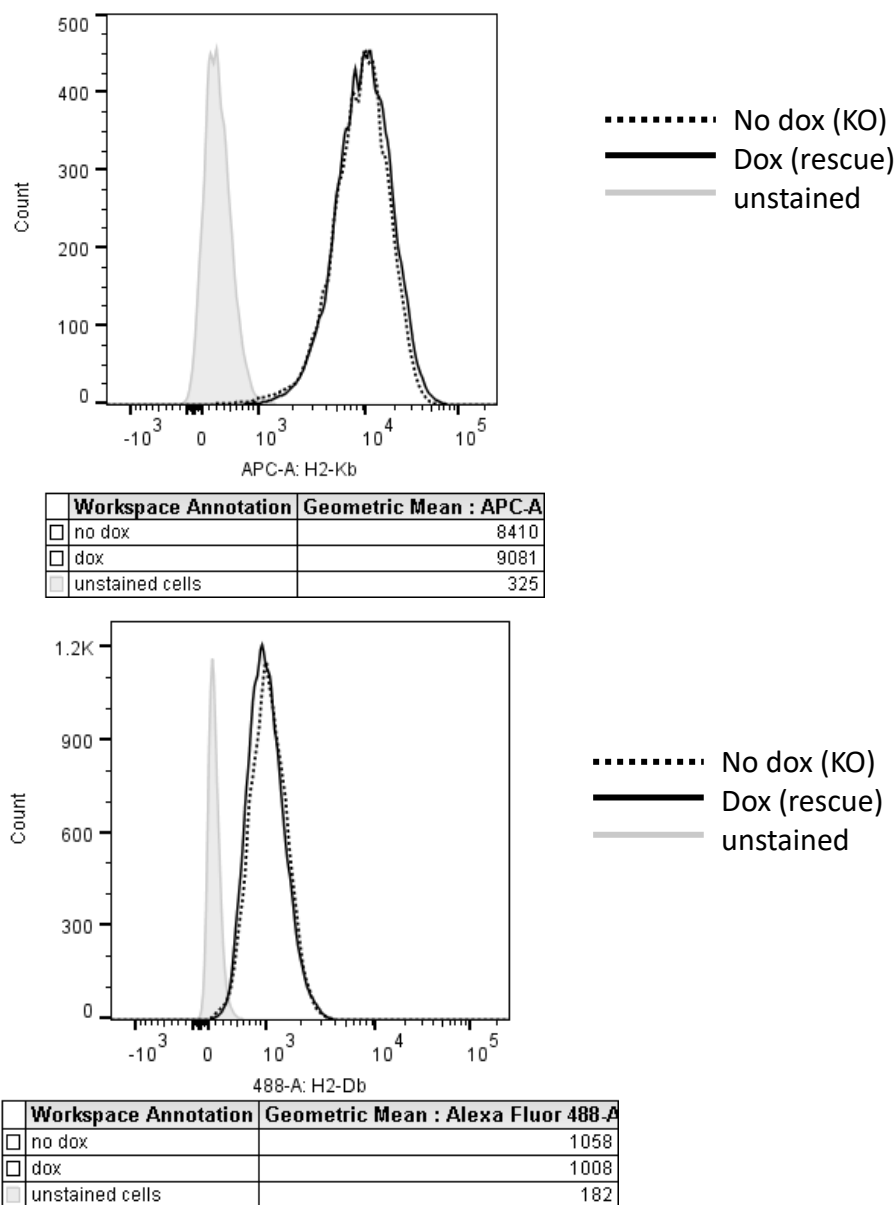
Figure 26. **Rab39a rescue does not change steady state surface MHC Class I levels.**
1.25 x 10^5 DC3.2-Rab39aKO-Rab39a-L^d cells were incubated with or without 1 μg/ml dox for 48 hours at 37°C in a 12 well plate. Cells were trypsinized, washed and stained for surface Class I (H2-K^b and H2-D^b). Shown are gMFIs of the indicated stains

F. Rab39a is localized to late endosomes as well as antigen containing phagosomes

Before studying the possible roles of Rab39a in the phagosomal steps of XPT, we sought to reconfirm the findings that it was indeed endosomally localized and was recruited to antigen containing phagosomes (102).

In order to do this, we rescued our generated knockout cells with doxycycline (DC3.2 Rab39aKO-Rab39a) and stained Rab39a (via an HA tag) as well as endosomal markers for confocal microscopy. Confirming the previous reports, Rab39a colocalized with both Rab7 (Figure 27) and Lamp2 (Figure 28), both markers of late endosomes.

We also rescued the knockout cells with an mcherry tagged Rab39a. This allowed for live cell observations during microscopy. Rab39a assumed a punctate pattern. When cells were fed overnight with lysosensor dextran (which fluoresces at 521 nm when in acidic conditions), Rab39a could be seen surrounding the antigen (Figure 29). It has been reported that the terminal destination of endocytosed dextrans are Lamp1 positive, Rab7 positive compartments (122). Thus, Rab39a localized with late endosomal compartments in live cells.

Mcherry-Rab39a also colocalized with internalized beads in the live cell imaging experiments (Figure 30). Thus, Rab39a was recruited not just to endosomes, but also to particulate containing phagosomes.
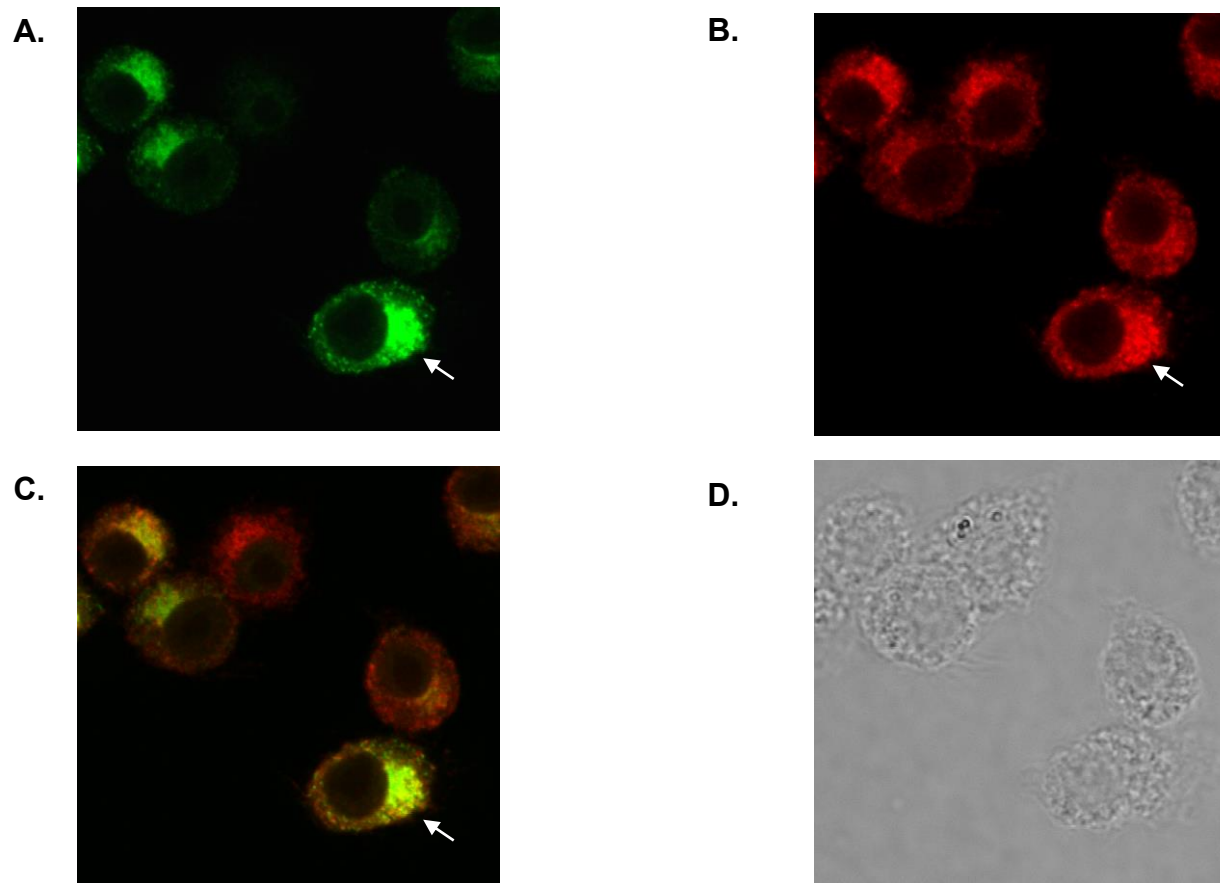
Figure 27. **Rab39a colocalizes with Rab7.**
DC3.2-Rab39aKO-Rab39a were grown in round coverslips placed in a 12 well plate. After overnight incubation with 1 µg/ml doxycycline, cells on coverslips were washed, fixed and stained according to the listed protocol and antibodies. A. Green = Rab39a (HA tag), B. Red = Rab7, C. Merge, D. Brightfield. Arrows highlight colocalization.
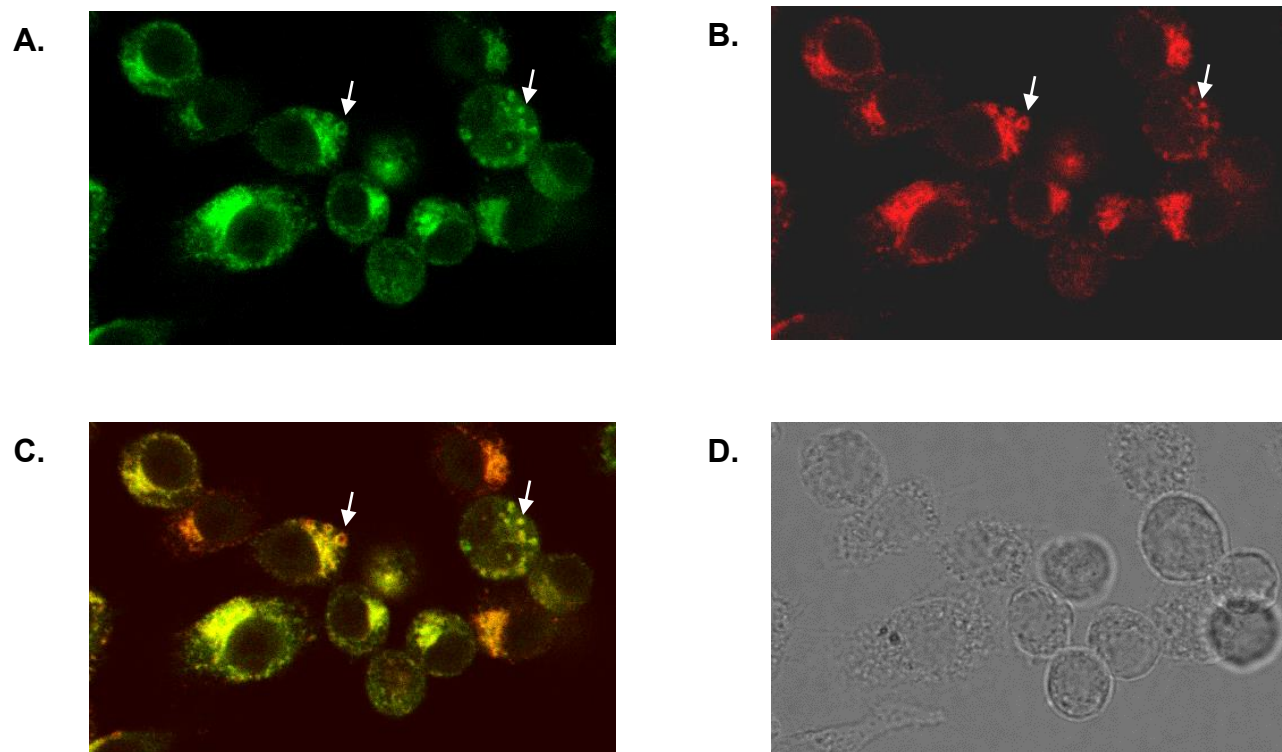
Figure 28. **Rab39a colocalizes with Lamp2.**
DC3.2-Rab39aKO-Rab39a were grown in round coverslips placed in a 12 well plate. After overnight incubation with 1 µg/ml doxycycline, cells on coverslips were washed, fixed and stained according to the listed protocol and antibodies. A. Green = rab39a (HA tag), B. Red = Lamp2, C. Merge, D. Brightfield. Arrows highlight punctate structures with colocalization
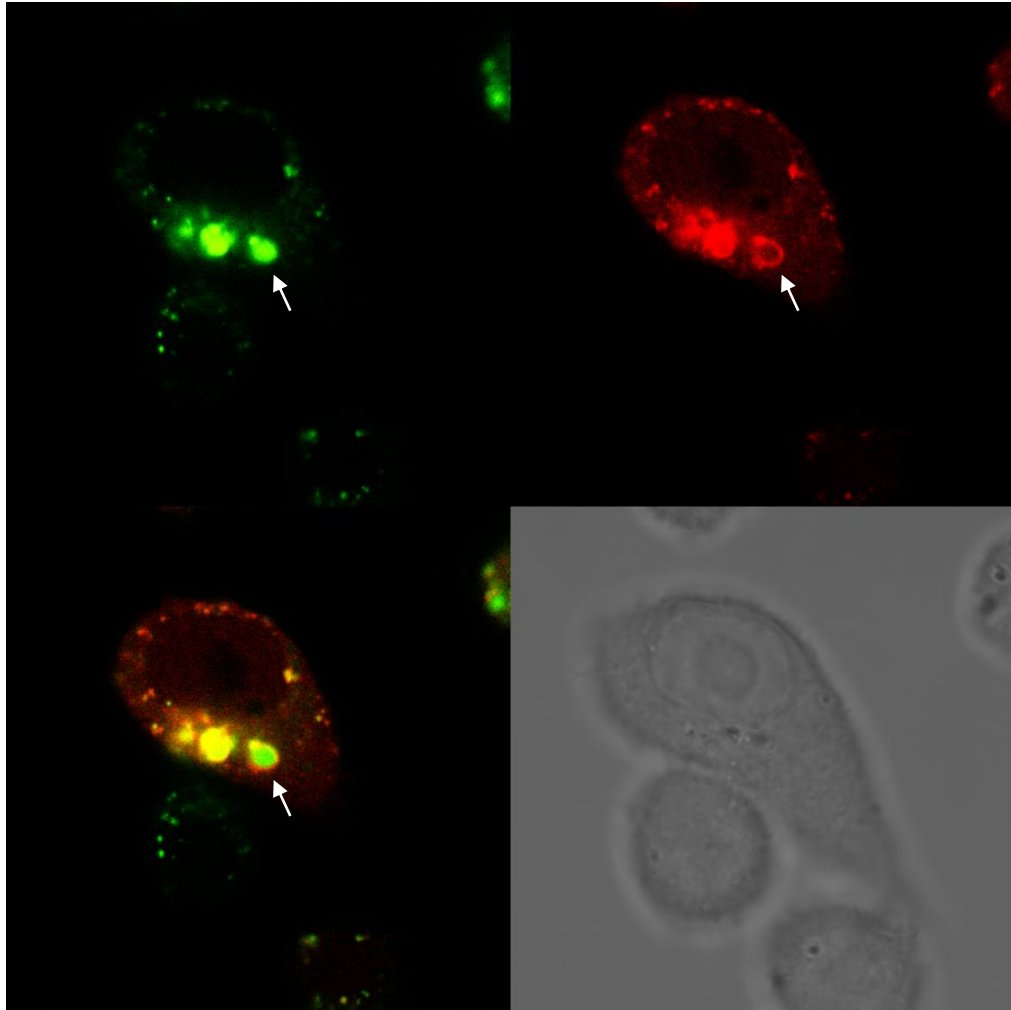
Figure 29. **Rab39a colocalizes with acidic vesicles.**
DC3.2-Rab39aKO cells were transduced with a doxycycline inducible construct containing mcherry-Rab39a. Cells were plated in 35 mm glass bottom dishes (MatTek) overnight with 1 µg/ml dox. The next day, cells were incubated with 1mg/ml lysosensor yellow/blue dextran. After overnight incubation at 37°C, cells were imaged under a Leica TCS SP5 confocal microscope. Green = lysosensor emission at 521 nm showing acidic compartments.. Red = mcherry- rab39a. Arrows highlight internalized dextran surrounded by Rab39a.
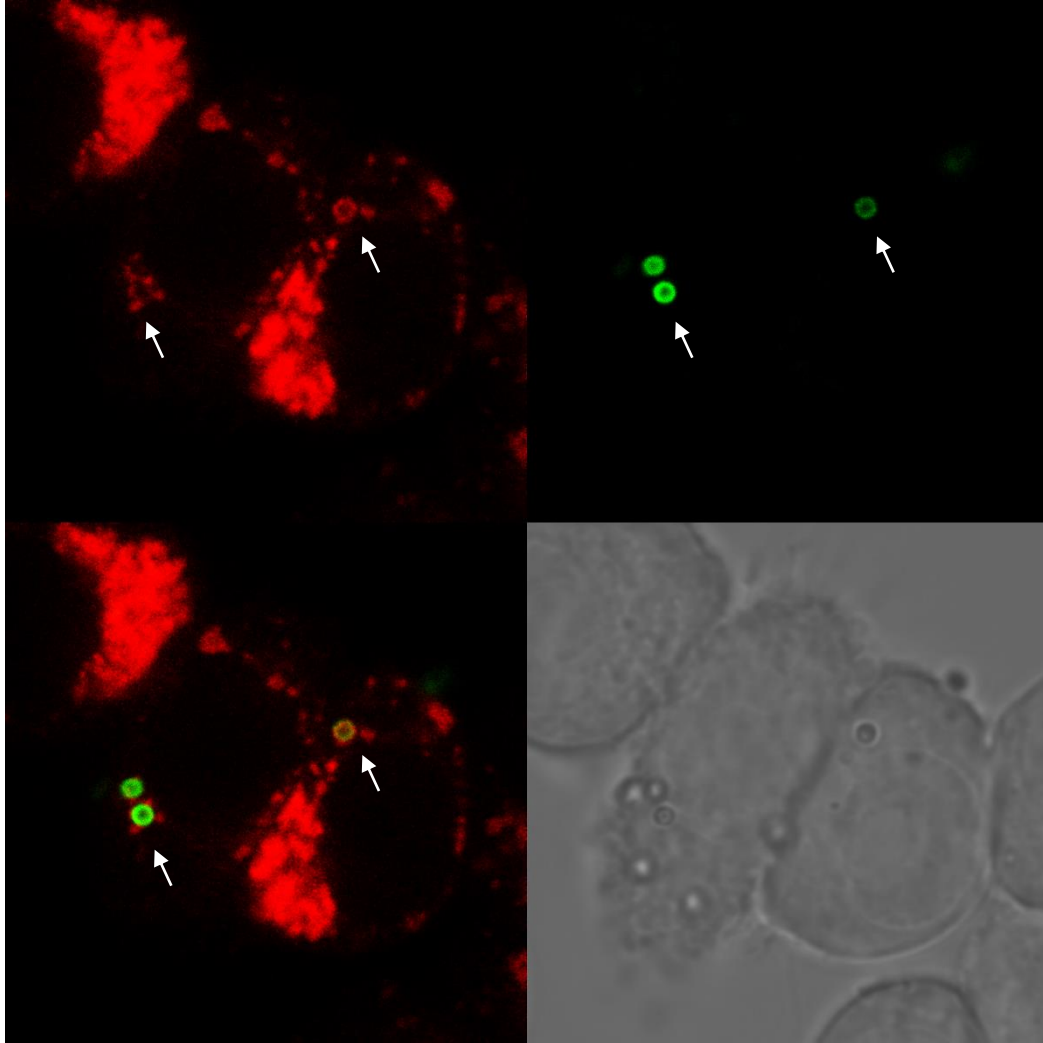
Figure 30. **Rab39a colocalizes with phagocytosed latex beads.**
DC3.2-Rab39aKO cells were transduced with a doxycycline inducible construct containing mcherry-Rab39a. Cells were plated in 35 mm glass bottom dishes (MatTek) overnight with 1 µg/ml dox. The next day, 1 µm latex beads conjugated with Alexa 488-NHS (1 bead / cell) were added. After 2 hours at 37°C, cells were imaged under a Leica TCS SP5 confocal microscope. Green = Alexa 488 labeled beads. Red = mcherry-rab39a. Arrows highlight internalized beads surrounded by Rab39a.

G. Flow cytometric analysis of isolated phagosomes (PhagoFACS)

Recent studies have indicated that certain processes involved in XPT occur at the individual phagosome level. For instance, MHC Class I from the ER-golgi intermediate compartment (ERGIC) have been shown to be recruited to specific phagosomes containing TLR4 ligands (71). In another case, it has been shown that XPT efficiency was enhanced when the antigen and a TLR signal was present in the same compartment, as opposed to pretreating cells with TLR ligands prior to antigen exposure (123). Because these phagosomal events might occur in a minority of the overall phagosomes in the cell, we needed to develop a method to be able analyze individual phagosomes at a sensitivity and resolution higher than that afforded microscopy.

Because of this, we performed flow cytometric analysis on isolated phagosomes (PhagoFACS), following and further optimizing the protocol as presented in a previous work (124). In this protocol, we fed dendritic cells with magnetic beads, then isolated these beads after cell disruption. The magnetic phagosomes were able to be efficiently separated from the rest of the cell components, greatly reducing background signal usually found during microscopy. This also allowed us to analyze phagosomes at an individual level, and distinguish subclasses of phagosomes present in the cells. The gating strategy we employed in this analysis is shown (Figure 31).
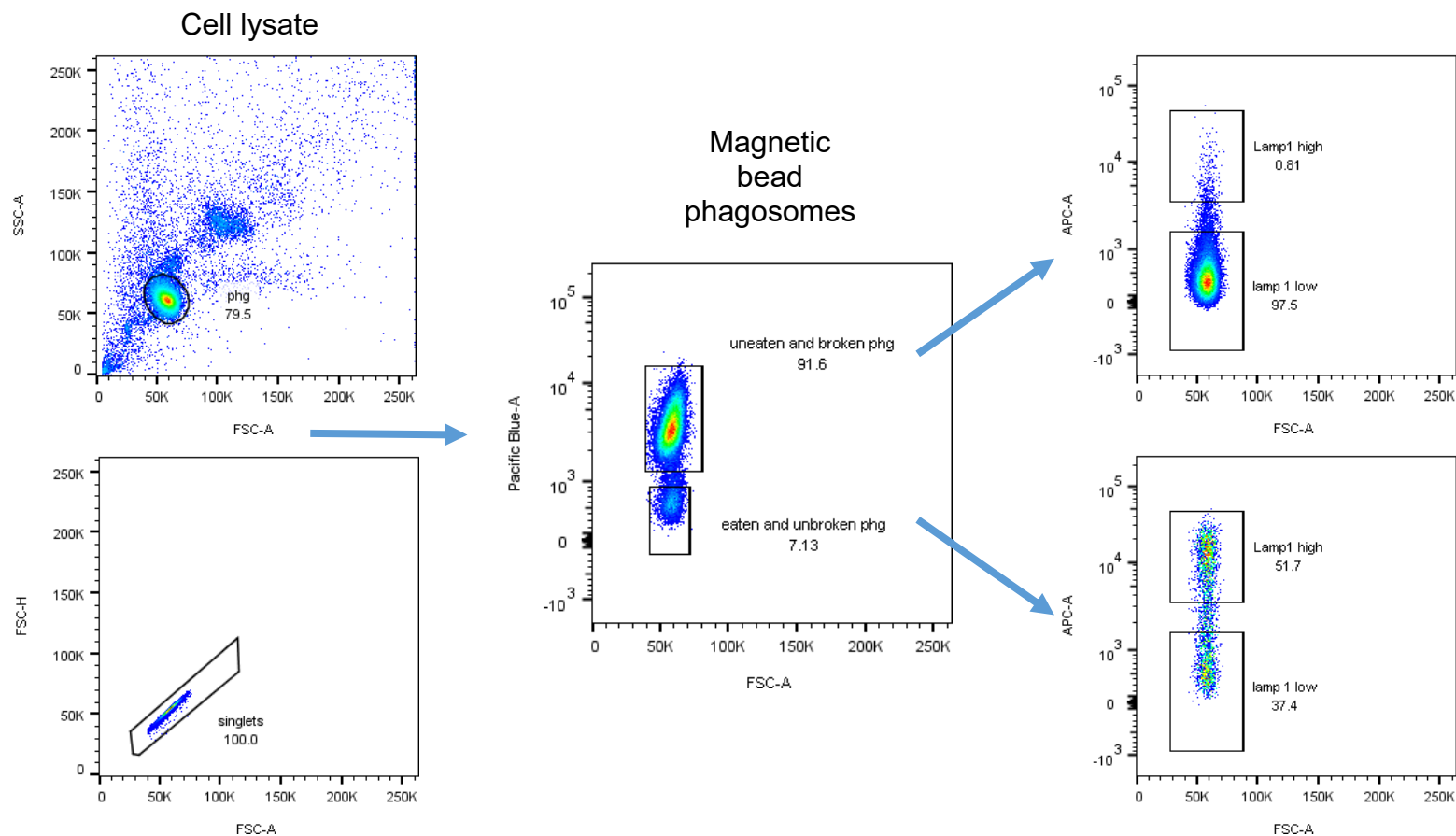
Figure 31. **Gating strategy for phagosomes.**

1.25×10^5 DC3.2-Rab39aKO-Rab39a-L^d cells were incubated with or without 1 μg/ml dox for 48 hours in a 12 well plate. Cells were fed at 1 bead / cell of biotinylated 6 μm magnetic beads for 2 hours. Then, the cells were exposed to Streptavidin-Pacific blue to stain uneaten beads. Phagosomes were then isolated using the listed protocol and broken phagosomes were stained through another round of Streptavidin- Pacific Blue. Isolated phagosomes were washed, permeabilized and stained for Lamp-1 (shown on APC channel).

H. Rab39a is recruited to late phagosomes but is not necessary for phagosome maturation.

We used PhagoFACS to study phagosomal Rab39a in our generated KO vs reconstituted cells (DC3.2-Rab39aKO-Rab39a). As shown in (Figure 32), Rab39a was recruited to magnetic bead containing phagosomes. The signal was specific as no staining was observed when the cells did not express Rab39a. In agreement with previous findings (102, 105) , Rab39a was a late endosomal Rab GTPase, as most of the phagosomes were positive for Rab39a only at later time points. Rab39a had similar kinetics to Lamp1 and its presence or absence did not affect Lamp1 recruitment, in agreement with previous reports (105) (Figure 33). These data showed that Rab39a was recruited as the phagosome matured, and its recruitment to the phagosome membrane was not required for phagosome maturation.
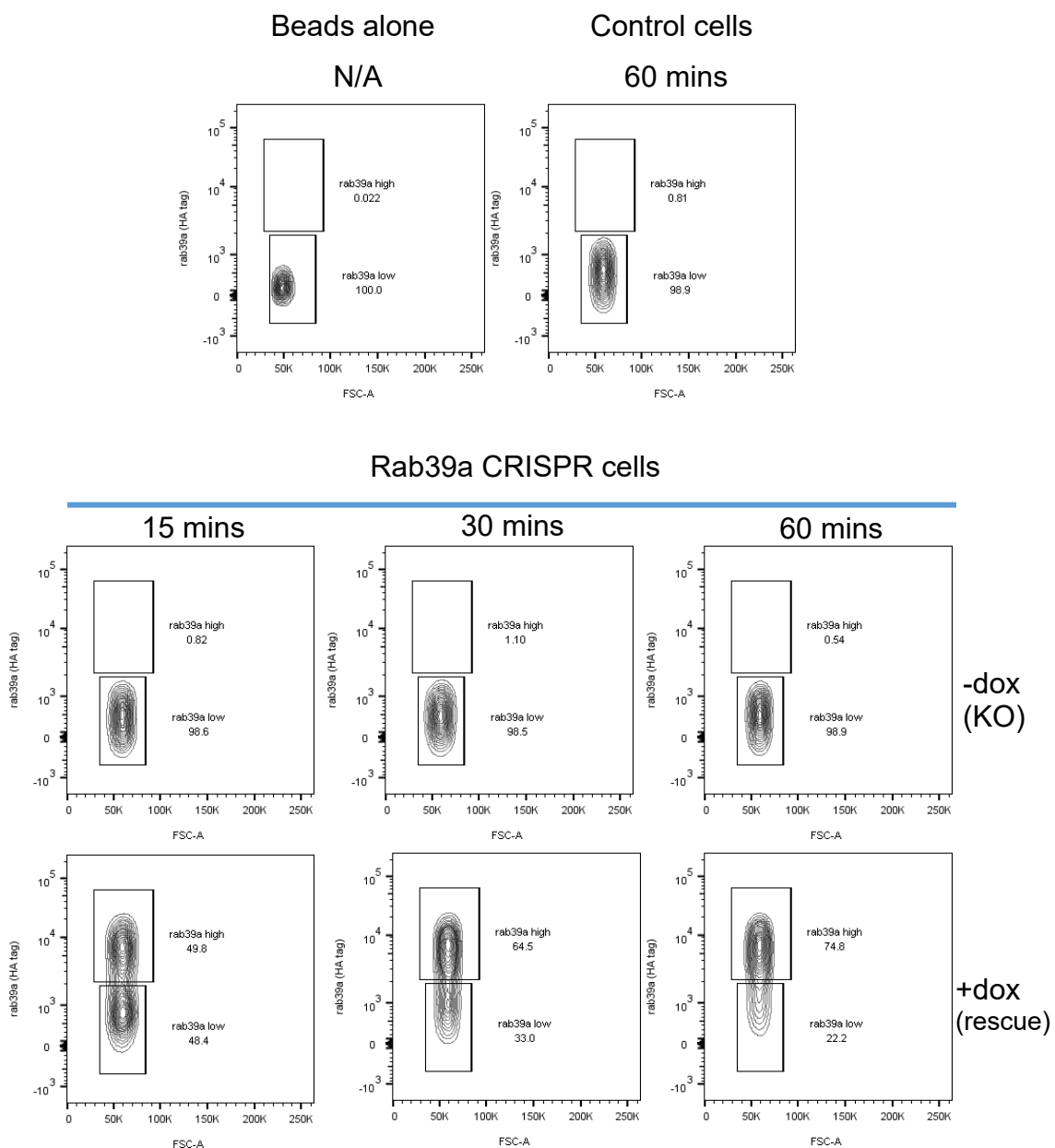
Figure 32. R**ab39a is recruited to magnetic bead phagosomes.**

5×10^5 DC3.2-Rab39aKO-Rab39a cells were incubated with or without 1 µg/ml dox for 24 hours in a 6 well plate. Cells were fed at 1 bead / cell of biotinylated 6 µm magnetic beads for the indicated lengths of time. Magnetic bead phagosomes were isolated using the listed protocol. Phagosomes were washed, permeabilized and stained for Rab39a (HA-tag). Data shown represents one experiment of $\geq$3.
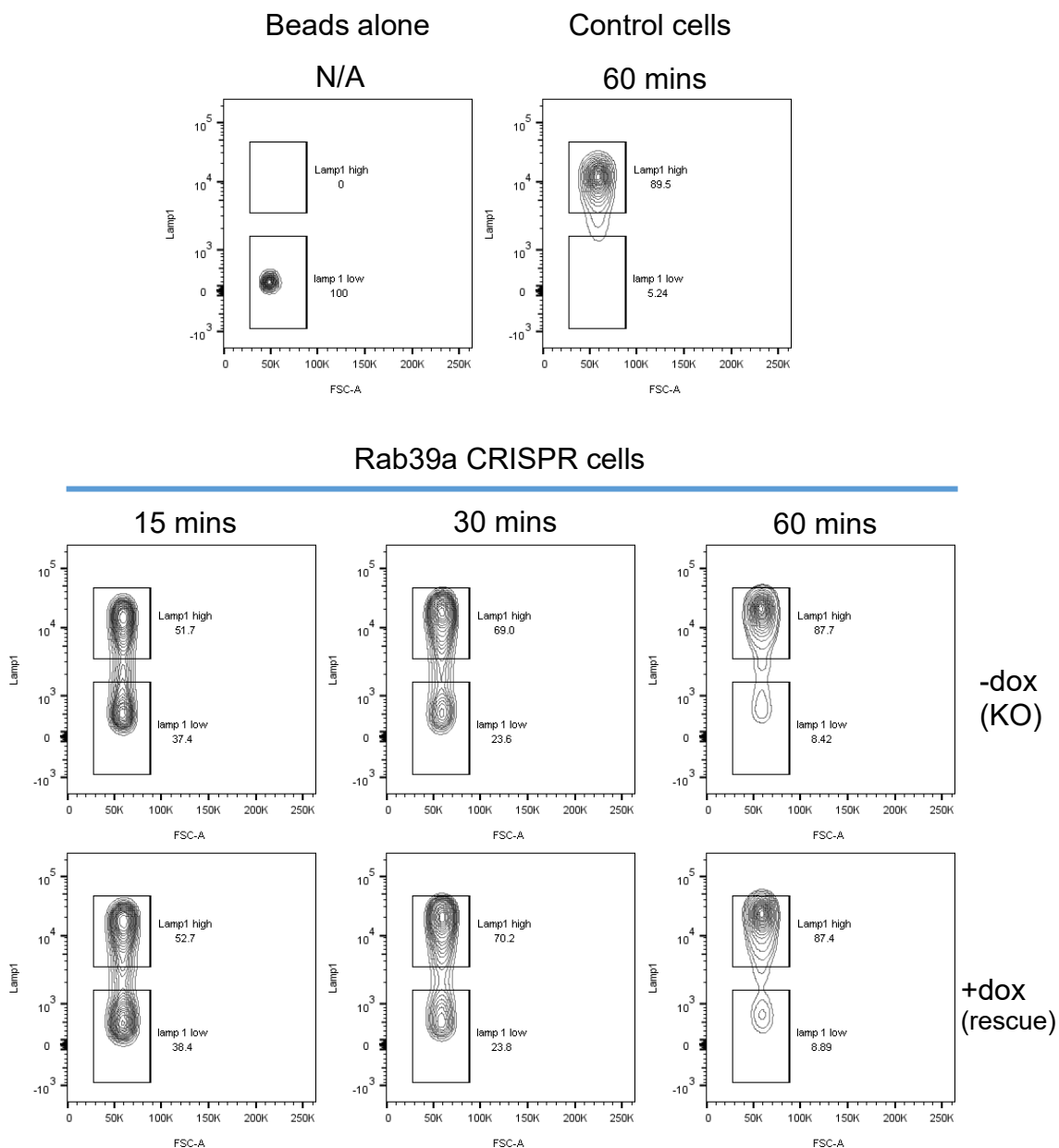
Figure 33. **Rab39a does not affect Lamp-1 recruitment to phagosomes.**

5×10^5 DC3.2-Rab39aKO-Rab39a cells were incubated with 1 µg/ml dox for 24 hours in a 6 well plate. Cells were fed at 1 bead / cell of biotinylated 6 µm magnetic beads for the indicated lengths of time. Magnetic bead phagosomes were isolated using the listed protocol. Phagosomes were washed, permeabilized and stained for Lamp-1. Data shown represents one experiment of ≥ 3.

I. Wt and CA Rab39a localizes to the phagosome but the DN form does not

We then looked if the DN and CA mutants of Rab39a were being recruited to phagosomes, to see if this explained the lack of phenotype we observed during our rescue experiments. Using PhagoFACS, we saw that that while the wt and CA forms of Rab39a were recruited to the phagosome, the DN form was not (Figure 34). This was perhaps due to the high turnover rate of DN in dendritic cells. Nevertheless, a previous study has shown that at least in HeLa cells, the DN form acquired a disperse/cytosolic localization as compared to the wt form, which mainly localized to late endosomes and vesicular structures (108). The CA form did not rescue XPT despite being recruited to the phagosomes (Figure 21). Further studies are needed to clarify this observation.
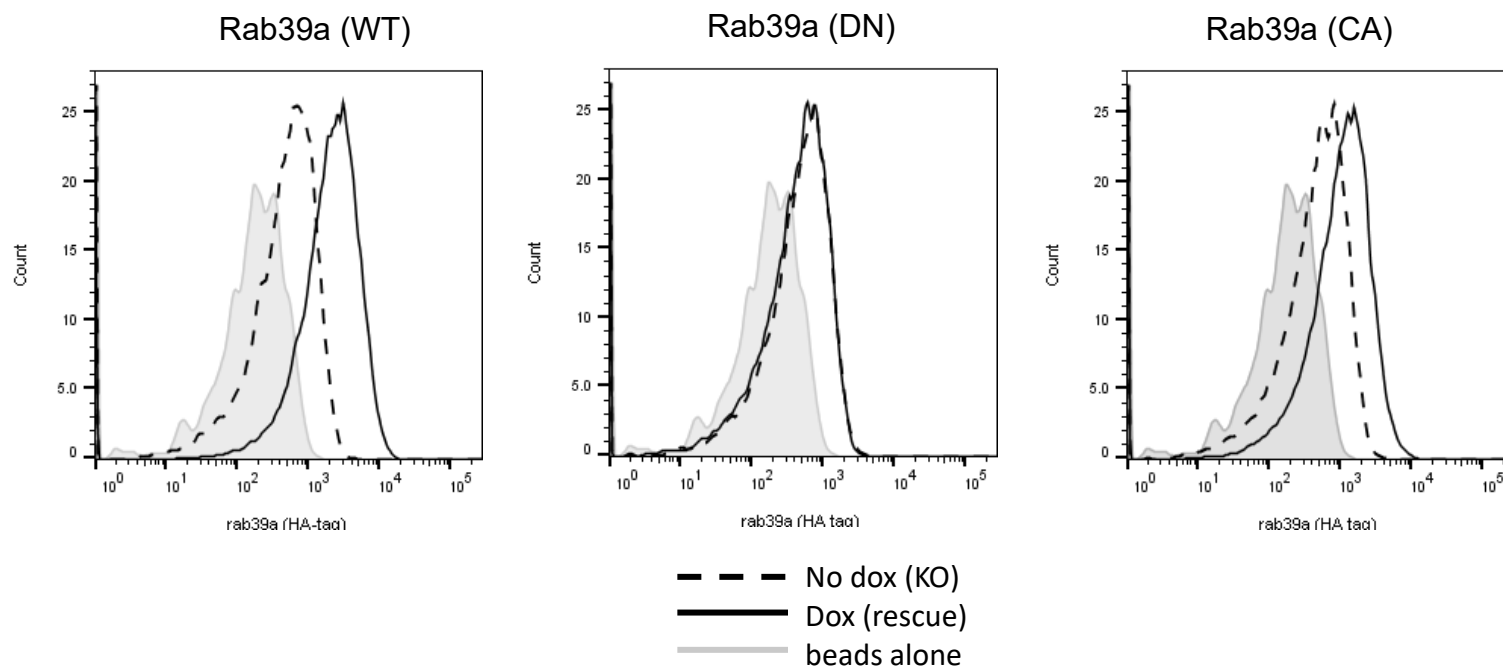
Figure 34. **WT and CA, but not DN Rab39a are recruited to magnetic bead containing phagosomes.**
DC3.2-Rab39aKO cells were transduced with doxycycline inducible constructs containing the wt sequence of Rab39a, or its DN (S22N), or CA (Q72L) mutants and selected with puromycin. 1.25×10^{5} cells were incubated with or without 1 µg/ml dox for 48 hours in a 12 well plate. Cells were fed at 1 bead / cell of biotinylated 6 µm magnetic beads for 2 hours. Phagosomes were isolated using the listed protocol. Isolated phagosomes were washed, permeabilized and stained for Rab39a (HA-tag). Shown are phagosomal gMFI of indicated stains. Data shown represents one experiment of $\geq$3.

J. Silencing Rab39a reduces XPT of vacuolar pathway antigens

Because Rab39a was phagosomal and did not affect the Classical

Pathway of XPT, we then asked if Rab39a would affect the Vacuolar Pathway of

XPT. The vacuolar pathway did not share the cytosolic steps involved in the

Classical Pathway such as proteasome processing and TAP transport of

peptides. Antigens that routed through the vacuolar pathway did not even need

transport from the phagosome to the cytosol. Assaying the effect of Rab39a on

this pathway would also shed light if Rab39a was playing a role in this transport

process.

Our lab has previously described a vacuolar pathway for XPT of polymer-

based beads and cell associated antigen (27). This pathway was shown to be

TAP independent, and primarily used phagosomal proteases such as Cathepsin

S to process antigen, bypassing the proteasome altogether. Other forms of

antigen, such as bacteria, have been described to follow a similar route (46, 47).

We therefore used heat-killed *E. coli* expressing GST fused to either SIINFEKL

or ASNENMETM as a source of vacuolar pathway / TAP-independent antigen. In

cells wherein Rab39a was knocked down via siRNA, XPT of these bacterial

forms of antigen was reduced (Figure 35).

The observed data further supports our hypothesis that Rab39a was

affecting XPT in a process that was occurring within the phagosomes. The

bacterial antigens we used had no need for TAP, suggesting that they had no

need for phagosome to cytosol transfer (as TAP is used for ER or phagosome entry from the cytosol). Because of this, we also hypothesized that the effect of Rab39a on XPT was not just due to a role in phagosome to cytosol transport of antigen.
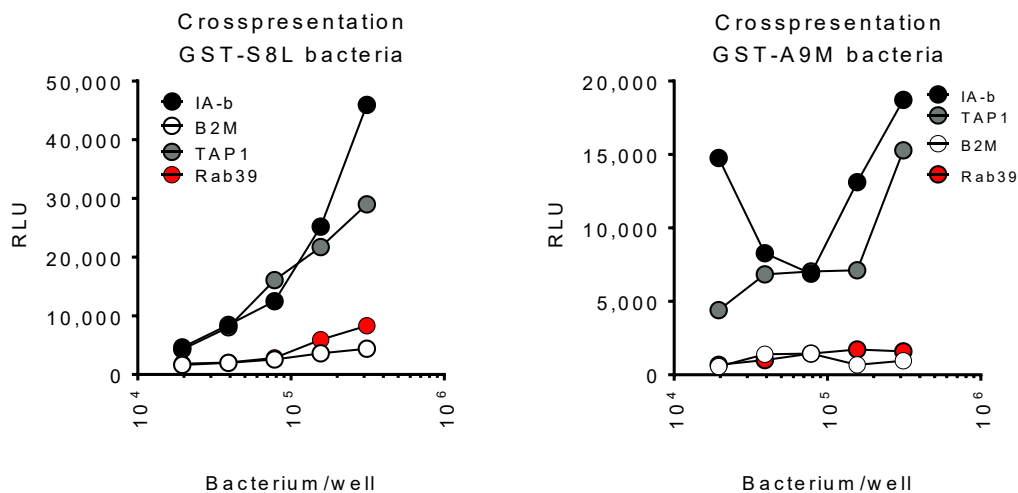
Figure 35. **Rab39a affects crosspresentation of TAP independent bacterial antigens.**

1.25 x10^4 DC3.2R cells were transfected with 50 nM sirna pools using Lipofectamine RNAiMax. After 48 hours, 5 x 10^4 Rf33-Luc or 12.64-Luc cells were added along with the indicated amounts of heat killed bacteria *(E.coli)*. After overnight incubation (~18 hours), Luciferase activity of the T cells were read using Oneglo reagent (Promega). (Experiment done by Colbert, J)

K. Rab39a inhibits phagosomal degradation of antigens

In the case of biomag-ova, latex bead-ova and soluble ova, one way Rab39a could have affected the XPT of these antigens was through the modulation of antigen degradation in the phagosomes. These forms of antigen were previously shown to be processed mainly in the cytosol by the proteasome, as proteasome inhibitors completely abolished presentation (in this case, ova-beads) (33). Furthermore, the presentation of these antigens was resistant to chloroquine, a weak base that inhibits phagosomal proteases by increasing phagosome pH (33). Supporting this, excessive antigen degradation in the phagosomes was shown to be detrimental to the XPT of these antigens (73, 125). Dendritic cells express the NADPH oxidase (NOX2) complex that alkalinizes the phagosomes, preventing excessive degradation of antigen (73). When this complex was perturbed, crosspresentation of ova was reduced. When the transcription factor TFEB was overexpressed in DCs, XPT of ova was decreased due to enhanced phagosomal proteolytic activity (125). In APCs, TFEB positively regulated phagocytosis and lysosomal functions. Thus, it was possible that the lack of Rab39a somehow caused increased degradation of ova in our experiments that led to decreased XPT.

To test this, we fed knockout or Rab39a rescued DCs with beads conjugated to DQ-ovalbumin (DQ-ova). DQ-ova is ovalbumin attached to Bodipy FL dye. While the ova protein is intact, the high concentration and proximity of the attached dyes cause them to self-quench, resulting in low fluorescence. Upon

ova degradation, the dyes are freed, resulting in bright fluorescence. When we analyzed whole cells (Figure 36), we saw a very slight decrease in ova degradation in cells that expressed Rab39a.

However, when we looked at isolated phagosomes, we saw a much bigger phenotype. Knockout or rescued cells were fed with magnetic beads conjugated to ovalbumin. After the phagosomes have been isolated, the level of ovalbumin remaining on the beads/phagosomes was determined by staining with a monoclonal anti-ova antibody. This assay has shown that Rab39a reduced ova degradation in the phagosomes (Figure 37).

Because of this finding, one could hypothesize that Rab39a was preventing excessive antigen degradation in the phagosomes, thereby preserving more antigen that could feed into the XPT pathway.
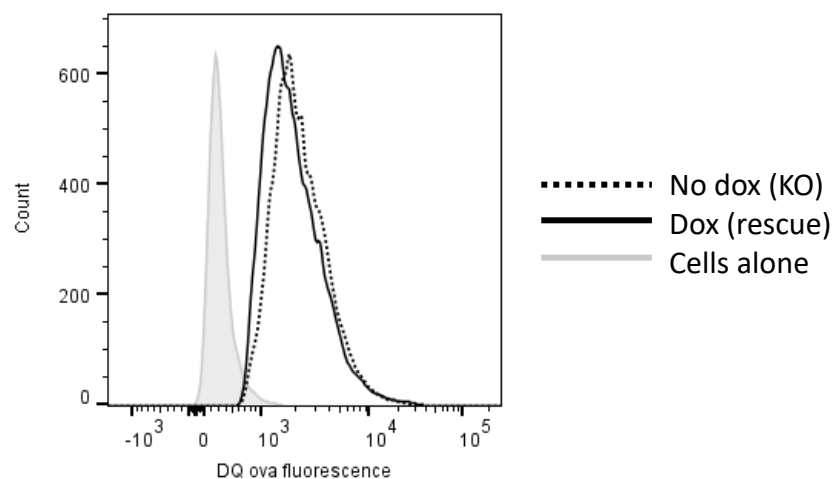
	Workspace Annotation	Geometric Mean : Alexa Fluor 488-A
☐	dox	1914
☐	no dox	2195
▨	cells alone	328

Figure 36. **Rab39a slightly reduces overall ova degradation.**

1.25×10^5 DC3.2-Rab39aKO-Rab39a cells were incubated with 1 µg/ml dox for 24 hours in a 12 well plate. Cells were fed at 1 bead / cell of 6 µm magnetic beads conjugated with DQ ova 4 hours at 37°C. Wells were washed and the cells were detached with versene, washed in 1%FCS-PBS then run for facs analysis. Shown are gMFI of cells that have eaten beads. Data shown represents one experiment of $\geq$3.
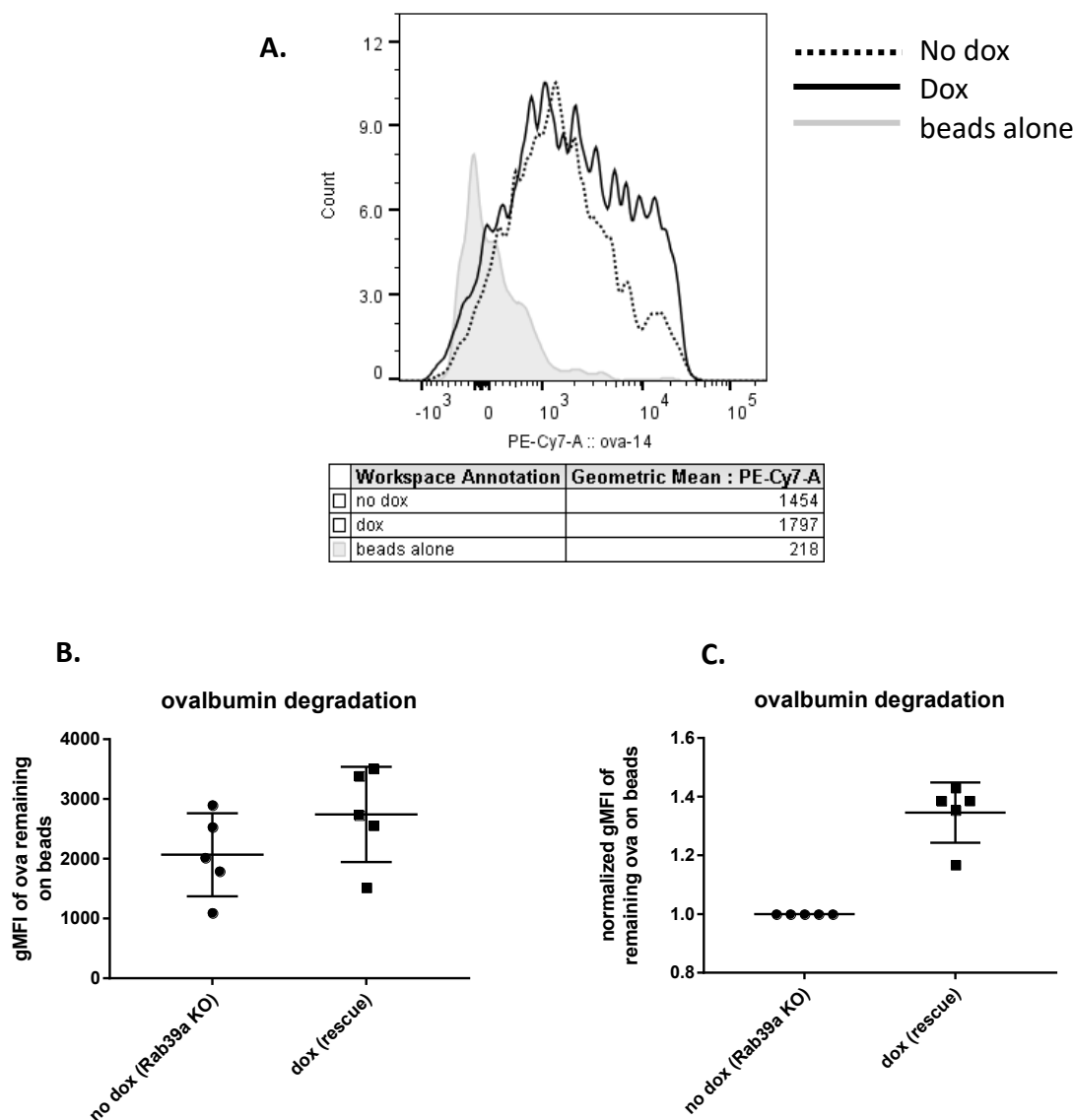
Figure 37. Phagosomes from Rab39a positive cells are less degradative

A. Representative experiment. 1.25 x 10^5 DC3.2-rab39aKO-rab39a-L^d cells were incubated with or without 1 μg/ml dox for 48 hours in a 12 well plate. Cells were fed at 1 bead / cell of biotinylated-ova conjugated to 6 μm magnetic beads for 4 hours. Isolated phagosomes were washed, permeabilized and stained for ovalbumin. **B.** As in A, but showing combined data for 5 independent experiments. The paired student's t-test is p=0.0025. **C.** As in B, but the MFI of dox setups was normalized to no dox to show extent of inhibition of ova degradation.

i. Rab39a does not enhance XPT by limiting degradation of ovalbumin

While we observed that Rab39a was inhibiting phagosomal degradation of ova, we wanted to know if this inhibition of degradation was responsible for the augmentation of XPT seen in Rab39a expressing cells. This was because we also found that Rab39a was necessary for the efficient XPT of vacuolar pathway antigens - a process that heavily depended on phagosomal proteases (27). Thus, if Rab39a inhibited degradation of antigen to preserve them for the phagosome to cytosol pathway (biomag-ova), then its knockdown should have enhanced the presentation of vacuolar bacteria-ova.

To examine this, we deliberately inhibited phagosomal degradation by treating knockout or Rab39a rescued dendritic cells with leupeptin - a broad inhibitor of cysteine and serine proteases. Once again, Rab39a expressing cells were better at XPT as compared to the knockout (Figure 38). Furthermore, the advantage of Rab39a rescued cells over the knockout remained in the presence of inhibitor.

Because the deliberate inhibition of phagosomal degradation did not abolish the XPT advantage of Rab39a expressing cells, we hypothesized that Rab39a improved DC XPT in a mechanism(s) distinct from just the inhibition of antigen degradation.
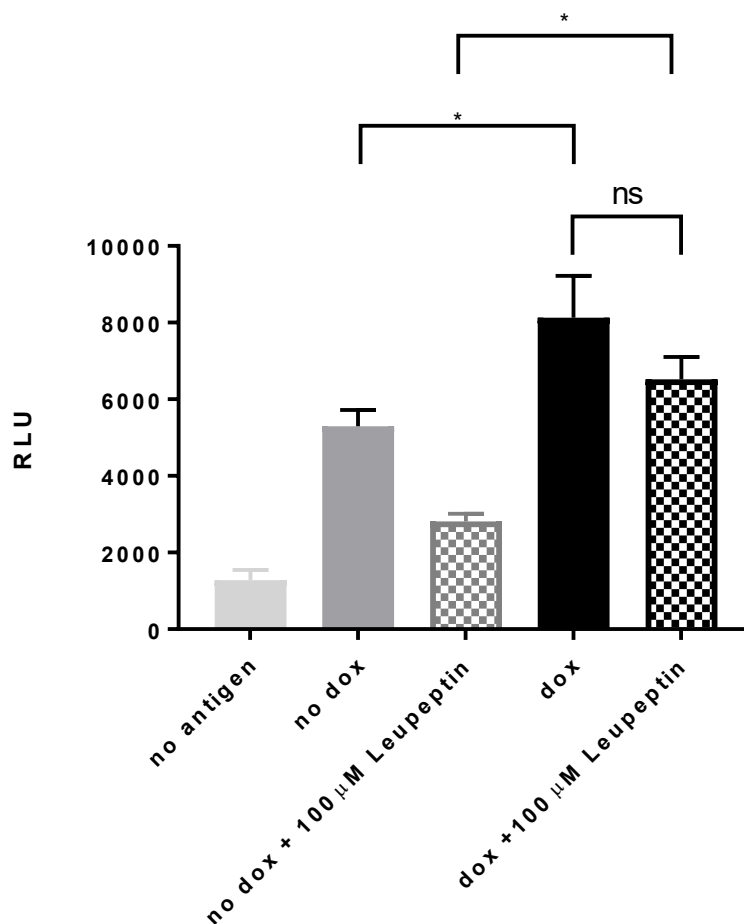
Figure 38. Leupeptin does not increase xpt and does not abolish rab39a phenotype.

1.25×10^4 DC3.2-Rab39aKO-Rab39a cells were incubated with 1 μg/ml dox for 48 hours in a 96 well plate. Then, biomag-ova beads (μg of ova) were added along with 5 x 10^4 Rf33-Luc with or without the listed final concentration of leupeptin. After overnight incubation, luciferase activity from the T cells were quantified using Oneglo reagent (Promega). Error bars indicate standard deviation between triplicate wells. * $p \leq 0.05$ based on ANOVA. Data represents one experiment of 3.

L. Rab39a affects peptide loading in the phagosome

Our experiments have so far suggested that Rab39a was playing a role in the phagosomes that was not involved in antigen processing. We then reasoned that perhaps Rab39a was facilitating XPT by enhancing peptide loading in the phagosomes. This could be achieved through several ways. Rab39a could have been delivering MHC Class I molecules to the phagosome for loading. It could also have been delivering specialized chaperones that mediate peptide loading onto Class I (similar to H2-DM and DO in the Class II pathway). Perhaps it could also have been modulating the phagosome environment to optimize Class I loading (though we did not observe a significant effect on pH by Rab39a).

To test if Rab39a affected peptide loading in the phagosomes, we initially made use of N and C terminally extended SIINFEKL beads (peptide beads). We extended the SIINFEKL peptide by a cysteine containing amino acid stretch at the N or C terminal end, allowing us to conjugate these peptides to magnetic beads via a disulfide bond.

The rationale of this was that these peptides would not need proteases to be released from the beads, as opposed to covalently bound full length ova. Instead, these peptides would be released from the beads due to the reducing environment dendritic cells generate in their phagosomes. This phenomenon has been shown to be mediated by the Gamma-interferon-inducible lysosomal thiol reductase (GILT) (126). Once released, the short peptides (particularly the N-

terminal extended ones) would only need a little trimming (mediated by phagosomal petidases such as IRAP) before they were loaded onto phagosomal Class I.

We thus fed siRNA treated dendritic cells with either N-extended CQLE(SIINFEKL) or C-extended (SIINFEKL)TEWC peptide beads. Our results have shown that efficient XPT of both these beads still depended on Rab39a (Figure 39). Because both N and C terminal extended beads were affected, we ruled out the possibility that Rab39a was specifically used to just recruit N or C terminal exopeptidases to the phagosome (such as IRAP) and hypothesized that Rab39a was instead affecting Class I loading.

To further refine this experiment, we modified the SIINFEKL peptide through the generation of cysteine mutants (data not shown). We searched for a position in SIINFEKL wherein T cell recognition of the peptide MHC was not abolished even if this position was mutated to a cysteine. We found that CIINFEKL, bound to H2-K^b, was still able to be recognized by our reporter T cells (RF33-Luc).

We now had a peptide that did not even require trimming. This peptide only needed to be released from beads – after which, it was ready to bind available Class I. When we fed siRNA treated cells with CIINFEKL beads, we observed that even with this form of antigen, efficient XPT required Rab39a (Figure 40). Rab39a rescue of knockout cells also increased XPT of this form of

antigen (Figure 41). Furthermore, this form of antigen was TAP-independent. This meant that CIINFEKL loading onto MHC Class I was occurring within the bead containing phagosome itself. This was because TAP1 is primarily used to transfer cytosolically processed peptides into the ER (127) or back into the phagosome (41). The CIINFEKL construct therefore was presented via a completely phagosomal route still dependent on Rab39a.

The same effect was seen when DCs were fed with a CSNENMETM flu peptide conjugated in the same manner (Figure 42). The peptide bound H2-D[b] and was recognized by reporter 12.64-Luc cells in a TAP independent but Rab39a dependent manner. Thus, Rab39a was shown to also affect loading on a different MHC-I allele.

The above results strongly supported our hypothesis that Rab39a was enhancing phagosomal Class I loading in the phagosomes, rather than affecting XPT through a different process such as pH modulation or antigen processing.

xpt of disulfide linked CQLESIINFEKL

xpt of disulfide linked SIINFEKLTEWC
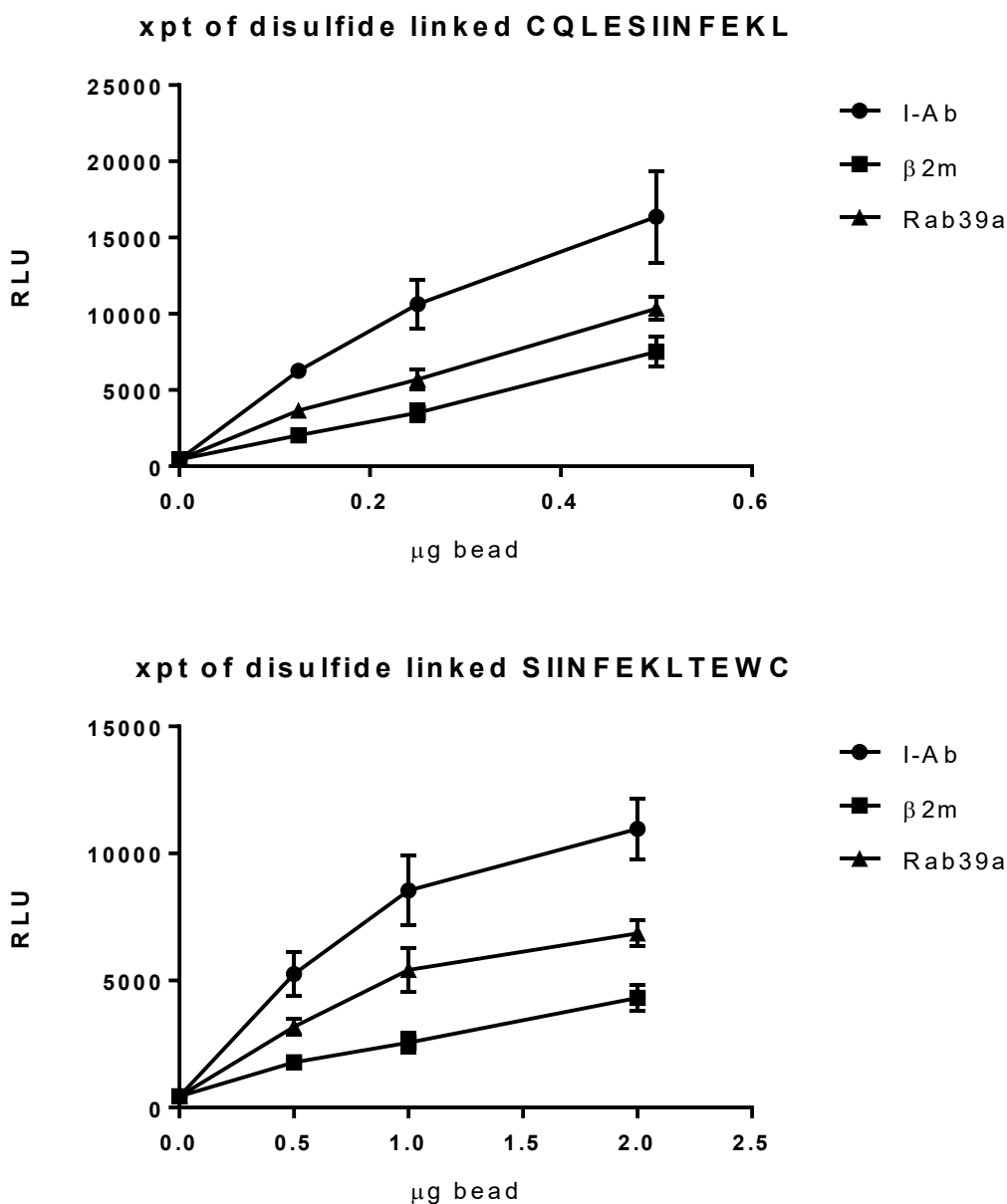
Figure 39. **Rab39a sirna decreases presentation of disulfide conjugated peptide beads.**

2.5×10^3 DC3.2R cells were transfected with 50 nM sirna using Lipofectamine RNAiMax in reducing agent free media (cDMEM). After 48 hours, 1×10^4 Rf33-Luc were added along with the indicated amounts of biomag conjugates. After overnight incubation (~18 hours), Luciferase activity of the T cells were read using Oneglo reagent (Promega). Error bars indicate the standard deviation between triplicate wells. Data shown represents one experiment of $\geq$ 3. All wells with antigen have p-values (ANOVA) $\leq$ 0.05 between β2m or Rab39a vs negative control I-Ab.

xpt of disulfide linked ovalbumin

xpt of disulfide linked CIINFEKL
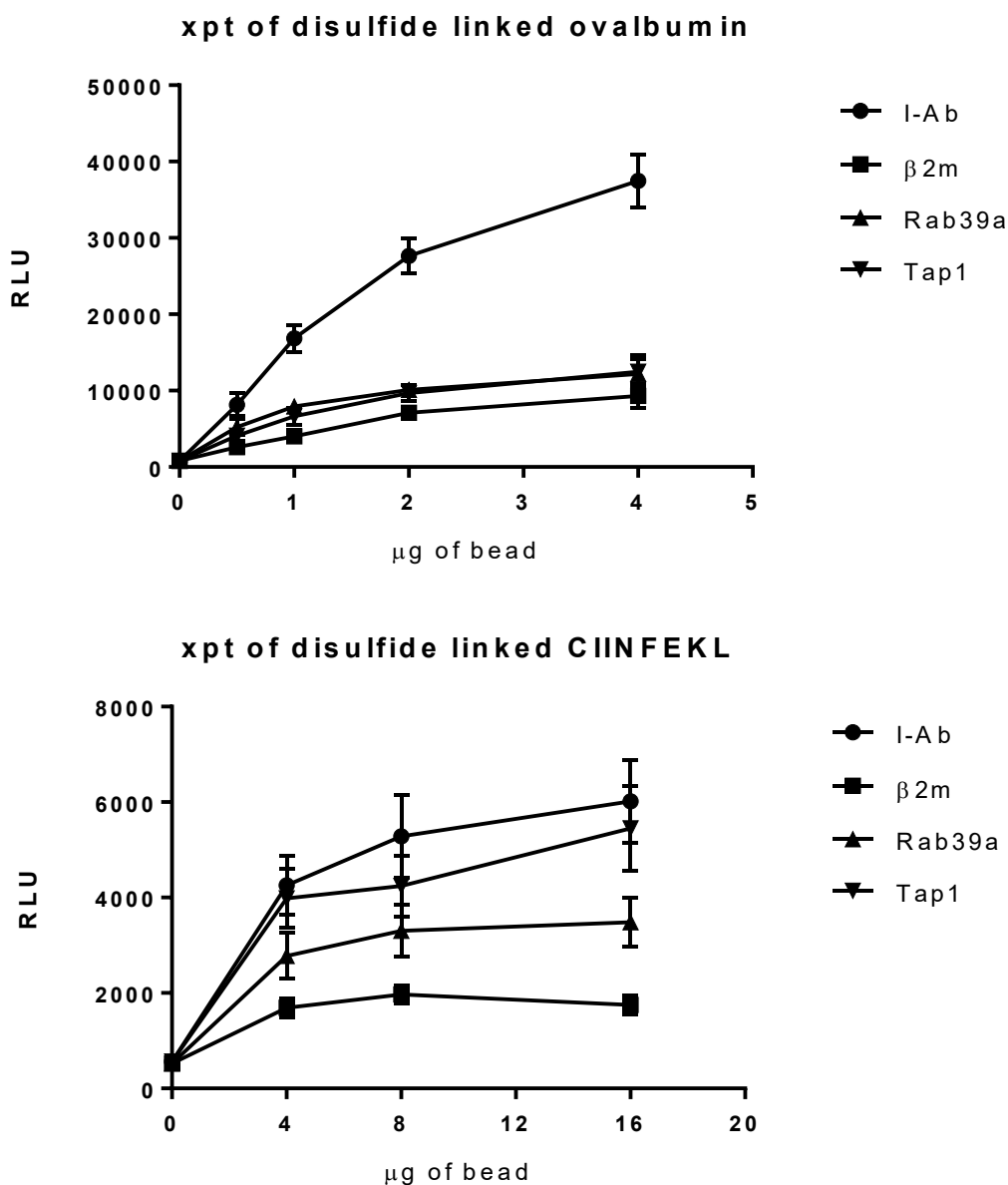
Figure 40. **Rab39a sirna decreases presentation of preformed peptide.**
2.5 x10^3 DC3.2R cells were transfected with 50 nM sirna pools using Lipofectamine RNAiMax in reducing agent free media (cDMEM). After 48 hours, 1 x 10^4 Rf33-Luc were added along with the indicated amounts of biomag conjugates. After overnight incubation (~18 hours), Luciferase activity of the T cells were read using Oneglo reagent (Promega). Error bars indicate the standard deviation between triplicate wells. Data shown represents one experiment of $\geq$ 3. All wells with antigen have p-values (ANOVA) $\leq$ 0.05 between β2m or Rab39a vs negative control I-Ab. For CIINFEKL, none of the wells for Tap1 are significant vs the control.

xpt of disulfide linked CIINFEKL
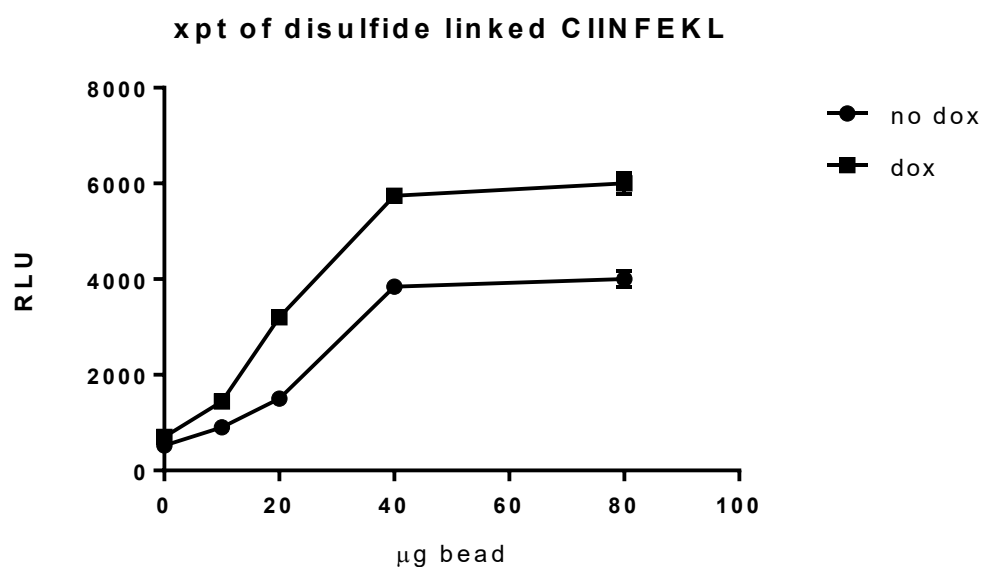
Figure 41. Rab39a rescue of knockout DCs increases crosspresentation of peptide beads.

1.25×10^4 DC3.2-Rab39aKO-Rab39a cells were incubated with 1 µg/ml dox for 48 hours in a 96 well plate. Then, the indicated amounts of biomag-CIINFEKL beads were added along with 5×10^4 Rf33-Luc. After overnight incubation, luciferase activity from the T cells were quantified using Oneglo reagent (Promega). Error bars indicate the standard deviation between triplicate wells. Data shown represents one experiment of ≥ 3. All wells with antigen have p-values (ANOVA) ≤ 0.05 between no dox and dox.
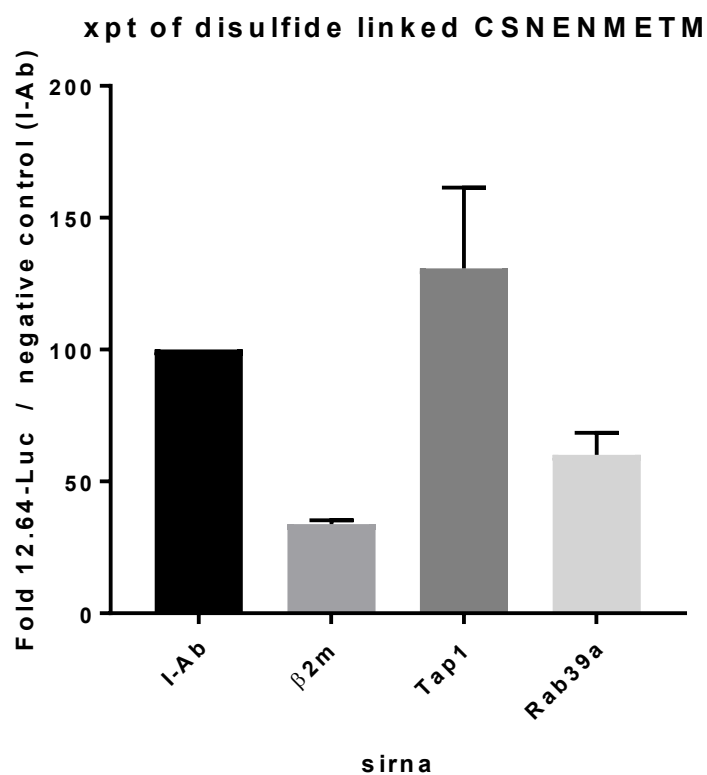
Figure 42. **Rab39a sirna decreases presentation of preformed peptide.**
2.5 x10^3 DC3.2R cells were transfected with 50 nM sirna pools using Lipofectamine RNAiMax in reducing agent free media (cDMEM). After 48 hours, 1 x 10^4 Rf33-Luc were added along with the indicated amounts of biomag conjugates. After overnight incubation (~18 hours), Luciferase activity of the T cells were read using Oneglo reagent (Promega).
This experiment was performed by Jeff Colbert

M. Rab39a increases open conformers in phagosomes

Our findings that showed that Rab39a is required for the optimal XPT of an antigen that neither requires processing nor cytosolic transfer led us to hypothesize that Rab39a facilitates either delivery of MHC Class I to the phagosome, and/or peptide loading on MHC Class I already present there. To study this, we transduced the conditional Rab39a knockout DC line with H2-L^d, a Class I allele not normally present in C57BL/6 mice from which the DC line was derived. H2-L^d was a useful tool for studying peptide-Class I loading because there were antibodies that specifically recognized peptide empty forms (64-3-7 antibody) or peptide occupied forms (30-5-7s antibody) of the Class I molecule (128). This would help us measure phagosomal Class I loading.

Analysis of phagosomes derived from Rab39a positive cells showed a unique pattern of open and closed H2-L^d (Figure 43). While the majority of phagosomes were either negative or very low in either form of H2-L^d, a subset of these vesicles contained moderate to high amounts of both. There was also a subpopulation that mainly contained just the open or just the closed form of H2-L^d. An interesting finding of this assay was that in Rab39a KO cells (-dox), there was a significantly lower subset of phagosomes with only open H2-L^d molecules as compared to the Rab39a-reconstituted cells (+dox) (Figure 44). Rescuing the KO cells with either the DN or CA forms of Rab39a did not recover this subset (Figure 45). This phenotype seemed to be specific for open H2-L^d molecules as

the levels of MHC Class II and Lamp1 in the phagosomes were not affected

(Figure 46).
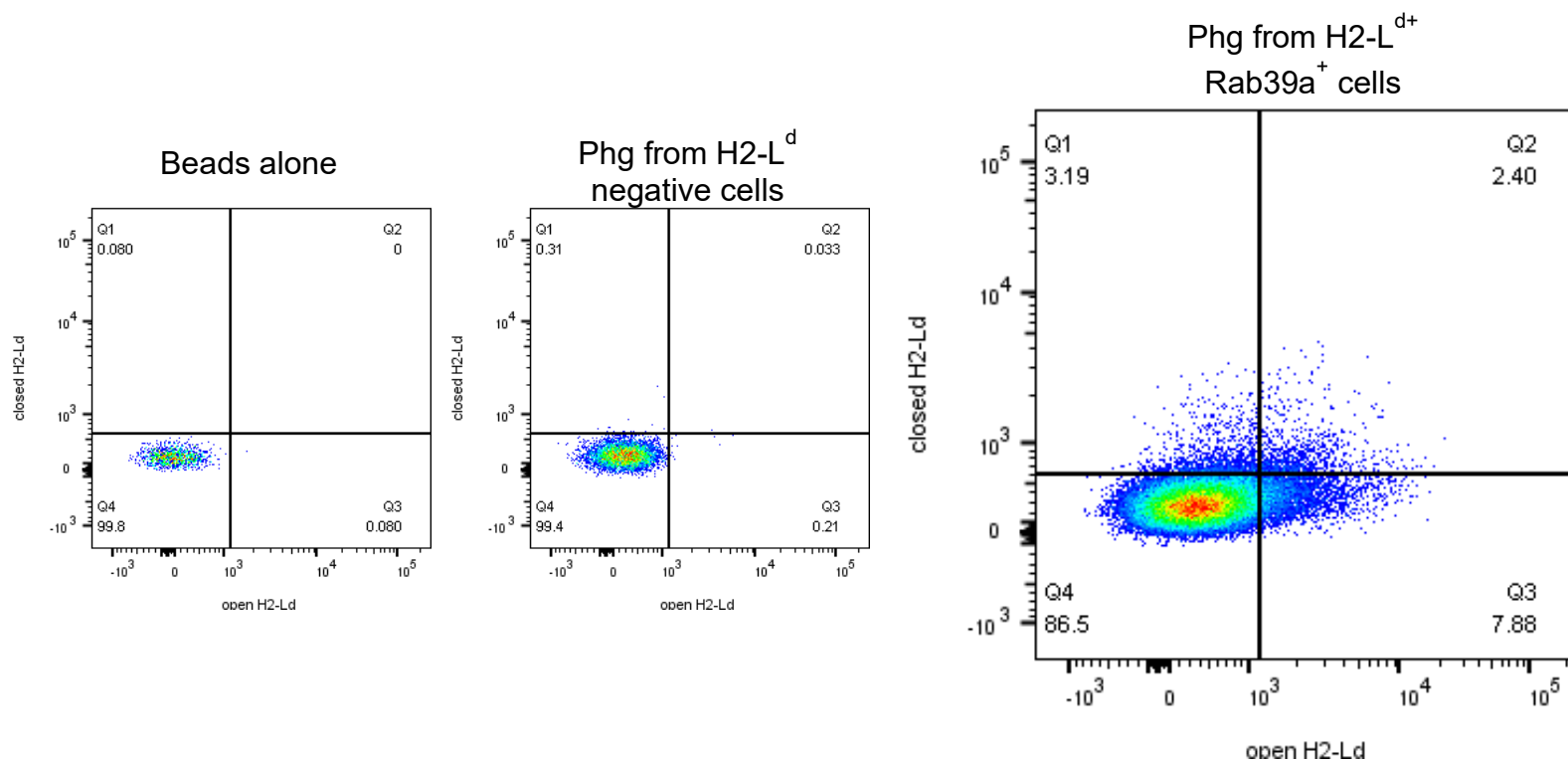
Figure 43. **Open and closed forms of H2-L^d are enriched in different subsets of phagosomes.**

1.25 x 10^5 DC3.2-Rab39aKO-Rab39a-L^d cells were incubated with 1 µg/ml dox for 48 hours in a 12 well plate. Cells were fed at 1 bead / cell of biotinylated 6 µm magnetic beads for 2 hours. Phagosomes were isolated using the listed protocol. Isolated phagosomes were washed, permeabilized and stained for open and closed H2-L^d. As a control, phagosomes were also isolated from dendritic cells lacking H2-L^d. Data shown represents one experiment of ≥3.
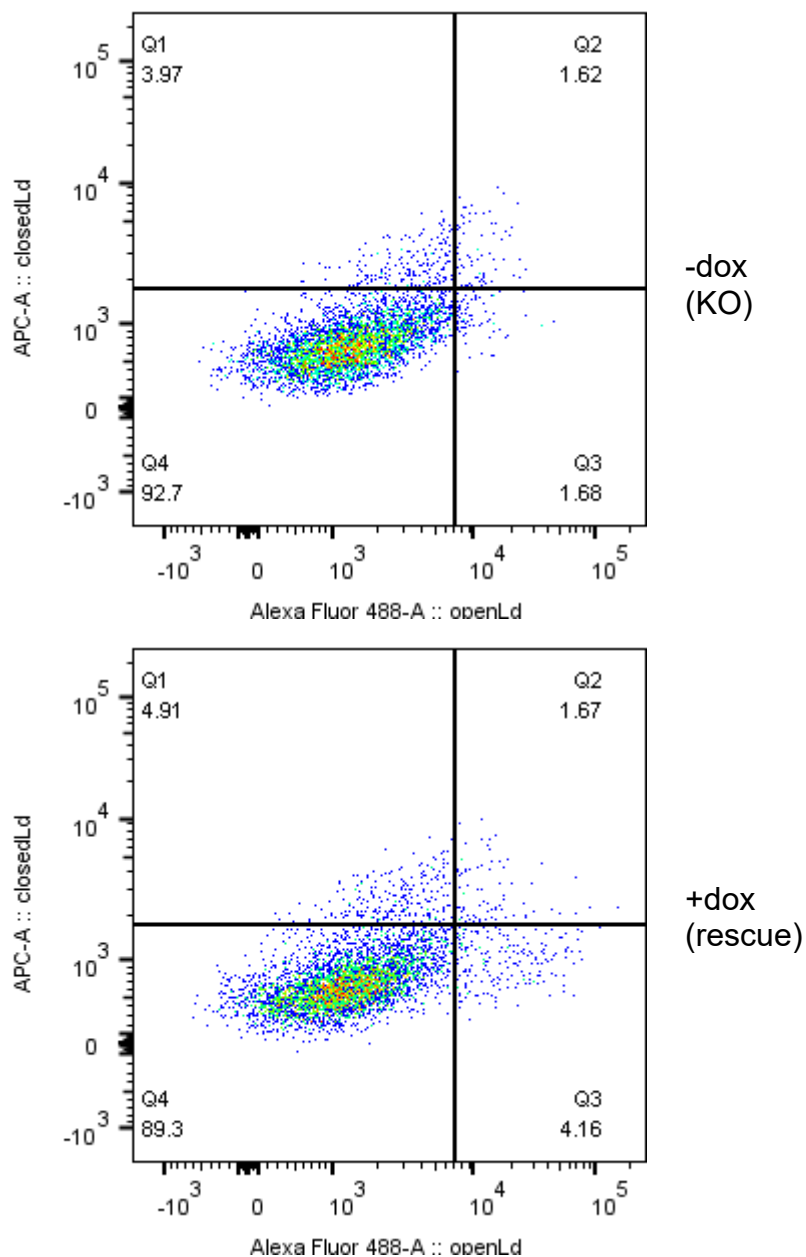
Figure 44. **Open H2-L^{d} conformers is enriched in phagosomes from Rab39a positive cells.**

1.25 x 10^{5} DC3.2-Rab39aKO-Rab39a-L^{d} cells were incubated with or without 1 µg/ml dox for 48 hours in a 12 well plate. Cells were fed at 1 bead / cell of biotinylated 6 µm magnetic beads for 4 hours. Magnetic bead phagosomes were isolated using the listed protocol. Phagosomes were washed, permeabilized and stained for open (64-3-7) and closed (30-5-7s) forms of H2-L^{d}. Data shown represents one experiment of $\geq$3.
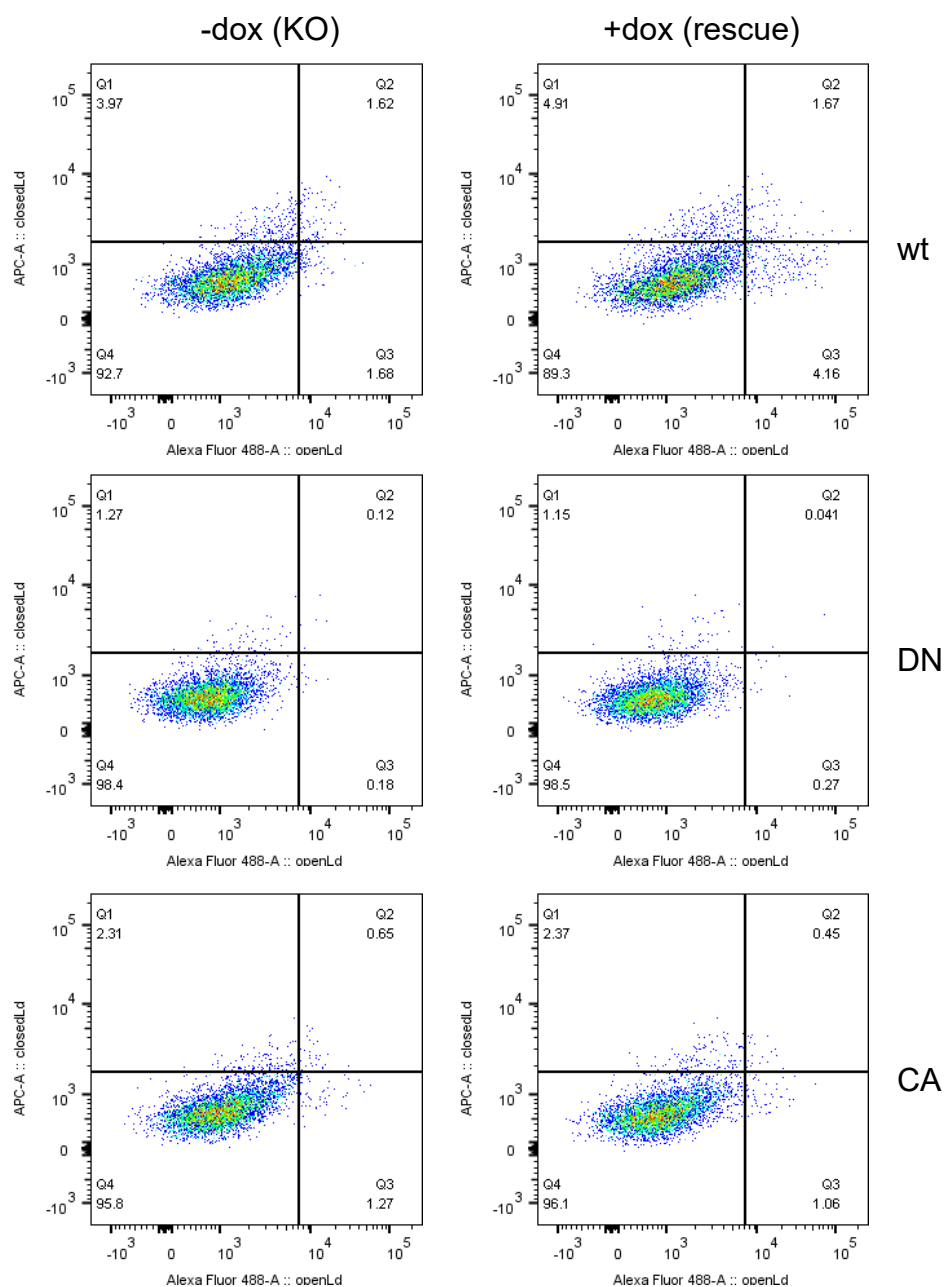
Figure 45. **Only the wt form of Rab39a is able to increase open H2-L^d in the phagosomes.**

1.25 x 10^5 of cells with wt, DN or CA Rab39a were incubated with or without 1 µg/ml dox for 48 hours in a 12 well plate. Cells were fed at 1 bead / cell of biotinylated 6 µm magnetic beads for 4 hours. Magnetic bead phagosomes were isolated using the listed protocol. Phagosomes were washed, permeabilized and stained for open and closed forms of H2-L^d. Top panels representing wt Rab39a are the same as in the previous figure (Figure 44). Data shown represents one experiment of $\geq$3.
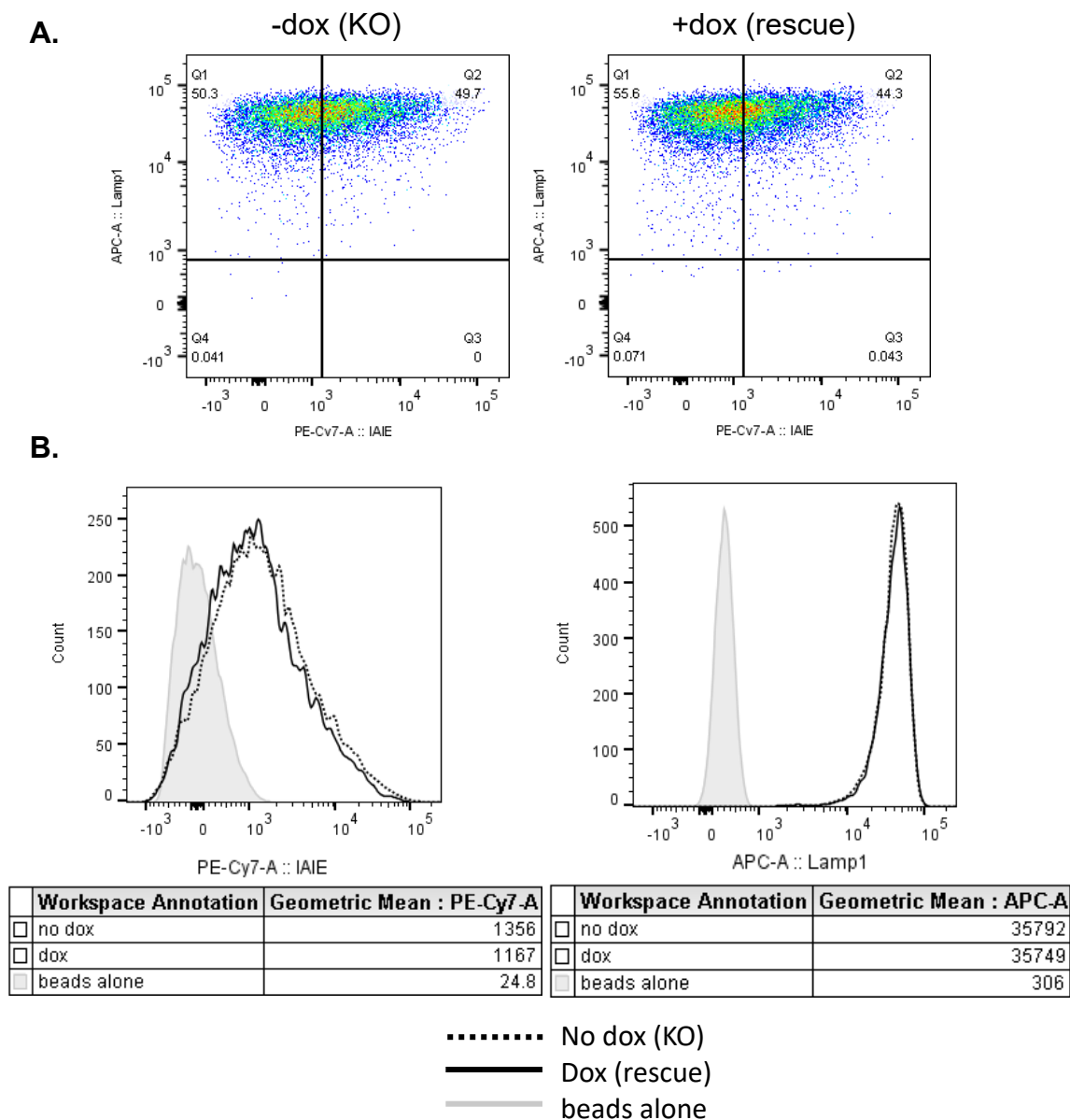
Figure 46. **Rab39a rescue does not change phagosomal MHC Class II or Lamp-1 levels.**

(A) 1.25 x 10^5 DC3.2-Rab39aKO-Rab39a-L^d cells were incubated with or without 1 µg/ml dox for 48 hours in a 12 well plate. Cells were fed at 1 bead / cell of biotinylated 6 µm magnetic beads for 4 hours. Magnetic bead phagosomes were isolated using the listed protocol. Phagosomes were washed, permeabilized and stained for MHC Class II (I-A / I-E) and Lamp1. (B) Shown are phagosomal gMFI of indicated stains. Data shown represents one experiment of ≥3.

i. Rab39a does not increase surface open or closed forms of H2-L^d

The increase in open conformers mediated by Rab39a was found selectively in phagosomes, as steady state cell surface levels of both open and closed H2-L^d were not affected (Figure 47). Incubating the cells at 25°C increased overall Class I on the surface by allowing trafficking of unstable Class I from the ER and slowing down their internalization from the surface. Knockout and rescued cells had similar levels of H2-L^d despite this. Because of this finding, we hypothesized that the overall increase of open MHC Class I in the phagosomes mediated by Rab39a was not due to an overall increase in Class I expression.

A.

Open H2-L^d Closed H2-L^d 37°C

Workspace Annotation	Geometric Mean : Alexa Fluor 488-A
☐ no dox - 37C	389
☐ dox - 37C	344
☐ unstained cells	115

Workspace Annotation	Geometric Mean : Pacific Blue-A
☐ no dox - 37C	3034
☐ dox - 37C	3326
☐ unstained cells	181

B.

25°C

Workspace Annotation	Geometric Mean : Alexa Fluor 488-A
☐ no dox - 25C	973
☐ dox - 25C	889
☐ unstained cells	115

Workspace Annotation	Geometric Mean : Pacific Blue-A
☐ no dox - 25C	4159
☐ dox - 25C	5172
☐ unstained cells	181

```
........  No dox (KO)
———————  Dox (rescue)
———————  Unstained cells
```

Figure 47. **Rab39a rescue does not change cell surface levels of open or closed H2-L^d.**

1.25×10^5 DC3.2-Rab39aKO-Rab39a-L^d cells were incubated with or without 1 µg/ml dox for 24 hours at 37°C in a 12 well plate. Then, cells were transferred to either (A) 37°C or (B) 25°C for overnight incubation. Cells were detached and stained for the open and closed forms of H2-L^d. Data shown represents one experiment of ≥3.

N. Phagosomal open conformers of Class I can be loaded with peptide

Open forms of Class I in the phagosome could potentially be ones that become loaded with peptides. Thus, with the antigen, phagosomal proteases / trimming peptidases (27), components of the peptide-loading complex (40, 41) and now the MHC Class I molecule itself, the phagosome becomes a self-contained organelle capable of crosspresentation.

The 64-3-7 antibody used in our assays detected open forms of MHC Class I whether the Class I was bound to β2-microglobulin (β2m) or was β2m free (129). It has been shown that β2m free Class I can be detected on the surface and can be utilized in other cell processes besides XPT, such as in NK cell recognition (130). Furthermore, open MHC Class I has been shown to be unstable and is internalized quickly for degradation (131, 132). Thus, it was important to determine whether the open H2-L^d enrichment found in the phagosomes of Rab39a positive cells can actually be used for antigen presentation.

To do this, phagosomes were obtained from KO or Rab39a positive cells, permeabilized *in vitro* with saponin and pulsed with SPSYVYHQF, a peptide that can bind to H2-L^d (133). Figure 48 shows that with peptide, the open H2-L^d in the phagosomes decreased, while closed H2-L^d increased (though sometimes the

increase in closed H2-L^d was very small). This result showed that the form of

Class I enriched in Rab39a positive cells was functional and peptide receptive.

Pulsing with an irrelevant peptide (SIINFEKL) had no effect (Figure 49). It is

important to note that the peptide pulsing experiments were performed in a β2m-

free solution (1%BSA-pbs). This showed that at least a fraction of the open

conformers in the phagosomes must be associated with β2m and are ready to

accept peptides.

Open H2-L^d

Workspace Annotation	Geometric Mean : Alexa Fluor 488-A
□ no peptide	1495
□ 5 uM S9F	1021
▨ beads alone	193

Closed H2-L^d

Workspace Annotation	Geometric Mean : PE-A
□ no peptide	1168
□ 5 uM S9F	1652
▨ beads alone	66.9
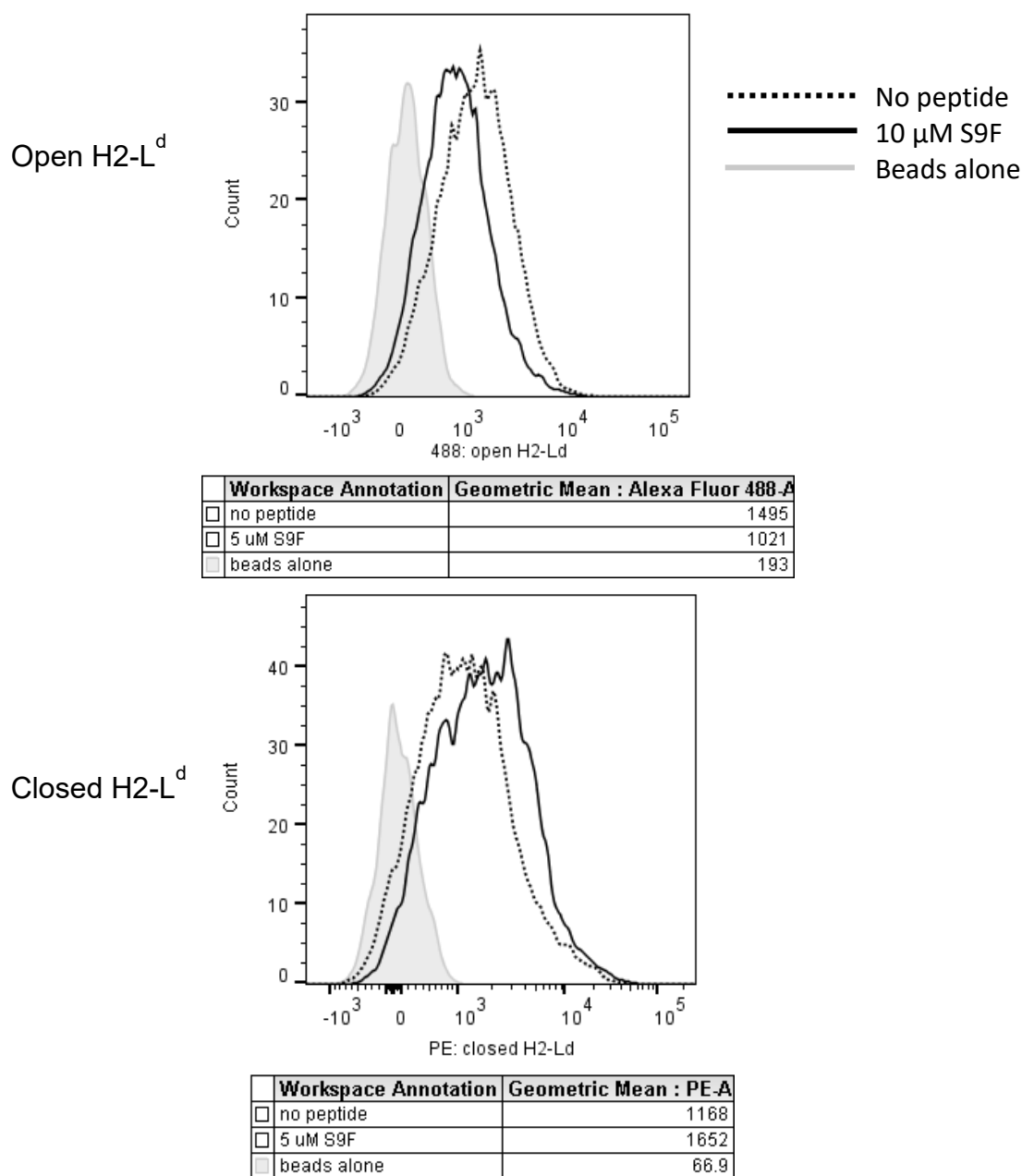
Figure 48. A fraction of phagosomal open H2-Ld are peptide receptive.

1.25×10^5 DC3.2-Rab39aKO-Rab39a-L^d cells were incubated with 1 µg/ml dox for 48 hours in a 12 well plate. Cells were fed at 1 bead / cell of biotinylated 6 µm magnetic beads for 1 hour. Isolated phagosomes were washed, permeabilized and pulsed for 3 hours with the indicated peptide at 25°C. Phagosomes were then washed and stained for the open and closed forms of H2-L^d. Data shown represents one experiment of $\geq$3.

Open H2-L^d

	Workspace Annotation	Geometric Mean : Alexa Fluor 488-A
☐	no peptide	724
☐	10 uM S8L	759
☐	10 uM S9F	462
☐	beads alone	60.4

Closed H2-L^d

	Workspace Annotation	Mean : APC-A
☐	10 uM S9F	296
☐	10 uM S8L	255
☐	no peptide	241
☐	beads alone	112
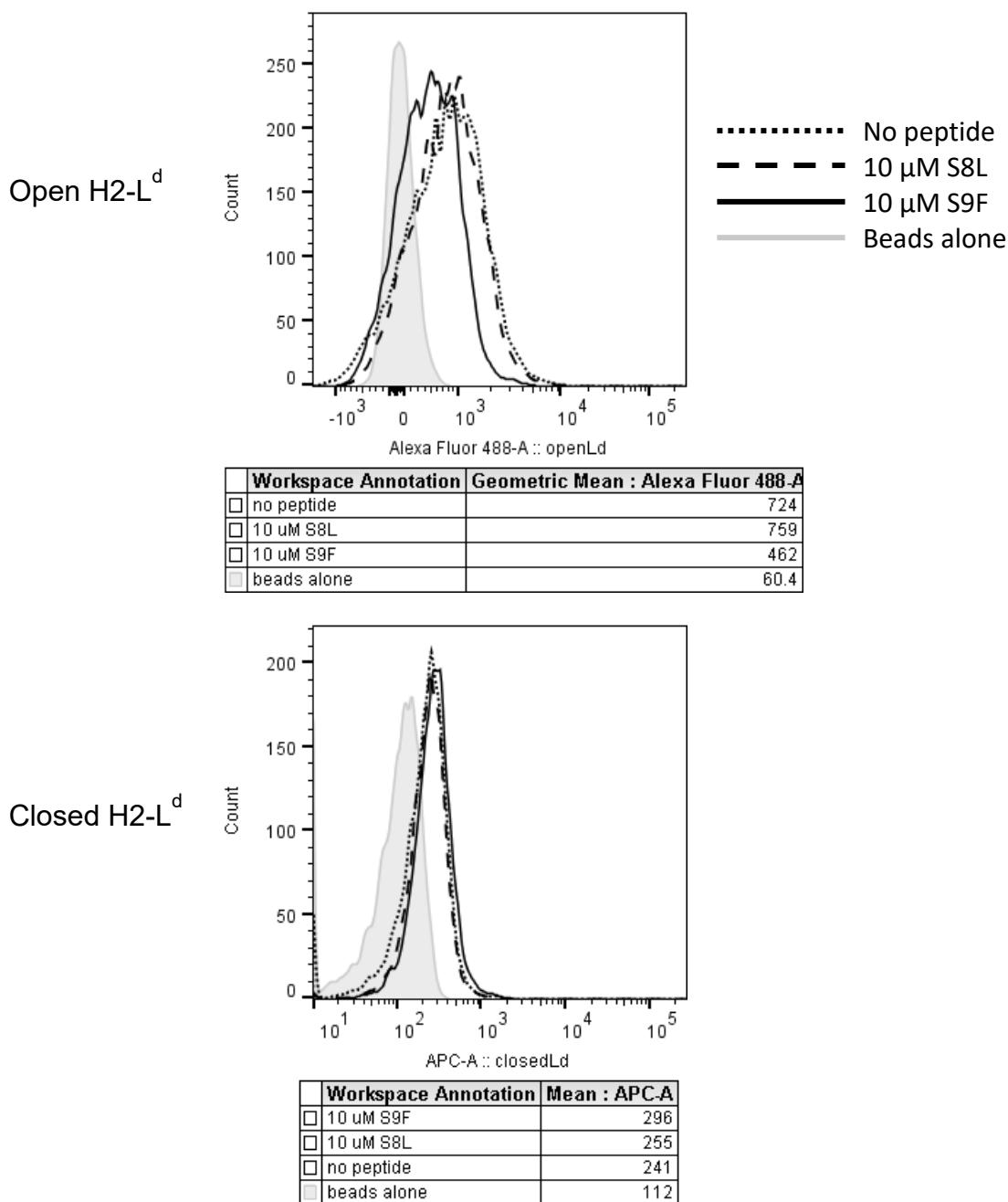
Figure 49. Only the correct peptide can load phagosomal open H2-L^d.

1.25 x 10^5 DC3.2-Rab39aKO-Rab39a-L^d cells were incubated with 1 µg/ml dox for 48 hours in a 12 well plate. Cells were fed at 1 bead / cell of biotinylated 6 µm magnetic beads for 4 hours. Isolated phagosomes were washed, permeabilized and pulsed for 3 hours with the indicated peptides dissolved in 1% BSA-PBS at 25°C. Phagosomes were then washed and stained for the open and closed forms of H2-L^d. Data shown represents one experiment of ≥3.

O. Phagosomal open conformers are sensitive to endosomal proteases

The percentage of phagosomes that are solely enriched with open H2-L^d greatly varied between experiments, but in all cases, rescue with Rab39a increased this percentage at least twofold compared to KO cells. Because of this variability, we extensively searched for factors that might influence the appearance of this seemingly unique population of phagosomes.

In this search, we have found that the open form of H2-L^d was extremely sensitive to protease degradation, as addition of a serine and cysteine protease inhibitor (Leupeptin) greatly enriched its levels in the phagosomes (Figure 50 and 51). Interestingly, the closed form of H2-L^d was not increased, indicating that this form was resistant to degradation. Treatment of cells with bafilomycin, which not only inactivates proteases due to increasing pH but may also prevent receptor recycling (134), enriched both the open and closed forms of H2-L^d in the phagosomes.

We have previously shown that Rab39a expression reduced degradation in the phagosomes (Figure 37). Thus, it was possible that Rab39a was enriching internalized open H2-L^d in the phagosomes by preventing their degradation. Interestingly, both open and Closed H2-L^d were mainly in phagosomes with little ova degradation (Figure 52). However, it was also possible that Rab39a was

directly involved in delivering Class I molecules to the phagosome rather than just facilitating Class I persistence.
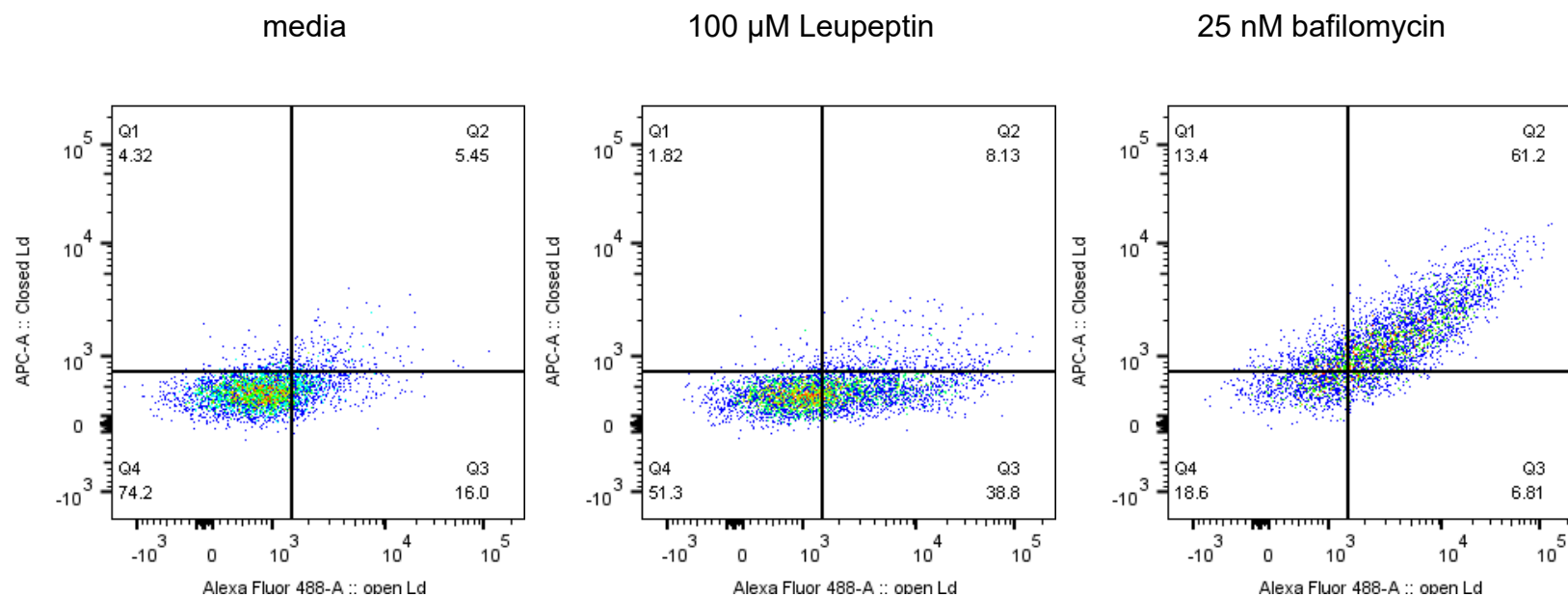
Figure 50. **Open and closed forms of H2-L^d are differentially affected by inhibitors.**
1.25 x 10^5 DC3.2-Rab39aKO-Rab39a-L^d cells were incubated with 1 µg/ml dox for 48 hours in a 12 well plate. Cells were fed at 1 bead / cell of biotinylated ova conjugated to 6 µm magnetic beads for 4 hours with the indicated inhibitors. Phagosomes were isolated using the listed protocol. Isolated phagosomes were washed, permeabilized and stained for open and closed H2-L^d. Data shown represents one experiment of $\geq$3.
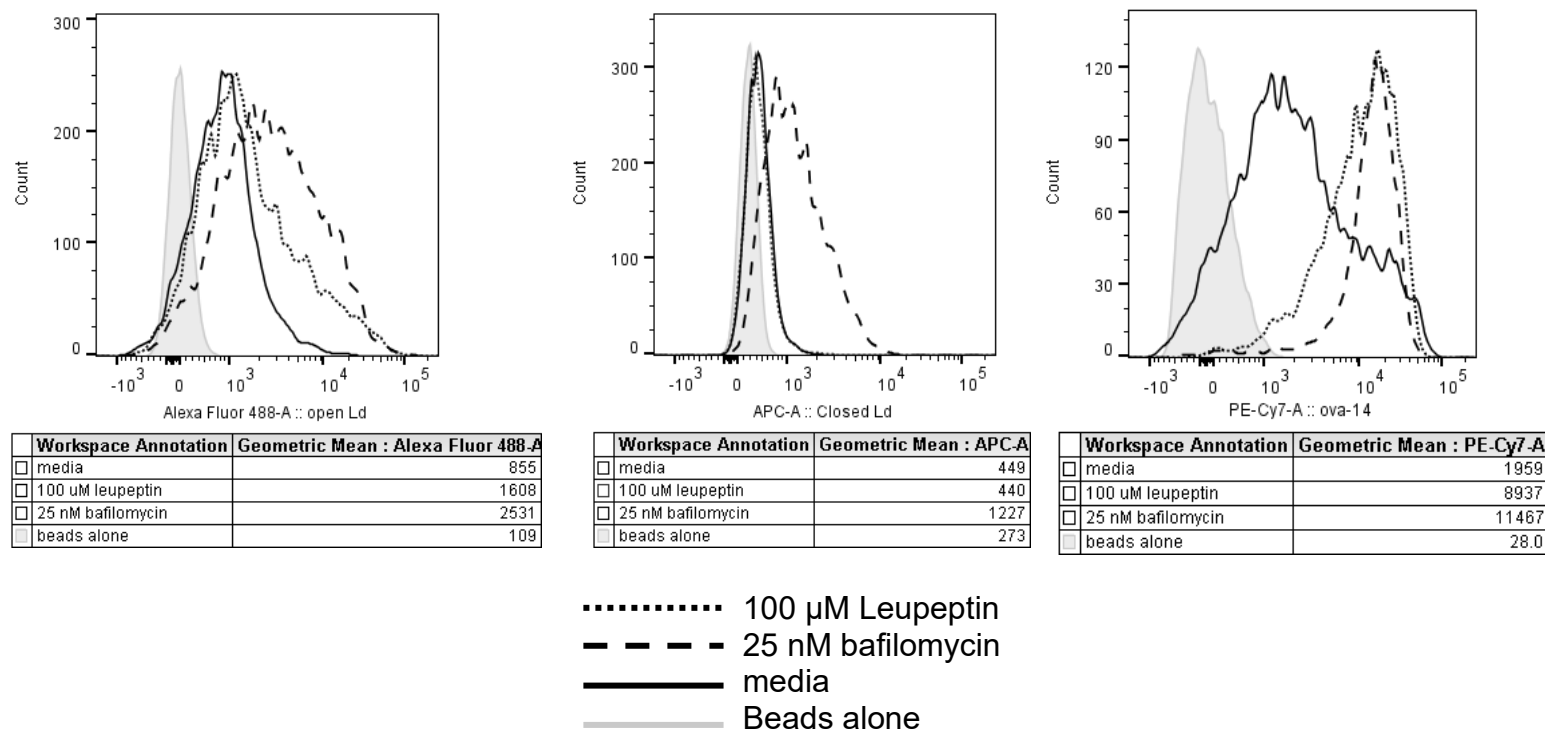
Figure 51. **Open and closed forms of H2-L^d are differentially affected by inhibitors.**
1.25 x 10^5 DC3.2-Rab39aKO-Rab39a-L^d cells were incubated with 1 μg/ml dox for 48 hours in a 12 well plate. Cells were fed at 1 bead / cell of biotinylated ova conjugated to 6 μm magnetic beads for 4 hours with the indicated inhibitors. Phagosomes were isolated using the listed protocol. Isolated phagosomes were washed, permeabilized and stained for open and closed H2-L^d as well as ovalbumin. Shown are phagosomal gMFI of indicated stains. Data shown represents one experiment of $\geq$3.
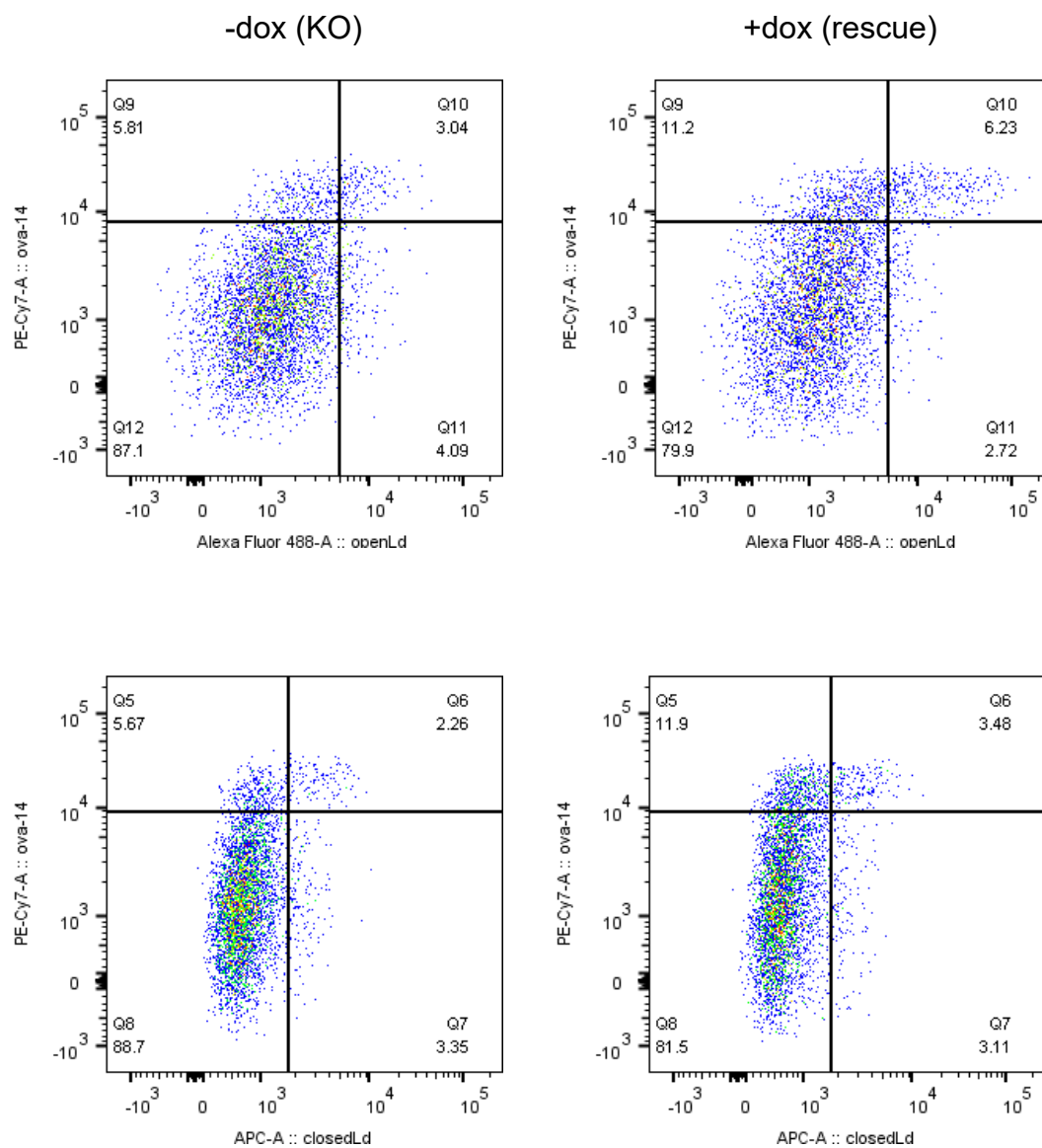
Figure 52. H2-L^{d} is enriched in less degradative phagosomes.

1.25 x 10^{5} DC3.2-Rab39aKO-Rab39a-L^{d} cells were incubated with or without 1 μg/ml dox for 48 hours in a 12 well plate. Cells were fed at 1 bead / cell of biotinylated-ova conjugated to 6 μm magnetic beads for 4 hours. Isolated phagosomes were washed, permeabilized and stained for ovalbumin and open/closed H2-L^{d}. Arbitrary gates divide the plots to show distinct phagosome populations. Data shown represents one experiment of $\geq$3.

P. Brefeldin A reduces Rab39a-dependent open H2-L^d molecules in phagosomes.

In order to shed light on the source of the enriched open H2-L^d we observed in the phagosomes, we treated Rab39a knockout or rescued cells with brefeldin A (BFA). The rationale of this was that if the MHC molecules were coming from the ER-golgi compartment, then BFA would block it. Surface derived MHC would in contrast be resistant to short term brefeldin A treatment.

PhagoFACS analysis has shown that when DCs were treated with BFA, Rab39a expression failed to increase the subset of phagosomes enriched with open H2-L^d (Figure 53). This suggested that MHC Class I was coming from an internal source (presumably the ER-golgi compartment) and were being delivered to the phagosome in part by Rab39a. As BFA was added along with the beads, surface Class I levels remained intact just prior to phagocytosis. If the increase in phagosomal Class I was due to surface MHC, then BFA should have had no effect.

On the other hand, we also observed that BFA abolished the inhibition of phagosomal antigen degradation conferred by Rab39a (Figure 54). Thus, it was possible that Rab39a was delivering stabilizing factors such as cathepsin inhibitors (cystatins) to the phagosome. Since MHC open conformers were sensitive to degradation (Figure 50), the Rab39a-mediated delivery of these

factors might be the reason why open MHC was enriched in the phagosomes,

rather than direct delivery of MHC to these compartments.
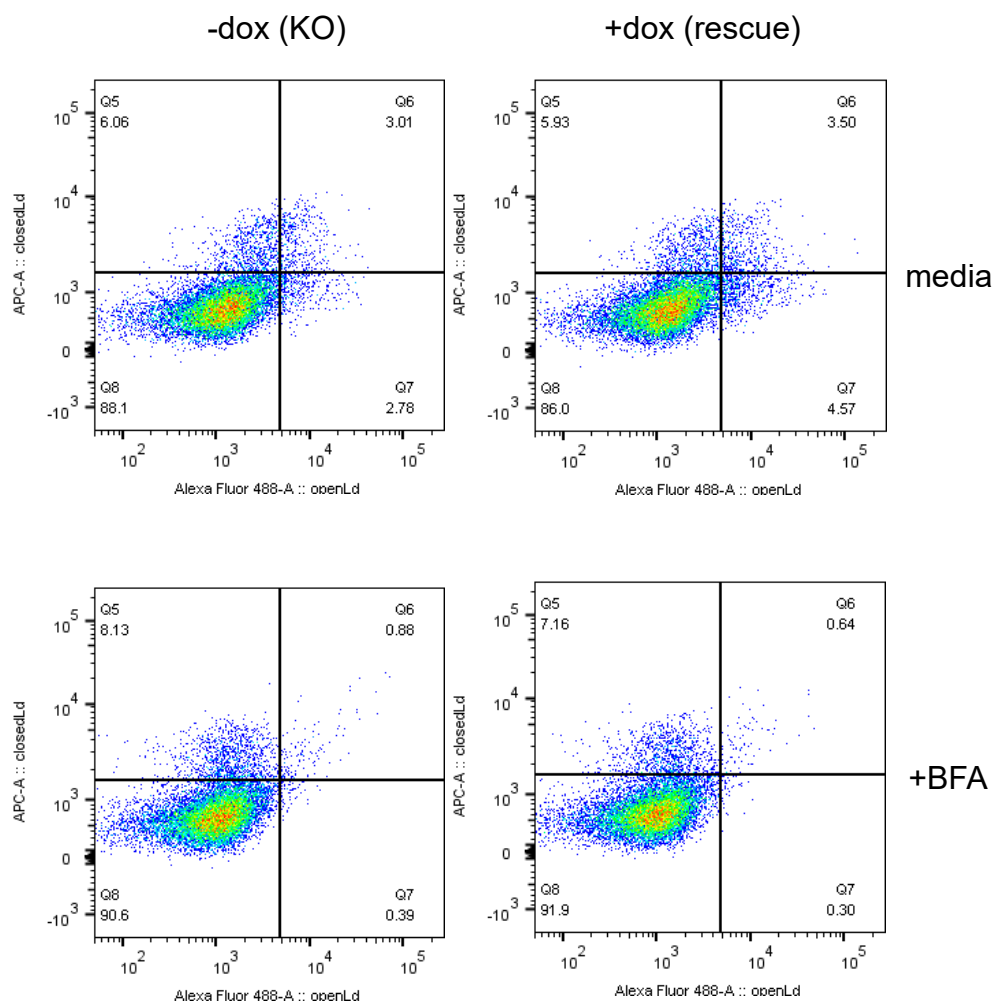
Figure 53. Brefeldin A abolishes phagosomal H2-L^d enrichment conferred by Rab39a.

1.25 x 10^5 DC3.2-Rab39aKO-Rab39a-L^d cells were incubated with or without 1 µg/ml dox for 48 hours in a 12 well plate. Cells were fed at 1 bead / cell of biotinylated-ova conjugated to 6 µm magnetic beads for 4 hours with or without 1:1000 golgiplug. Isolated phagosomes were washed, permeabilized and stained for open/closed H2-L^d. Data shown represents one experiment of $\geq$3.

media

+BFA
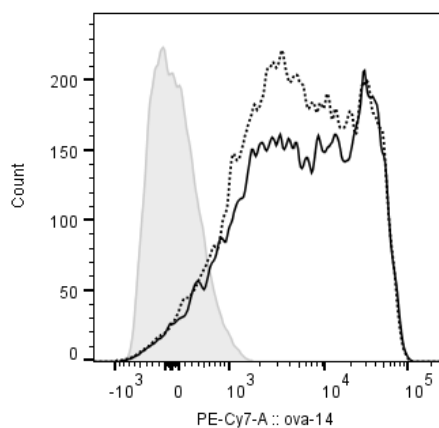
Workspace Annotation	Geometric Mean : PE-Cy7-A
no dox	4732
dox	5142
beads alone	34.5
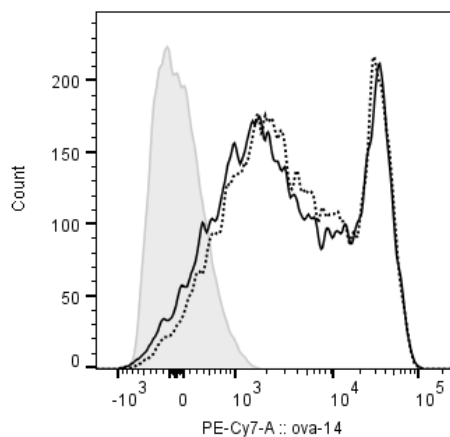
Workspace Annotation	Geometric Mean : PE-Cy7-A
no dox, +golgiplug	3892
dox, + golgiplug	3360
beads alone	34.5

No dox
Dox
beads alone

Figure 54. Brefeldin A abolishes phagosomal inhibition of degradation conferred by Rab39a.

1.25×10^5 DC3.2-Rab39aKO-Rab39a-L^d cells were incubated with or without 1 µg/ml dox for 48 hours in a 12 well plate. Cells were fed at 1 bead / cell of biotinylated-ova conjugated to 6 µm magnetic beads for 4 hours with or without 1:1000 golgiplug. Isolated phagosomes were washed, permeabilized and stained for ovalbumin. Data shown represents one experiment of $\geq$3.

Q. Brefeldin A blocks Rab39a recruitment to the phagosomes

Our previous data showed that Rab39a was perhaps involved in bringing ER-derived components to the phagosome. These components might include the MHC Class I molecule. In order to determine if Rab39a shuttled from ER-golgi compartments to the phagosomes, we looked at the effect of BFA treatment on phagosomal Rab39a.

Recruitment of Rab39a to the bead containing phagosome was inhibited by addition of BFA (Figure 55). In contrast to this, Rab7, implicated in controlling endosome maturation and lysosome biogenesis (135), reached the phagosomes despite BFA treatment. Phagosomal Lamp1, a component of the lysosome and another marker for phagosome maturation (136), was also not decreased (Figure 56). These data showed that BFA treatment still allowed phagosome maturation to occur normally, and Rab39a was not likely playing a role in this process. Rab39a might instead have been delivering ER-golgi derived components to the developing phagosome, as disruption of this compartment reduced phagosomal Rab39a. Perhaps the non phagosomal GDP bound form of Rab39a was localized to non phagosomal organelles such as the ER-golgi compartment, and once activated shuttled cargo from these sources to the phagosome.
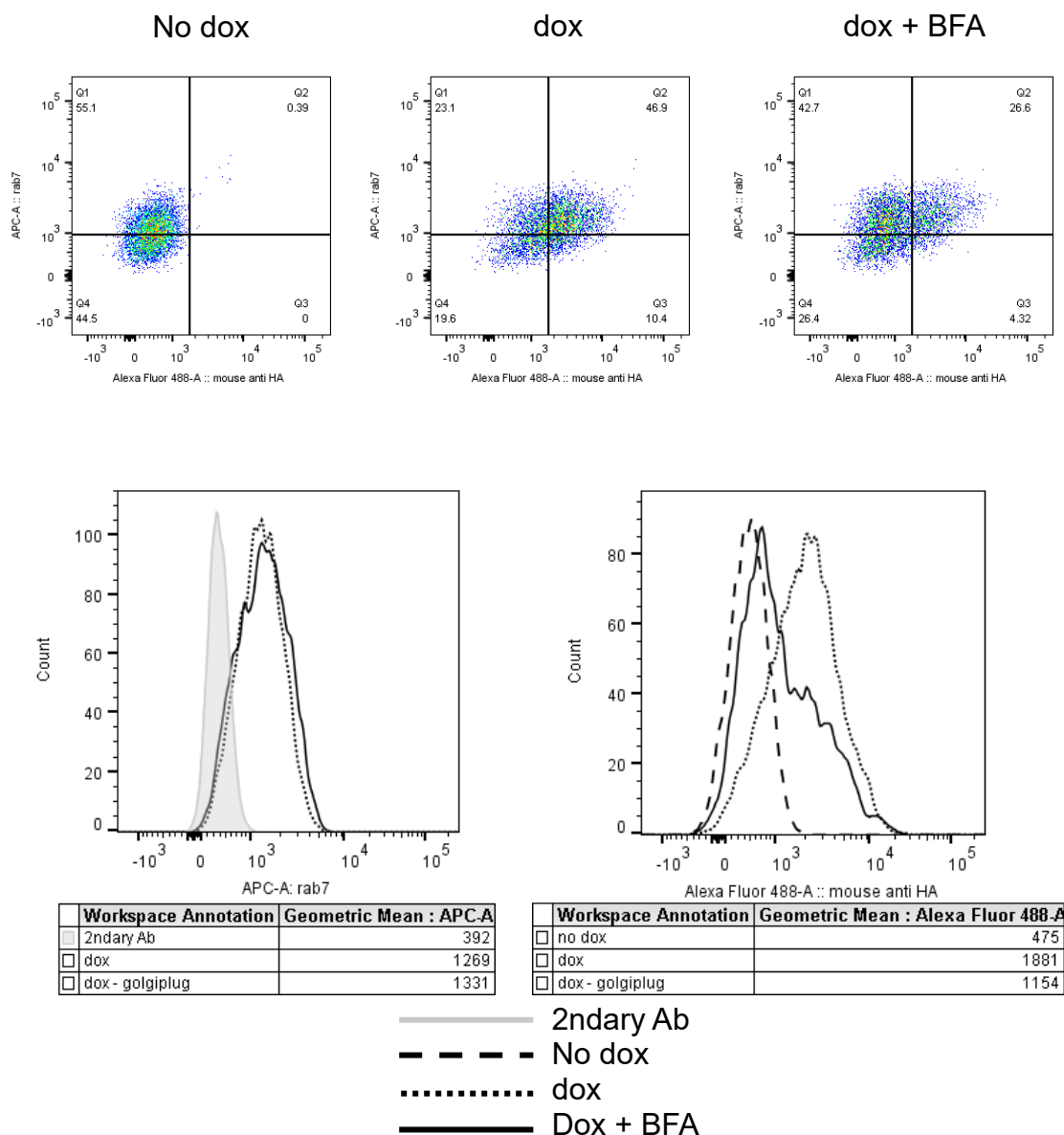
Figure 55. **Brefeldin A inhibits rab39a but not rab7 recruitment to the phagosome.**

1.25×10^5 DC3.2-Rab39aKO-Rab39a-L^d cells were incubated with or without 1 µg/ml dox for 48 hours at 37^oC in a 12 well plate. Cells were fed at 1 bead / cell of biotinylated-ova 6 µm magnetic beads for 3 hours with or without 1:1000 BFA (golgiplug, BD). Phagosomes were isolated using the listed protocol. Isolated phagosomes were washed, permeabilized and stained. Below are phagosomal gMFI of indicated stains. *Rab39a stained via HA-tag. Data shown represents one experiment of $\geq$3.

No dox   dox   dox + BFA

Workspace Annotation	Geometric Mean : APC-A
2ndary Ab	305
dox	44036
dox - golgiplug	37758

Workspace Annotation	Geometric Mean : Alexa Fluor 488-A
no dox	549
dox	2120
dox - golgiplug	1202

——— 2ndary Ab
– – – – No dox
·············· dox
——— Dox + BFA
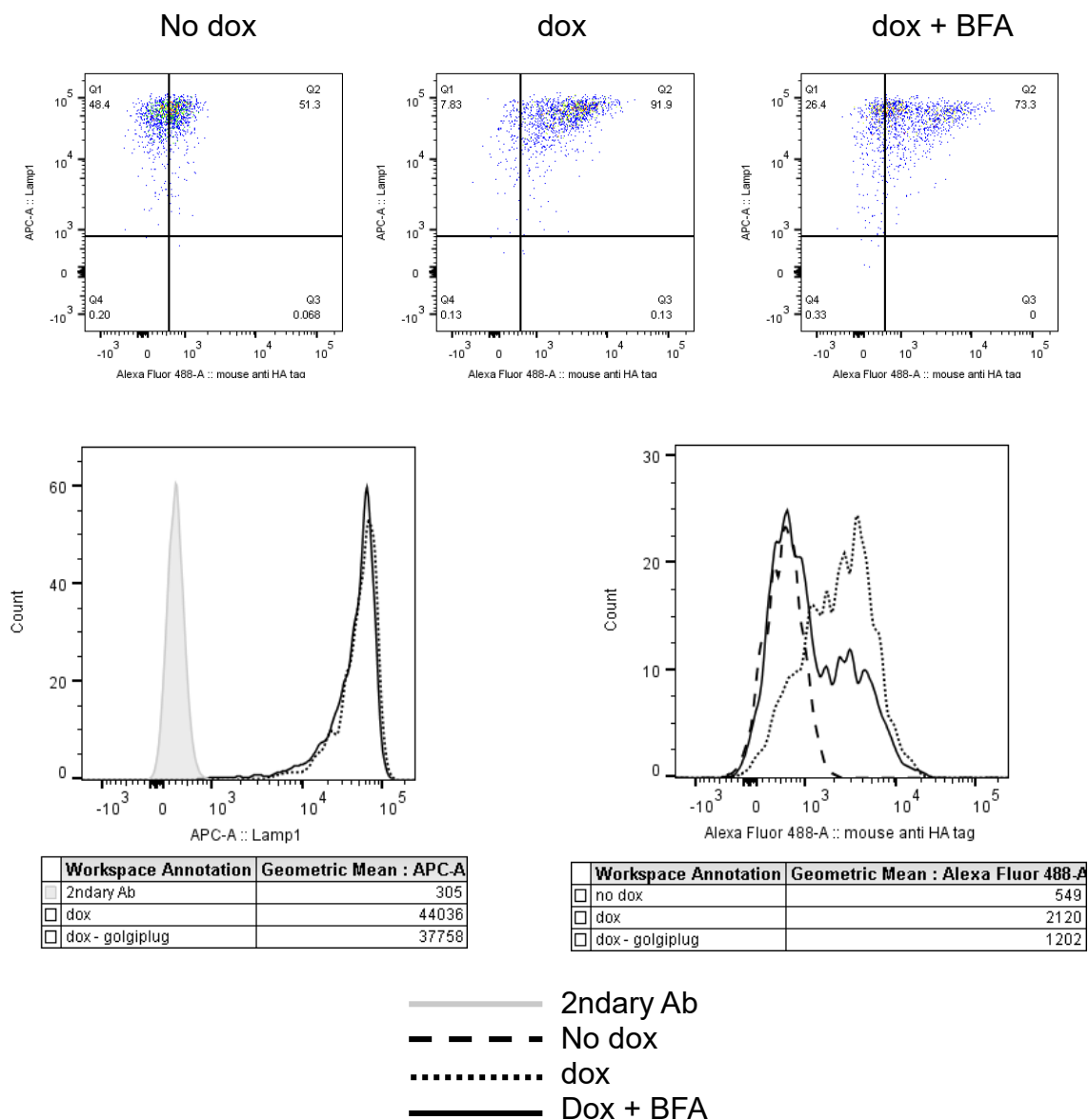
Figure 56. **Brefeldin A inhibits rab39a but not Lamp1 recruitment to the phagosome.**

1.25×10^5 DC3.2-Rab39aKO-Rab39a-L^d cells were incubated with or without 1 µg/ml dox for 48 hours at 37^oC in a 12 well plate. Cells were fed at 1 bead / cell of biotinylated-ova 6 µm magnetic beads for 3 hours with or without 1:1000 BFA (golgiplug, BD). Phagosomes were isolated using the listed protocol. Isolated phagosomes were washed, permeabilized and stained. Below are phagosomal gMFI of indicated stains. *Rab39a stained via HA-tag. Data shown represents one experiment of $\geq$3.

R. Rab39a expression increases Sec22b levels in the phagosome

Because Rab39a was seemingly shuttling components of the ER-golgi compartment to the phagosome, we looked at how Rab39a affected Sec22b, an ERGIC localized SNARE that was published to be important in XPT (59). In that study, Sec22b knockdown caused a defect in XPT and an increase in phagosomal degradation of antigen. Knockdown of the gene also did not cause a defect in MHC Class II presentation, similar to our results. Sec22b, along with syntaxin 4, was shown to mediate delivery of ERGIC derived components to the phagosome. These components included known players of the PLC (TAP, Tapasin, Calnexin). It was also proposed that the delivery of ERGIC components to the phagosome promotes phagosome to cytosol transfer of antigens.

We used phagoFACS to determine if Sec22b levels in phagosomes from KO or Rab39a rescued cells were changed. When Rab39a knockout or rescued cells were fed with beads, we observed that Sec22b levels were increased (~25%) in phagosomes from rescued cells (Figure 57). We also observed a very small (~10%) but consistent increase in the levels of phagosomal TAP1 upon rescue with Rab39a (Figure 58). This was in agreement with the previous worked that showed PLC delivery to the phagosomes was mediated by Sec22b (59).

Workspace Annotation	Geometric Mean : APC-A
☐ wt - no dox	2524
☐ wt - dox	3128
☐ secondary Ab	357
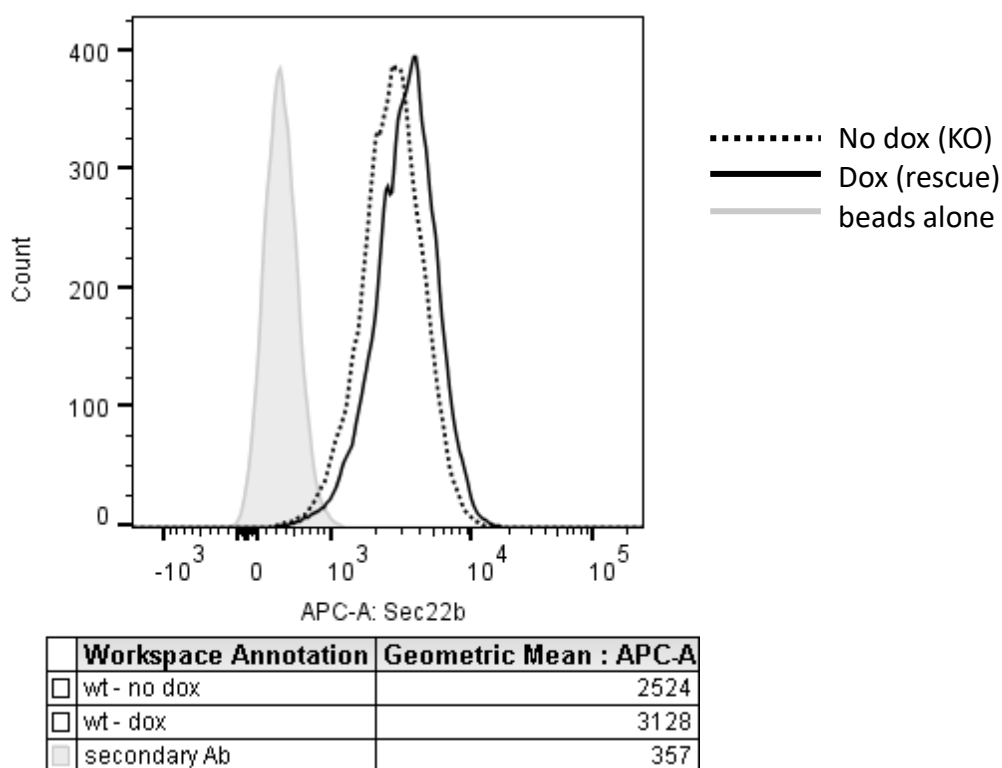
Figure 57. **Rab39a recruits Sec22b to phagosomes.**
1.25×10^5 DC3.2-Rab39aKO-Rab39a-L^d cells were incubated with or without 1 µg/ml dox for 48 hours at 37°C in a 12 well plate. Cells were fed at 1 bead / cell of biotinylated 6 µm magnetic beads for 3 hours. Phagosomes were isolated using the listed protocol. Isolated phagosomes were washed, permeabilized and stained for Sec22b. Shown are phagosomal gMFI of indicated stains. Data shown represents one experiment of $\geq$3.
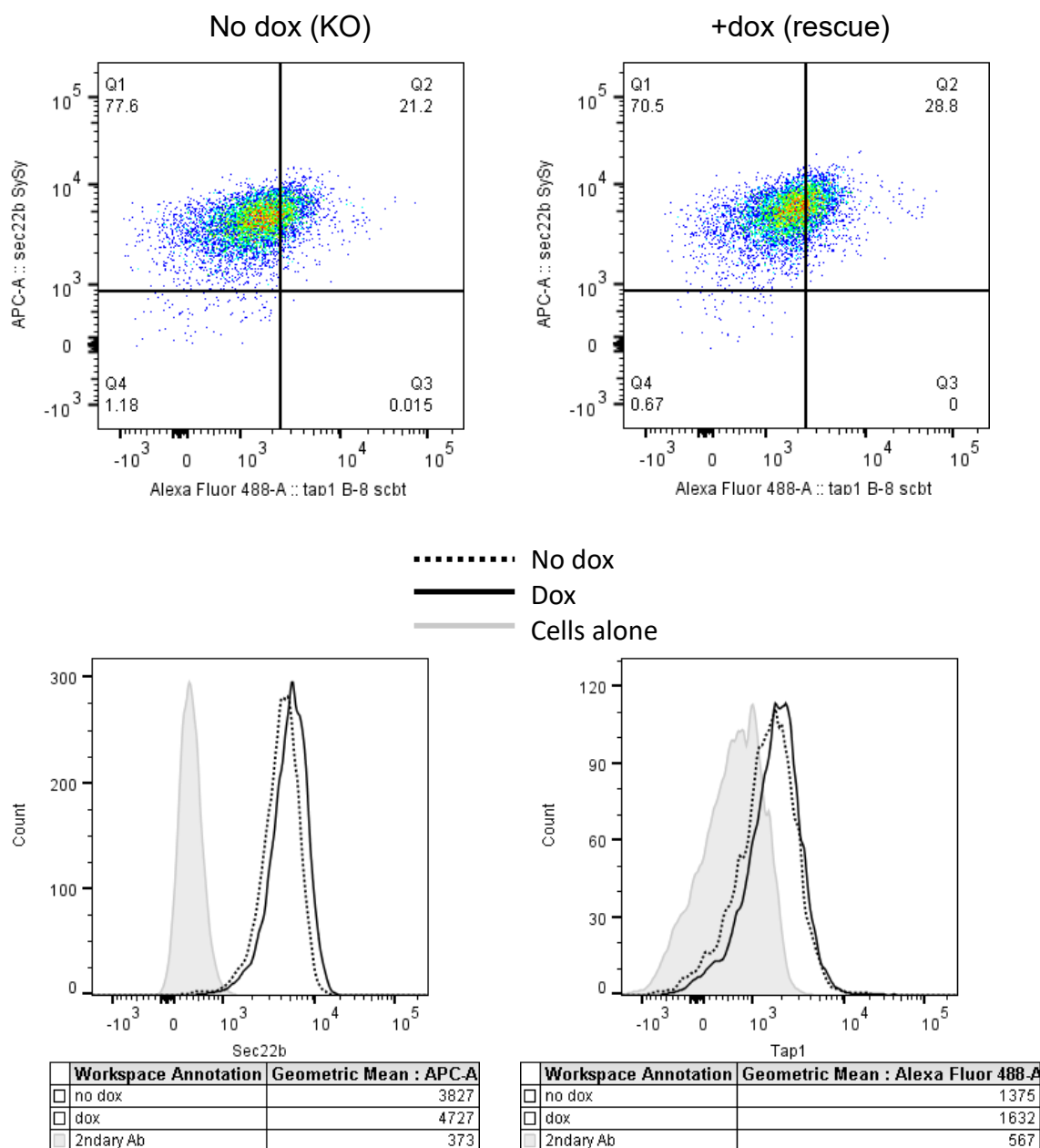
Figure 58. **Rab39a expression increases Sec22b and Tap1 levels in the phagosome.**

1.25×10^5 DC3.2-Rab39aKO-Rab39a-L^d cells were incubated with or without 1 µg/ml dox for 48 hours at 37^oC in a 12 well plate. Cells were fed at 1 bead / cell of biotinylated 6 µm magnetic beads for 3 hours. Phagosomes were isolated using the listed protocol. Isolated phagosomes were washed, permeabilized and stained for Sec22b and Tap1. Below are phagosomal gMFI of indicated stains. Data shown represents one experiment of $\geq$3.

IV.   Discussion

Through a genomewide siRNA screen, we have identified Rab39a as a gene involved in XPT. Despite being a Rab GTPase associated with late endosomal compartments, loss of Rab39a inhibited only XPT, while leaving Class II presentation intact. The presentation of endogenously expressed proteins through the Classical Pathway was also unaffected. This led us to hypothesize that Rab39a affected XPT at the phagosome level. Experiments using TAP independent antigens, including preformed MHC peptides conjugated to beads further supported this hypothesis.

Our experiments showed that expression of Rab39a inhibited degradation in the phagosomes. This could lead to the interpretation that Rab39a enhanced XPT by promoting antigen persistence. Supporting this, previous studies have shown that dendritic cells, as opposed to macrophages, had the capability to modulate phagosomal protease activity (73, 125). This inhibition of degradation can also be used to explain how a peptide bead (CIINFEKL) still required Rab39a activity for XPT despite having no need for processing. The effect of Rab39a on phagosomes may have led to the preservation of very sensitive antigens (such as short peptides) and provided the necessary time and peptide concentration for optimal loading to MHC Class I.

While Rab39a may very well exert its effects through the modulation of antigen degradation, we have also shown that Rab39a expressing cells still had

XPT advantages over knockouts despite the deliberate inhibition of phagosomal proteases. Even in the presence of Leupeptin, Rab39a expression caused an increase in XPT. Moreover, the form of antigen we used (biomag-ova) depended little on phagosomal proteases, and mostly required cytosolic processing through the proteasome to generate the necessary MHC-I peptides.

Though previous studies have demonstrated that magnetic bead conjugated ova was both proteasome and TAP dependent, we have shown that reducing ova to the minimal peptide (in our case CIINFEKL), removed this dependency. The antigen, despite being conjugated to the same bead material, became TAP independent, being loaded onto Class I in the phagosome itself similar to the vacuolar pathway that certain antigens route to. Loss of Rab39a still diminished presentation of this antigen. This led us to hypothesize that Rab39a was playing a role not in antigen processing, but in the phagosomal loading of peptides onto Class I. We wondered if the role of Rab39a was to deliver Class I to the phagosome.

Through the use of phagosome flow cytometry, we have shown that expression of Rab39a increased the levels of open MHC Class I in the phagosomes. This increase was specific, as other phagosomal molecules such as MHC Class II and Lamp 1 were not affected. The significance of this finding was that a fraction of these open conformers were shown to be peptide

receptive. The presence of peptide receptive MHC-I in the phagosome explains how peptides can be loaded onto Class I while bypassing the ER. Both the vacuolar (CatS dependent) and IRAP dependent (P2C2P) pathways do not undergo an ER transport step, and Rab39a may provide the necessary Class I for their loading.

One of the lingering questions in the field of XPT pertains to the source of phagosomal MHC Class I. Some antigens are released into the cytosol for proteasomal processing but then go back into the phagosome through TAP for N-terminal trimming and Class I loading (41, 43). Other antigens do not need to leave the phagosome at all, and require phagosomal proteases (27). These two observations indicate that functional MHC Class is in the phagosomes ready to receive peptides. How MHC Class I reaches the phagosomes and in what form is under intensive study. Several models have been proposed for this.

One of the models proposed that surface MHC molecules can be internalized with the antigen, and, with low pH and the activity of proteases, these MHCs can be loaded with crosspresented antigen peptides (65, 66, 119). A unique property of fully formed peptide-MHC Class I to recycle back to the surface instead of being degraded in the lysosomes then allowed XPT. To further complicate matters, it has been shown that both the closed (peptide bound) and open (peptide free) forms of Class I were present on the surface and were internalized (131). This being the case, were peptides loaded on internalized closed or open MHC molecules? Lucin et al. has shown that the two forms did

not traffic equally - it was the open form of Class I that reached late endosomal compartments while the closed form was rapidly recycled back to the surface (137-139).

We hypothesize that it is the open form of MHC Class I that accepts peptides destined for XPT. It is the form present throughout endosome/phagosome maturation, where the antigen undergoes continuous processing. It is also the form that can most readily bind free peptide, as the closed form would require low pH and/or specialized chaperones to facilitate peptide exchange.

Supporting this hypothesis, our results showed that through Rab39a, the levels of open MHC Class I in late phagosomes (>2hrs) were increased. At this time point, there was also very low levels of Closed MHC Class I. Thus, at the location where antigen was processed, the open form of Class I was the one present to receive XPT peptides. This was particularly important for antigens that routed through the vacuolar pathway, as these needed processing in late endosomes. Furthermore, a fraction of the open MHC Class I was peptide receptive. Addition of peptide alone to isolated phagosomes in a β2m-free solution was enough to facilitate Class I loading. This suggested that Rab39a allowed phagosomes, particularly late phagosomes, to become self-sufficient XPT compartments by increasing their peptide receptive Class I.

If Rab39a increased open MHC in the phagosomes, how did it do so? This enrichment could be due in part through Rab39a mediated inhibition of degradation, as we have also shown that the open form of MHC-I was very sensitive to protease digestion. Thus, one could hypothesize that Rab39a caused an increase in phagosomal open conformers by preventing its degradation, rather than delivering them there. These open conformers could have come from the cell surface, internalized together with the magnetic bead antigen.

On the other hand, we hypothesized that Rab39a mediated delivery of newly synthesized MHC Class I from the ER to the antigen containing phagosome. This was because our results have shown that the increase in open conformers, as well as the inhibition of degradation mediated by Rab39a, was abolished by BFA. Rab39a itself was inhibited from being recruited to the phagosomes upon BFA treatment. This suggested that Rab39a was coming from the ER-golgi before reaching the phagosome. If this was the case, then it might have been delivering ER-golgi components (which can include Class I and the PLC) to the antigen containing phagosome. Moreover, phagosomes from Rab39a positive cells had increased levels of Sec22b, an ER-golgi t-SNARE that conferred a strikingly similar phenotype to that of Rab39a (59).

Sec22b was shown to inhibit antigen degradation in the phagosomes. It was also shown to mediate delivery of ER-golgi derived components to the phagosome. Of particular note were components involved in Class I presentation (TAP1, Tapasin, Calnexin, though Class I itself was not looked at). The delivery

of ER-golgi components also promoted phagosome to cytosol transfer of whole antigens. Thus, at least for particles/beads containing full length ovalbumin, Rab39a might have also played a role in this cytosolic transfer, by mediating delivery of Sec22b labeled vesicles to the phagosomes.

The Sec22b data showed that the Rab39a-mediated delivery of ER-golgi components to the phagosome likely has multiple effects in XPT. Inhibition of degradation in the phagosomes promoted antigen and open MHC persistence. For whole antigens, ER-golgi components facilitated phagosome to cytosol transfer. For peptide and vacuolar pathway antigens, the enrichment of open MHC in the phagosome allowed for peptide loading.

The phenomenon of nascent, MHC Class I molecules being delivered to the antigen containing compartment has been described before, in the context of human DC presentation of long peptides (120). In that model, it was proposed that nascent MHC, loaded with suboptimal peptide, were delivered to the endosome through a novel secretory mechanism independent of Sec22b and CD74. The delivered MHC, with unstable peptide, then underwent peptide exchange with the more stable long peptide antigen. While our results showed that Rab39a expression increased both Sec22b and open conformers of H2-L^d in the phagosome, we could not definitively say that the increase in open conformers was due to Sec22b recruitment. It was possible that Rab39a may also have played a role in the proposed MHC-I secretory mechanism. It would also be very interesting to see if the open conformers we observed in the

phagosome arrived there already peptide free, or were in fact MHC with suboptimal peptides that have subsequently lost their cargo.

Another model for phagosomal MHC trafficking, proposed by Nair-Gupta et.al (71), involved a pool of MHC Class I molecules in a compartment distinct from the ERGIC, which were then recruited to phagosomes containing TLR4 ligand. The antibody they used for their experiments was AF6-88.4; this antibody recognized the closed form of H2-K^b as pulsing H2-K^b positive cells with SIINFEKL peptide increased staining (our unpublished data). Thus, their experiments showed an intracellular pool of peptide bound Class-I molecules being trafficked to the phagosome. How these closed molecules were loaded with new crosspresented peptides is unclear – as loaded Class I molecules are not known to readily exchange peptides. Perhaps the open form of H2-K^b also resided in this intracellular pool and was recruited similarly. It was also possible that TLR ligand containing phagosomes recruited other factors such as pH modulators and chaperones that mediated peptide exchange, similar to what happens in the MHC Class II pathway. Their experiments have shown that this trafficking of Class I was independent of Sec22b, which suggested that this pathway might be distinct from the phenomenon we have observed. Furthermore, we have performed our experiments using both ova coated beads (which might contain LPS) and plain biotinylated beads (which have no LPS) and saw similar results. This suggested multiple pathways of phagosome MHC

recruitment - that mediated by Rab39a/Sec22b and that of a Rab11a/Snap23 related pathway involved in TLR containing antigen.

Several studies could provide some insight on the possible role for Rab39a in bridging internal cellular components and the phagosomal compartment. In a study involving the intracellular parasite *Chlamydia*, it was shown that Rab39a was recruited to the bacterial inclusions (108). Its proposed role was to deliver multivesicular bodies, as well as spingolipids to the parasituous vacuole, which are then used for parasite growth. Interestingly, that study also showed that Rab39a labeled a subset vesicles that were Lamp1 positive but lacked Cathepsin D. Perhaps this could explain the reduction of antigen degradation we have observed. Another group performed an extensive study to characterize the interactions of various Rab GTPases in dendritic cells (140). They have shown that Rab39a, which is late endosomal, was able to interact with the golgi localized Rab39b. Furthermore, at least in Neuro2A cells, both Rab39a and b shared a common effector, UACA (uveal autoantigen with coiled-coil domains and Ankyrin repeats) (104). Thus it is possible that Rab39a played a role in mediating ER-golgi and endosome/phagosome interactions.

The contribution of the ER and other organelles to the formation of phagosomal membranes is not a new idea, but its contribution to XPT is the subject of intense debate. When attempting to eat particularly large antigen, phagocytes such as macrophages have been shown to recruit membranes from organelles in order to facilitate engulfment. This was termed "frustrated

phagocytosis" (141, 142). When macrophages were exposed to a surface coated with immune complexes, the cells tried to eat it. The impossibly large size of the surfaced caused macrophage golgi (141) and lysosomal (142) compartments to localize to the site of phagocytosis, to potentially contribute extra membrane. In dendritic cells, it was observed that latex bead phagosomes acquired proteins normally localized in the ER (61). These included transporters such as Sec61, Sec62, and TAP, as well as members of the PLC (Calnexin, Tapasin, Erp57). Therefore, it was proposed that dendritic cells use ER derived membranes to form phagosomes, and these were delivered via ER-phagosome fusion. Moreover, as the ER contained the classical players of MHC I presentation, ER-phagosome fusion was a proposed method to facilitate XPT directly in the phagosome compartment.

However, other groups contended that ER-phagosome fusion did not occur (143). In that study, very little if any Calnexin and PDI (both ER localized proteins) were detected in phagosomes using electron microscopy. APCs were also made to express ER localized GFP through a fusion with KDEL, an ER retention sequence. When these cells were made to internalize beads, the investigators could find no trace of GFP on the phagosomes. In a modification of this experiment, avidin-KDEL was expressed on cells, which were subsequently fed with biotin-beads. Still, even with the increased sensitivity of avidin-biotin interactions, no pull down of ER avidin was observed.

A potential resolution to this debate was presented by Desjardins et.al. (144). Through proteomics, it was shown that bead-containing phagosomes isolated from macrophages did indeed contain ER resident proteins. What was novel about this work was that it was also found that only a subset of ER proteins was trafficking to the phagosomes. For instance, mVenus fused to Stx18 was found in the phagosome proteasome while GFP-KDEL was not. This work showed that while phagosomes could recruit membranes from the ER, the mechanism of this recruitment was probably not wholesale ER fusion. Perhaps the ER/ER-golgi compartment generated secretory vesicles that were then trafficked to phagosomes, similar to the classic secretion pathways. These vesicles would have required specialized adaptors and Rab GTPases to facilitate their proper targeting and trafficking. They would also have required proper SNARES to mediate fusion with their intended targets. Rab39a and Sec22b might have provided these requirements.

While our data suggests a novel pathway for the XPT of both TAP dependent and independent antigens, several unanswered questions remain. First, we cannot definitively pinpoint the source of open MHC we observed to be enriched in the phagosomes. Both surface MHC or internal sources can contribute to this. This is complicated by the observation that Rab39a expression inhibits degradation in the phagosomes. Brefeldin A treated cells do not enrich open MHC in the phagosomes despite the presence of Rab39a. While this might imply that MHC is coming from within the cell, BFA might also block internally

derived phagosome modulators that limit antigen degradation. These modulators, which may include cystatins and Nox2, can contribute to the preservation of surface derived open MHC-I.

In our phagosome FACS assays, we saw that only a small subset of phagosomes was enriched for open H2-L^d (while containing low levels of closed H2-L^d). While our experiments showed that rescue with Rab39a increased this population vis-à-vis the knockout, the percentage of this population varied between experiments. Despite our efforts, we were not able to find a way to increase this population besides using protease inhibitors. Treatment of cells with TLR ligands or recycling inhibitors did not seem to have any effect (data not shown). What we did observe was that this subset was more visible in later timepoints (>2 to 4 hours, kinetics data not shown). Because of this, we consistently fed cells with beads for 2-4 hours, in order to hopefully maximize this population. However, we could not find a timepoint that had consistently high numbers of these phagosomes as the percentage of these open MHC enriched phagosomes still varied between experiments. One possible explanation was that open H2-L^d was continuously being loaded by peptides in the phagosome, and the MHC, now closed, was being rapidly shuttled to the cell surface. Indeed, when we did experiments to determine the kinetics of phagosomal open and closed MHC, we observed that while majority of phagosomes were double positive for both MHC forms at very early timepoints (~15 mins, data not shown), the closed form of Class I disappears or is greatly decreased by 30 mins. The

open form on the other hand, gradually decreases but somehow is stabilized at 2

hours and onwards, presumably by delivery of new open Class I (or by inhibition

of degradation in the phagosomes). However, these observations must be

verified by better controlled experiments as we had technical issues in

synchronizing the phagocytosis of the beads by dendritic cells.

Another unanswered question is how Rab39a expression manages to

reduce phagosomal degradation. Both Rab39a and Sec22b have been shown to

have this effect, but the mechanism is as yet unclear. One of the ways dendritic

cells manage to do this is by recruiting Nox2 to the phagosomal membrane.

Nox2 promotes ROS production, which in turn causes an increase in

phagosomal pH. This prevents the activation of a variety of proteases, thus

preserving phagocytosed antigen for efficient XPT.

While we have attempted to address the role of Nox2 in our observed

phenotype, the antibodies we used did not give sufficient signal in our

PhagoFACS assays. Perhaps further optimization, or use of alternative assays

such as confocal microscopy will be able to definitively look at the mechanism of

antigen persistence mediated by Rab39a.

A caveat in our analysis of phagosomes was that we were limited into

observing magnetic bead containing vesicles. However, it has been shown that

phagosomes undergo several fusion and fission events, many of which

contribute to XPT. For instance, MHC Class I, once loaded by an optimal peptide

in the phagosome, was then shuttled to the surface for presentation. Though this mechanism is still under study, it has been proposed that vesicles, through the action of Rab11a and other effectors, budded out of the phagosome and were "recycled" back to the surface (145). These steps in XPT were missed in our PhagoFACS analysis as they were no longer part of our magnetic bead preparations. Another missing event was the activity of Rab39a before it reached the antigen/bead containing vesicle. It would be interesting to characterize the content and determine the precise source of the cargo Rab39a delivered to the phagosome. In previous studies, the GDP bound form of Rab39a was shown to be dispersed in the cell, while the GTP bound form was endosomal (108). Perhaps the GDP bound form allows Rab39a to gather cargo from non endosomal sources (such as the ER-golgi) and once activated by GTP, deliver them to phagosomes.

Furthermore, while we propose that the delivery of open MHC Class I was responsible for the increase in crosspresentation by Rab39a positive cells, our phagoFACS experiments looked at the open and closed forms of a transduced H2-L^d molecule. However, our XPT experiments (with reporter T cells) made use of the endogenous H2-K^b expressed by the cells. This discrepancy was brought about by the lack of / availability of tools needed for the experiments. The reporter T cells which we used were only specific for peptides on H2-K^b (or D^b for 12.64 hybridoma) but only H2-L^d has antibodies for its open and closed forms. While the epitope recognized by the 64-3-7 antibody (for the open form of H2-L^d)

can be transferred to a synthetic construct of H2-K^b, the dendritic cells that we use already had their own endogenous H2-K^b, and this will complicate the results. While we believe that the trafficking of open H2-K^b is the same or very similar to that of H2-L^d, one must be aware that in our experiments, the open MHC that we have observed within the phagosomes are not the ones being used to present ovalbumin peptides to our reporter T cells.

V.   Proposed model of Rab39a in XPT

Given these data, we hypothesize that Rab39a regulates a transport mechanism that delivers ER-golgi derived vesicles to the developing phagosome. Perhaps the GDP bound form of Rab39a, that we failed to detect on magnetic bead phagosomes, localizes extraphagosomally, on membranes of the ER-golgi compartment or its associated vesicles. Once activated, the GTP bound form of Rab39a, via adaptors and the cytoskeleton, then delivers its cargo of Sec22b labelled vesicles to the phagosome. As SNARES are primarily used for vesicle fusion, Sec22b on the Rab39 delivered vesicle then mediates fusion. Thus, ER-golgi derived components, which may include degradation inhibitors (eg Cystatins), the PLC and possibly MHC Class I itself, are delivered into the phagosome lumen where they would be available for crosspresentation. These factors enhance crosspresentation by promoting antigen persistence, allowing phagosome to cytosol transfer of antigen, providing Tap1 as a peptide re-entry point to the phagosome and enriching receptive open MHC Class I molecules for peptide loading (Figure 59).
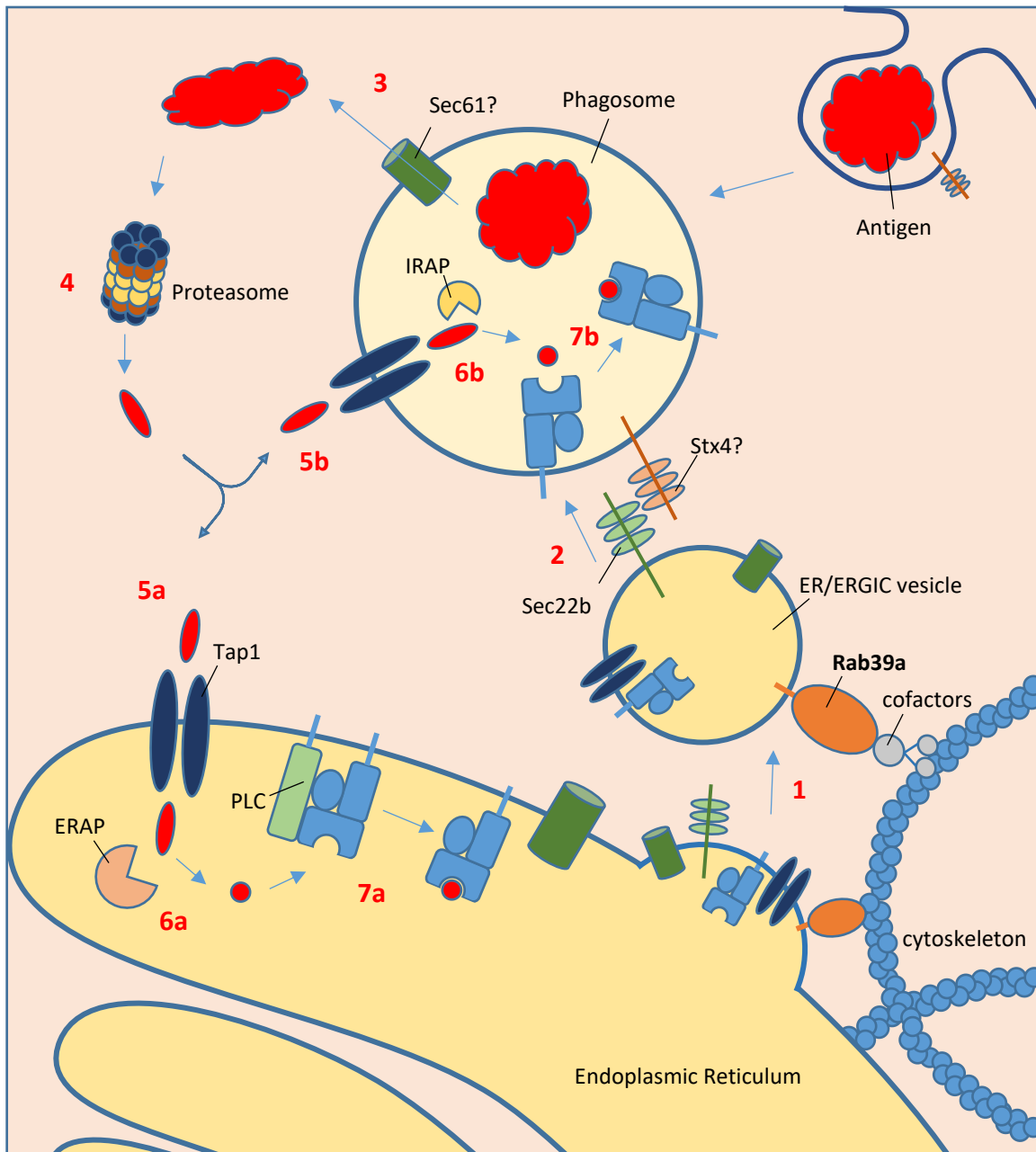
Figure 59. **Model of Rab39a mediated enhancement of crosspresentation.** Rab39a mediates delivery of ER derived cargo to antigen containing phagosomes **(1)**. These cargo include Sec22b **(2)** (for targeting phagosomes), factors that allow P2C transfer of antigen (proposed to be Sec61), members of the PLC such as Tap1, and open MHC-I molecules. Antigen is then transferred to the cytosol **(3)** for proteasome processing **(4)**. The generated peptides enter through Tap1 to reach the ER **(5a)** or the phagosome **(5b)**. After trimming by ERAP **(6a)** or IRAP **(6b)**, peptides are loaded onto empty/open MHC Class I molecules **(7a, 7b)**. Loaded MHCs are then trafficked to the surface for presentation to CD8 T cells.

VI.   Conclusion

In this work, we have successfully developed and utilized a genomewide siRNA screen to identify novel genes involved in XPT. The screen was able to identify genes that selectively affected the XPT or Class II pathways. These genes are currently under intense study (Cruz FM, Colbert JD, Merino E, Kriegsman BA).

The genomewide siRNA screen identified Rab39a as a gene involved in XPT. This Rab GTPase had no previously published role in antigen presentation. Furthermore, this study characterized the mechanism of how Rab39a affected XPT.

Through the use of both siRNA and CRISPR knockout cells, we have shown that Rab39a was selective for XPT, and did not affect the Classical Class I and the Class II pathways. We showed that Rab39a enhanced XPT of antigens that required cytosol trafficking, but also those that remained in the phagosome. Our data indicated that Rab39a did not do this by altering phagosomal pH or just modulating antigen degradation. Rather, Rab39a was being utilized by the cell to mediate the delivery of ER-golgi derived cargo to the phagosomes. This cargo could contain members of the peptide loading complex as well as peptide receptive forms of the MHC molecule. Rab39a expression increased Sec22b levels in the phagosome, suggesting that the fusion of this ER-golgi cargo with the antigen containing phagosome was mediated by this SNARE protein.

VII. References

1. Bevan MJ. 1976. Minor H antigens introduced on H-2 different stimulating cells cross-react at the cytotoxic T cell level during in vivo priming. *J Immunol* 117: 2233-8
2. Shen Z, Reznikoff G, Dranoff G, Rock KL. 1997. Cloned dendritic cells can present exogenous antigens on both MHC class I and class II molecules. *J Immunol* 158: 2723-30
3. Hildner K, Edelson BT, Purtha WE, Diamond M, Matsushita H, Kohyama M, Calderon B, Schraml BU, Unanue ER, Diamond MS, Schreiber RD, Murphy TL, Murphy KM. 2008. Batf3 deficiency reveals a critical role for CD8alpha+ dendritic cells in cytotoxic T cell immunity. *Science* 322: 1097-100
4. Jung S, Unutmaz D, Wong P, Sano G, De los Santos K, Sparwasser T, Wu S, Vuthoori S, Ko K, Zavala F, Pamer EG, Littman DR, Lang RA. 2002. In vivo depletion of CD11c+ dendritic cells abrogates priming of CD8+ T cells by exogenous cell-associated antigens. *Immunity* 17: 211-20
5. Kovacsovics-Bankowski M, Clark K, Benacerraf B, Rock KL. 1993. Efficient major histocompatibility complex class I presentation of exogenous antigen upon phagocytosis by macrophages. *Proc Natl Acad Sci U S A* 90: 4942-6
6. Rock KL, Rothstein L, Gamble S, Fleischacker C. 1993. Characterization of antigen-presenting cells that present exogenous antigens in association with class I MHC molecules. *J Immunol* 150: 438-46
7. Davey MS, Morgan MP, Liuzzi AR, Tyler CJ, Khan MW, Szakmany T, Hall JE, Moser B, Eberl M. 2014. Microbe-specific unconventional T cells induce human neutrophil differentiation into antigen cross-presenting cells. *J Immunol* 193: 3704-16
8. Milo I, Sapoznikov A, Kalchenko V, Tal O, Krauthgamer R, van Rooijen N, Dudziak D, Jung S, Shakhar G. 2013. Dynamic imaging reveals promiscuous crosspresentation of blood-borne antigens to naive CD8+ T cells in the bone marrow. *Blood* 122: 193-208
9. Kiesel JR, Buchwald ZS, Aurora R. 2009. Cross-presentation by osteoclasts induces FoxP3 in CD8+ T cells. *J Immunol* 182: 5477-87
10. Ebrahimkhani MR, Mohar I, Crispe IN. 2011. Cross-presentation of antigen by diverse subsets of murine liver cells. *Hepatology* 54: 1379-87
11. Jarry U, Jeannin P, Pineau L, Donnou S, Delneste Y, Couez D. 2013. Efficiently stimulated adult microglia cross-prime naive CD8+ T cells injected in the brain. *Eur J Immunol* 43: 1173-84
12. Hirosue S, Vokali E, Raghavan VR, Rincon-Restrepo M, Lund AW, Corthesy-Henrioud P, Capotosti F, Halin Winter C, Hugues S, Swartz MA. 2014. Steady-state antigen scavenging, cross-presentation, and CD8+ T cell priming: a new role for lymphatic endothelial cells. *J Immunol* 192: 5002-11
13. Mora JR, von Andrian UH. 2006. T-cell homing specificity and plasticity: new concepts and future challenges. *Trends Immunol* 27: 235-43
14. Sigal LJ, Crotty S, Andino R, Rock KL. 1999. Cytotoxic T-cell immunity to virus-infected non-haematopoietic cells requires presentation of exogenous antigen. *Nature* 398: 77-80

15. Huang AY, Golumbek P, Ahmadzadeh M, Jaffee E, Pardoll D, Levitsky H. 1994. Role of bone marrow-derived cells in presenting MHC class I-restricted tumor antigens. *Science* 264: 961-5

16. de Jersey J, Snelgrove SL, Palmer SE, Teteris SA, Mullbacher A, Miller JF, Slattery RM. 2007. Beta cells cannot directly prime diabetogenic CD8 T cells in nonobese diabetic mice. *Proc Natl Acad Sci U S A* 104: 1295-300

17. Calderon B, Unanue ER. 2012. Antigen presentation events in autoimmune diabetes. *Curr Opin Immunol* 24: 119-28

18. den Haan JMM, Lehar SM, Bevan MJ. 2000. Cd8+but Not Cd8−Dendritic Cells Cross-Prime Cytotoxic T Cells in Vivo. *The Journal of Experimental Medicine* 192: 1685-96

19. Pooley JL, Heath WR, Shortman K. 2001. Cutting edge: Intravenous soluble antigen is presented to CD4 T cells by CD8(-) dendritic cells, but cross-presented to CD8 T cells by CD8(+) dendritic cells. *Journal of Immunology* 166: 5327-30

20. Busche A, Jirmo AC, Welten SP, Zischke J, Noack J, Constabel H, Gatzke AK, Keyser KA, Arens R, Behrens GM, Messerle M. 2013. Priming of CD8+ T cells against cytomegalovirus-encoded antigens is dominated by cross-presentation. *J Immunol* 190: 2767-77

21. Hanc P, Fujii T, Iborra S, Yamada Y, Huotari J, Schulz O, Ahrens S, Kjaer S, Way M, Sancho D, Namba K, Reis e Sousa C. 2015. Structure of the Complex of F-Actin and DNGR-1, a C-Type Lectin Receptor Involved in Dendritic Cell Cross-Presentation of Dead Cell-Associated Antigens. *Immunity* 42: 839-49

22. Zelenay S, Keller AM, Whitney PG, Schraml BU, Deddouche S, Rogers NC, Schulz O, Sancho D, Reis e Sousa C. 2012. The dendritic cell receptor DNGR-1 controls endocytic handling of necrotic cell antigens to favor cross-priming of CTLs in virus-infected mice. *J Clin Invest* 122: 1615-27

23. Dudziak D, Kamphorst AO, Heidkamp GF, Buchholz VR, Trumpfheller C, Yamazaki S, Cheong C, Liu K, Lee HW, Park CG, Steinman RM, Nussenzweig MC. 2007. Differential antigen processing by dendritic cell subsets in vivo. *Science* 315: 107-11

24. Savina A, Peres A, Cebrian I, Carmo N, Moita C, Hacohen N, Moita LF, Amigorena S. 2009. The small GTPase Rac2 controls phagosomal alkalinization and antigen crosspresentation selectively in CD8(+) dendritic cells. *Immunity* 30: 544-55

25. Ding Y, Guo Z, Liu Y, Li X, Zhang Q, Xu X, Gu Y, Zhang Y, Zhao D, Cao X. 2016. The lectin Siglec-G inhibits dendritic cell cross-presentation by impairing MHC class I-peptide complex formation. *Nat Immunol* 17: 1167-75

26. Cruz FM, Colbert JD, Merino E, Kriegsman BA, Rock KL. 2017. The Biology and Underlying Mechanisms of Cross-Presentation of Exogenous Antigens on MHC-I Molecules. *Annu Rev Immunol* 35: 149-76

27. Shen L, Sigal LJ, Boes M, Rock KL. 2004. Important role of cathepsin S in generating peptides for TAP-independent MHC class I crosspresentation in vivo. *Immunity* 21: 155-65

28. Rock KL, Gramm C, Rothstein L, Clark K, Stein R, Dick L, Hwang D, Goldberg AL. 1994. Inhibitors of the Proteasome Block the Degradation of Most Cell-Proteins and the Generation of Peptides Presented on Mhc Class-I Molecules. *Cell* 78: 761-71

29. Rock KL, York IA, Goldberg AL. 2004. Post-proteasomal antigen processing for major histocompatibility complex class I presentation. *Nat Immunol* 5: 670-7

30.   Cresswell P, Bangia N, Dick T, Diedrich G. 1999. The nature of the MHC class I peptide loading complex. *Immunological Reviews* 172: 21-8

31.   Serwold T, Gonzalez F, Kim J, Jacob R, Shastri N. 2002. ERAAP customizes peptides for MHC class I molecules in the endoplasmic reticulum. *Nature* 419: 480-3

32.   York IA, Chang SC, Saric T, Keys JA, Favreau JM, Goldberg AL, Rock KL. 2002. The ER aminopeptidase ERAP1 enhances or limits antigen presentation by trimming epitopes to 8-9 residues. *Nat Immunol* 3: 1177-84

33.   Kovacsovics-Bankowski M, Rock KL. 1995. A phagosome-to-cytosol pathway for exogenous antigens presented on MHC class I molecules. *Science* 267: 243-6

34.   Norbury CC, Hewlett LJ, Prescott AR, Shastri N, Watts C. 1995. Class I MHC presentation of exogenous soluble antigen via macropinocytosis in bone marrow macrophages. *Immunity* 3: 783-91

35.   Lin ML, Zhan Y, Proietto AI, Prato S, Wu L, Heath WR, Villadangos JA, Lew AM. 2008. Selective suicide of cross-presenting CD8+ dendritic cells by cytochrome c injection shows functional heterogeneity within this subset. *Proc Natl Acad Sci U S A* 105: 3029-34

36.   Rodriguez A, Regnault A, Kleijmeer M, Ricciardi-Castagnoli P, Amigorena S. 1999. Selective transport of internalized antigens to the cytosol for MHC class I presentation in dendritic cells. *Nat Cell Biol* 1: 362-8

37.   Vivar OI, Magalhaes JG, Amigorena S. 2016. Measurement of Export to the Cytosol in Dendritic Cells Using a Cytofluorimetry-Based Assay. *Methods Mol Biol* 1423: 183-8

38.   Zehner M, Marschall AL, Bos E, Schloetel JG, Kreer C, Fehrenschild D, Limmer A, Ossendorp F, Lang T, Koster AJ, Dubel S, Burgdorf S. 2015. The translocon protein Sec61 mediates antigen transport from endosomes in the cytosol for cross-presentation to CD8(+) T cells. *Immunity* 42: 850-63

39.   Hornung V, Bauernfeind F, Halle A, Samstad EO, Kono H, Rock KL, Fitzgerald KA, Latz E. 2008. Silica crystals and aluminum salts activate the NALP3 inflammasome through phagosomal destabilization. *Nat Immunol* 9: 847-56

40.   Houde M, Bertholet S, Gagnon E, Brunet S, Goyette G, Laplante A, Princiotta MF, Thibault P, Sacks D, Desjardins M. 2003. Phagosomes are competent organelles for antigen cross-presentation. *Nature* 425: 402-6

41.   Ackerman AL, Kyritsis C, Tampe R, Cresswell P. 2003. Early phagosomes in dendritic cells form a cellular compartment sufficient for cross presentation of exogenous antigens. *Proceedings of the National Academy of Sciences* 100: 12889

42.   Lawand M, Abramova A, Manceau V, Springer S, van Endert P. 2016. TAP-Dependent and -Independent Peptide Import into Dendritic Cell Phagosomes. *J Immunol* 197: 3454-63

43.   Saveanu L, Carroll O, Weimershaus M, Guermonprez P, Firat E, Lindo V, Greer F, Davoust J, Kratzer R, Keller SR, Niedermann G, van Endert P. 2009. IRAP identifies an endosomal compartment required for MHC class I cross-presentation. *Science* 325: 213-7

44.   Weimershaus M, Maschalidi S, Sepulveda F, Manoury B, van Endert P, Saveanu L. 2012. Conventional dendritic cells require IRAP-Rab14 endosomes for efficient cross-presentation. *J Immunol* 188: 1840-6

45.   Saveanu L, Babdor J, Lawand M, van Endert P. 2013. Insulin-regulated aminopeptidase and its compartment in dendritic cells. *Mol Immunol* 55: 153-5

46.   Pfeifer JD, Wick MJ, Roberts RL, Findlay K, Normark SJ, Harding CV. 1993. Phagocytic processing of bacterial antigens for class I MHC presentation to T cells. *Nature* 361: 359

47.   Song R, Harding CV. 1996. Roles of proteasomes, transporter for antigen presentation (TAP), and beta 2-microgulbulin in the processing of bacterial or particulate antigens via an alternate class I MHC processing pathway. *J Immunol* 156: 4182-90

48.   Bertholet S, Goldszmid R, Morrot A, Debrabant A, Afrin F, Collazo-Custodio C, Houde M, Desjardins M, Sher A, Sacks D. 2006. Leishmania antigens are presented to CD8+ T cells by a transporter associated with antigen processing-independent pathway in vitro and in vivo. *J Immunol* 177: 3525-33

49.   Hari A, Ganguly A, Mu L, Davis SP, Stenner MD, Lam R, Munro F, Namet I, Alghamdi E, Furstenhaupt T, Dong W, Detampel P, Shen LJ, Amrein MW, Yates RM, Shi Y. 2015. Redirecting soluble antigen for MHC class I cross-presentation during phagocytosis. *Eur J Immunol* 45: 383-95

50.   Mant A, Chinnery F, Elliott T, Williams AP. 2012. The pathway of cross-presentation is influenced by the particle size of phagocytosed antigen. *Immunology* 136: 163-75

51.   Grotzke JE, Cresswell P. 2015. Are ERAD components involved in cross-presentation? *Mol Immunol* 68: 112-5

52.   Ruggiano A, Foresti O, Carvalho P. 2014. Quality control: ER-associated degradation: protein quality control and beyond. *J Cell Biol* 204: 869-79

53.   Wiertz EJ, Tortorella D, Bogyo M, Yu J, Mothes W, Jones TR, Rapoport TA, Ploegh HL. 1996. Sec61-mediated transfer of a membrane protein from the endoplasmic reticulum to the proteasome for destruction. *Nature* 384: 432-8

54.   Mehnert M, Sommer T, Jarosch E. 2014. Der1 promotes movement of misfolded proteins through the endoplasmic reticulum membrane. *Nat Cell Biol* 16: 77-86

55.   Carvalho P, Stanley AM, Rapoport TA. 2010. Retrotranslocation of a misfolded luminal ER protein by the ubiquitin-ligase Hrd1p. *Cell* 143: 579-91

56.   Giodini A, Cresswell P. 2008. Hsp90-mediated cytosolic refolding of exogenous proteins internalized by dendritic cells. *EMBO J* 27: 201-11

57.   Neefjes JJ, Stollorz V, Peters PJ, Geuze HJ, Ploegh HL. 1990. The biosynthetic pathway of MHC class II but not class I molecules intersects the endocytic route. *Cell* 61: 171-83

58.   Garstka MA, Neefjes J. 2013. How to target MHC class II into the MIIC compartment. *Mol Immunol* 55: 162-5

59.   Cebrian I, Visentin G, Blanchard N, Jouve M, Bobard A, Moita C, Enninga J, Moita LF, Amigorena S, Savina A. 2011. Sec22b regulates phagosomal maturation and antigen crosspresentation by dendritic cells. *Cell* 147: 1355-68

60.   Burgdorf S, Schölz C, Kautz A, Tampé R, Kurts C. 2008. Spatial and mechanistic separation of cross-presentation and endogenous antigen presentation. *Nature Immunology* 9: 558

61.   Guermonprez P, Saveanu L, Kleijmeer M, Davoust J, van Endert P, Amigorena S. 2003. ER–phagosome fusion defines an MHC class I cross-presentation compartment in dendritic cells. *Nature* 425: 397

62.   Burgdorf S, Kautz A, Bohnert V, Knolle PA, Kurts C. 2007. Distinct pathways of antigen uptake and intracellular routing in CD4 and CD8 T cell activation. *Science* 316: 612-6

63.   Chatterjee B, Smed-Sorensen A, Cohn L, Chalouni C, Vandlen R, Lee BC, Widger J, Keler T, Delamarre L, Mellman I. 2012. Internalization and endosomal degradation of

receptor-bound antigens regulate the efficiency of cross presentation by human dendritic cells. *Blood* 120: 2011-20

64. Shen KY, Song YC, Chen IH, Leng CH, Chen HW, Li HJ, Chong P, Liu SJ. 2014. Molecular mechanisms of TLR2-mediated antigen cross-presentation in dendritic cells. *J Immunol* 192: 4233-41

65. Basha G, Lizee G, Reinicke AT, Seipp RP, Omilusik KD, Jefferies WA. 2008. MHC class I endosomal and lysosomal trafficking coincides with exogenous antigen loading in dendritic cells. *PLoS One* 3: e3247

66. Lizee G, Basha G, Tiong J, Julien JP, Tian M, Biron KE, Jefferies WA. 2003. Control of dendritic cell cross-presentation by the major histocompatibility complex class I cytoplasmic domain. *Nat Immunol* 4: 1065-73

67. Zou L, Zhou J, Zhang J, Li J, Liu N, Chai L, Li N, Liu T, Li L, Xie Z, Liu H, Wan Y, Wu Y. 2009. The GTPase Rab3b/3c-positive recycling vesicles are involved in cross-presentation in dendritic cells. *Proceedings of the National Academy of Sciences* 106: 15801

68. Cebrian I, Croce C, Guerrero NA, Blanchard N, Mayorga LS. 2016. Rab22a controls MHC-I intracellular trafficking and antigen cross-presentation by dendritic cells. *EMBO reports*: e201642358

69. Weigert R, Yeung AC, Li J, Donaldson JG. 2004. Rab22a regulates the recycling of membrane proteins internalized independently of clathrin. *Mol Biol Cell* 15: 3758-70

70. Basha G, Omilusik K, Chavez-Steenbock A, Reinicke AT, Lack N, Choi KB, Jefferies WA. 2012. A CD74-dependent MHC class I endolysosomal cross-presentation pathway. *Nat Immunol* 13: 237-45

71. Nair-Gupta P, Baccarini A, Tung N, Seyffer F, Florey O, Huang Y, Banerjee M, Overholtzer M, Roche PA, Tampe R, Brown BD, Amsen D, Whiteheart SW, Blander JM. 2014. TLR signals induce phagosomal MHC-I delivery from the endosomal recycling compartment to allow cross-presentation. *Cell* 158: 506-21

72. Rock KL, Gamble S, Rothstein L. 1990. Presentation of exogenous antigen with class I major histocompatibility complex molecules. *Science* 249: 918-21

73. Savina A, Jancic C, Hugues S, Guermonprez P, Vargas P, Moura IC, Lennon-Dumenil AM, Seabra MC, Raposo G, Amigorena S. 2006. NOX2 controls phagosomal pH to regulate antigen processing during crosspresentation by dendritic cells. *Cell* 126: 205-18

74. Nakagawa TY, Rudensky AY. 1999. The role of lysosomal proteinases in MHC class II-mediated antigen processing and presentation. *Immunological Reviews* 172: 121-9

75. Chapman HA. 2006. Endosomal proteases in antigen presentation. *Current Opinion in Immunology* 18: 78

76. Villadangos JA, Bryant RAR, Deussing J, Driessen C, Lennon-Dumenil A-M, Riese RJ, Roth W, Saftig P, Shi G-P, Chapman HA, Peters C, Ploegh HL. 1999. Proteases involved in MHC dass II antigen presentation. *Immunological Reviews* 172: 109-20

77. Sadegh-Nasseri S, Kim A. 2015. Exogenous antigens bind MHC class II first, and are processed by cathepsins later. *Mol Immunol* 68: 81-4

78. Kim A, Sadegh-Nasseri S. 2015. Determinants of immunodominance for CD4 T cells. *Curr Opin Immunol* 34: 9-15

79. Blander JM, Medzhitov R. 2006. Toll-dependent selection of microbial antigens for presentation by dendritic cells. *Nature* 440: 808-12

80. Rock KL, Rothstein L, Gamble S. 1990. Generation of class I MHC-restricted T-T hybridomas. *J Immunol* 145: 804-11

81. Clipstone NA, Crabtree GR. 1992. Identification of calcineurin as a key signalling enzyme in T-lymphocyte activation. *Nature* 357: 695-7

82. Xu Y, Zhan Y, Lew AM, Naik SH, Kershaw MH. 2007. Differential Development of Murine Dendritic Cells by GM-CSF versus Flt3 Ligand Has Implications for Inflammation and Trafficking. *The Journal of Immunology* 179: 7577

83. Porgador A, Yewdell JW, Deng Y, Bennink JR, Germain RN. 1997. Localization, Quantitation, and In Situ Detection of Specific Peptide–MHC Class I Complexes Using a Monoclonal Antibody. *Immunity* 6: 715

84. Paul P, van den Hoorn T, Jongsma ML, Bakker MJ, Hengeveld R, Janssen L, Cresswell P, Egan DA, van Ham M, Ten Brinke A, Ovaa H, Beijersbergen RL, Kuijl C, Neefjes J. 2011. A Genome-wide multidimensional RNAi screen reveals pathways controlling MHC class II antigen presentation. *Cell* 145: 268-83

85. Grant EP, Rock KL. 1992. MHC class I-restricted presentation of exogenous antigen by thymic antigen-presenting cells in vitro and in vivo. *J Immunol* 148: 13-8

86. Deckhut AM, Allan W, McMickle A, Eichelberger M, Blackman MA, Doherty PC, Woodland DL. 1993. Prominent usage of V beta 8.3 T cells in the H-2Db-restricted response to an influenza A virus nucleoprotein epitope. *J Immunol* 151: 2658-66

87. Karttunen J, Sanderson S, Shastri N. 1992. Detection of rare antigen-presenting cells by the lacZ T-cell activation assay suggests an expression cloning strategy for T-cell antigens. *Proceedings of the National Academy of Sciences* 89: 6020

88. Huang da W, Sherman BT, Lempicki RA. 2009. Systematic and integrative analysis of large gene lists using DAVID bioinformatics resources. *Nat Protoc* 4: 44-57

89. Thomas PD, Campbell MJ, Kejariwal A, Mi H, Karlak B, Daverman R, Diemer K, Muruganujan A, Narechania A. 2003. PANTHER: a library of protein families and subfamilies indexed by function. *Genome Res* 13: 2129-41

90. Mi H, Lazareva-Ulitsky B, Loo R, Kejariwal A, Vandergriff J, Rabkin S, Guo N, Muruganujan A, Doremieux O, Campbell MJ, Kitano H, Thomas PD. 2005. The PANTHER database of protein families, subfamilies, functions and pathways. *Nucleic Acids Res* 33: D284-8

91. Kretzer NM, Theisen DJ, Tussiwand R, Briseno CG, Grajales-Reyes GE, Wu X, Durai V, Albring J, Bagadia P, Murphy TL, Murphy KM. 2016. RAB43 facilitates cross-presentation of cell-associated antigens by CD8alpha+ dendritic cells. *J Exp Med*

92. Schreibelt G, Klinkenberg LJ, Cruz LJ, Tacken PJ, Tel J, Kreutz M, Adema GJ, Brown GD, Figdor CG, de Vries IJ. 2012. The C-type lectin receptor CLEC9A mediates antigen uptake and (cross-)presentation by human blood BDCA3+ myeloid dendritic cells. *Blood* 119: 2284-92

93. Heng TS, Painter MW, Immunological Genome Project C. 2008. The Immunological Genome Project: networks of gene expression in immune cells. *Nat Immunol* 9: 1091-4

94. Sigoillot FD, King RW. 2011. Vigilance and validation: Keys to success in RNAi screening. *ACS Chem Biol* 6: 47-60

95. Grimm D, Streetz KL, Jopling CL, Storm TA, Pandey K, Davis CR, Marion P, Salazar F, Kay MA. 2006. Fatality in mice due to oversaturation of cellular microRNA/short hairpin RNA pathways. *Nature* 441: 537-41

96. Kincaid EZ, Che JW, York I, Escobar H, Reyes-Vargas E, Delgado JC, Welsh RM, Karow ML, Murphy AJ, Valenzuela DM, Yancopoulos GD, Rock KL. 2011. Mice completely lacking immunoproteasomes show major changes in antigen presentation. *Nat Immunol* 13: 129-35

97. Palmowski MJ, Gileadi U, Salio M, Gallimore A, Millrain M, James E, Addey C, Scott D, Dyson J, Simpson E, Cerundolo V. 2006. Role of immunoproteasomes in cross-presentation. *J Immunol* 177: 983-90

98. Ersching J, Vasconcelos JR, Ferreira CP, Caetano BC, Machado AV, Bruna-Romero O, Baron MA, Ferreira LR, Cunha-Neto E, Rock KL, Gazzinelli RT, Rodrigues MM. 2016. The Combined Deficiency of Immunoproteasome Subunits Affects Both the Magnitude and Quality of Pathogen- and Genetic Vaccination-Induced CD8+ T Cell Responses to the Human Protozoan Parasite Trypanosoma cruzi. *PLoS Pathog* 12: e1005593

99. Lundholt BK, Scudder KM, Pagliaro L. 2003. A simple technique for reducing edge effect in cell-based assays. *J Biomol Screen* 8: 566-70

100. Stenmark H. 2009. Rab GTPases as coordinators of vesicle traffic. *Nat Rev Mol Cell Biol* 10: 513-25

101. Jancic C, Savina A, Wasmeier C, Tolmachova T, El-Benna J, Dang PM, Pascolo S, Gougerot-Pocidalo MA, Raposo G, Seabra MC, Amigorena S. 2007. Rab27a regulates phagosomal pH and NADPH oxidase recruitment to dendritic cell phagosomes. *Nat Cell Biol* 9: 367-78

102. Seto S, Tsujimura K, Koide Y. 2011. Rab GTPases Regulating Phagosome Maturation Are Differentially Recruited to Mycobacterial Phagosomes. *Traffic* 12: 407

103. Chen T, Han Y, Yang M, Zhang W, Li N, Wan T, Guo J, Cao X. 2003. Rab39, a novel Golgi-associated Rab GTPase from human dendritic cells involved in cellular endocytosis. *Biochemical and Biophysical Research Communications* 303: 1114

104. Mori Y, Matsui T, Omote D, Fukuda M. 2013. Small GTPase Rab39A interacts with UACA and regulates the retinoic acid-induced neurite morphology of Neuro2A cells. *Biochemical and Biophysical Research Communications* 435: 113

105. Seto S, Sugaya K, Tsujimura K, Nagata T, Horii T, Koide Y. 2013. Rab39a Interacts with Phosphatidylinositol 3-Kinase and Negatively Regulates Autophagy Induced by Lipopolysaccharide Stimulation in Macrophages. *PLoS ONE* 8: e83324

106. Becker CE, Creagh EM, O'Neill LAJ. 2009. Rab39a Binds Caspase-1 and Is Required for Caspase-1-dependent Interleukin-1 Secretion. *Journal of Biological Chemistry* 284: 34531

107. Giannandrea M, Bianchi V, Mignogna ML, Sirri A, Carrabino S, D'Elia E, Vecellio M, Russo S, Cogliati F, Larizza L, Ropers H-H, Tzschach A, Kalscheuer V, Oehl-Jaschkowitz B, Skinner C, Schwartz CE, Gecz J, Van Esch H, Raynaud M, Chelly J, de Brouwer APM, Toniolo D, D'Adamo P. 2010. Mutations in the Small GTPase Gene RAB39B Are Responsible for X-linked Mental Retardation Associated with Autism, Epilepsy, and Macrocephaly. *The American Journal of Human Genetics* 86: 185

108. Tudela JG, Capmany A, Romao M, Quintero C, Miserey-Lenkei S, Raposo G, Goud B, Damiani MT. 2015. The late endocytic Rab39a GTPase regulates the interaction between multivesicular bodies and chlamydial inclusions. *Journal of Cell Science* 128: 3068

109. Shen L, Rock KL. 2004. Cellular protein is the source of cross-priming antigen in vivo. *Proc Natl Acad Sci U S A* 101: 3035-40

110. York IA, Bhutani N, Zendzian S, Goldberg AL, Rock KL. 2006. Tripeptidyl peptidase II is the major peptidase needed to trim long antigenic precursors, but is not required for most MHC class I antigen presentation. *J Immunol* 177: 1434-43

111. Towne CF, York IA, Watkin LB, Lazo JS, Rock KL. 2007. Analysis of the Role of Bleomycin Hydrolase in Antigen Presentation and the Generation of CD8 T Cell Responses. *The Journal of Immunology* 178: 6923-30

112. Hsu PD, Scott DA, Weinstein JA, Ran FA, Konermann S, Agarwala V, Li Y, Fine EJ, Wu X, Shalem O, Cradick TJ, Marraffini LA, Bao G, Zhang F. 2013. DNA targeting specificity of RNA-guided Cas9 nucleases. *Nat Biotechnol* 31: 827-32

113. Cong L, Ran FA, Cox D, Lin S, Barretto R, Habib N, Hsu PD, Wu X, Jiang W, Marraffini LA, Zhang F. 2013. Multiplex genome engineering using CRISPR/Cas systems. *Science* 339: 819-23

114. Belizaire R, Unanue ER. 2009. Targeting proteins to distinct subcellular compartments reveals unique requirements for MHC class I and II presentation. *Proc Natl Acad Sci U S A* 106: 17463-8

115. Shirane M, Nakayama KI. 2006. Protrudin induces neurite formation by directional membrane trafficking. *Science* 314: 818-21

116. van Weering JR, Toonen RF, Verhage M. 2007. The role of Rab3a in secretory vesicle docking requires association/dissociation of guanidine phosphates and Munc18-1. *PLoS One* 2: e616

117. Fukuda M, Kanno E, Ishibashi K, Itoh T. 2008. Large Scale Screening for Novel Rab Effectors Reveals Unexpected Broad Rab Binding Specificity. *Molecular & Cellular Proteomics* 7: 1031

118. Wandinger-Ness A, Zerial M. 2014. Rab proteins and the compartmentalization of the endosomal system. *Cold Spring Harb Perspect Biol* 6: a022616

119. Chefalo PJ, Grandea AG, 3rd, Van Kaer L, Harding CV. 2003. Tapasin-/- and TAP1-/- macrophages are deficient in vacuolar alternate class I MHC (MHC-I) processing due to decreased MHC-I stability at phagolysosomal pH. *J Immunol* 170: 5825-33

120. Ma W, Zhang Y, Vigneron N, Stroobant V, Thielemans K, van der Bruggen P, Van den Eynde BJ. 2016. Long-Peptide Cross-Presentation by Human Dendritic Cells Occurs in Vacuoles by Peptide Exchange on Nascent MHC Class I Molecules. *J Immunol* 196: 1711-20

121. Bachmair A, Finley D, Varshavsky A. 1986. In vivo half-life of a protein is a function of its amino-terminal residue. *Science* 234: 179-86

122. Humphries WHt, Szymanski CJ, Payne CK. 2011. Endo-lysosomal vesicles positive for Rab7 and LAMP1 are terminal vesicles for the transport of dextran. *PLoS One* 6: e26626

123. Schlosser E, Mueller M, Fischer S, Basta S, Busch DH, Gander B, Groettrup M. 2008. TLR ligands and antigen need to be coencapsulated into the same biodegradable microsphere for the generation of potent cytotoxic T lymphocyte responses. *Vaccine* 26: 1626-37

124. Ramachandra L, Sramkoski RM, Canaday DH, Boom WH, Harding CV. 1998. Flow analysis of MHC molecules and other membrane proteins in isolated phagosomes. *J Immunol Methods* 213: 53-71

125. Samie M, Cresswell P. 2015. The transcription factor TFEB acts as a molecular switch that regulates exogenous antigen-presentation pathways. *Nat Immunol* 16: 729-36

126. Singh R, Cresswell P. 2010. Defective cross-presentation of viral antigens in GILT-free mice. *Science* 328: 1394-8

127. Townsend A, Trowsdale J. 1993. The transporters associated with antigen presentation. *Semin Cell Biol* 4: 53-61

128. Hansen TH, Lybarger L, Yu L, Mitaksov V, Fremont DH. 2005. Recognition of open conformers of classical MHC by chaperones and monoclonal antibodies. *Immunological Reviews* 207: 100

129. Lie WR, Myers NB, Connolly JM, Gorka J, Lee DR, Hansen TH. 1991. The specific binding of peptide ligand to Ld class I major histocompatibility complex molecules determines their antigenic structure. *J Exp Med* 173: 449-59

130. Arosa FA, Santos SG, Powis SJ. 2007. Open conformers: the hidden face of MHC-I molecules. *Trends in Immunology* 28: 115

131. Mahmutefendić H, Blagojević G, Kučić N, Lučin P. 2006. Constitutive internalization of murine MHC class I molecules. *Journal of Cellular Physiology* 210: 445

132. Ljunggren HG, Stam NJ, Ohlen C, Neefjes JJ, Hoglund P, Heemels MT, Bastin J, Schumacher TN, Townsend A, Karre K, et al. 1990. Empty MHC class I molecules come out in the cold. *Nature* 346: 476-80

133. Rice J, Buchan S, Stevenson FK. 2002. Critical components of a DNA fusion vaccine able to induce protective cytotoxic T cells against a single epitope of a tumor antigen. *J Immunol* 169: 3908-13

134. Johnson LS, Dunn KW, Pytowski B, McGraw TE. 1993. Endosome acidification and receptor trafficking: bafilomycin A1 slows receptor externalization by a mechanism involving the receptor's internalization motif. *Mol Biol Cell* 4: 1251-66

135. Guerra F, Bucci C. 2016. Multiple Roles of the Small GTPase Rab7. *Cells* 5

136. Eskelinen E-L. 2006. Roles of LAMP-1 and LAMP-2 in lysosome biogenesis and autophagy. *Molecular Aspects of Medicine* 27: 495

137. Mahmutefendić H, Blagojević G, Tomaš MI, Kučić N, Lučin P. 2011. Segregation of open Major Histocompatibility Class I conformers at the plasma membrane and during endosomal trafficking reveals conformation-based sorting in the endosomal system. *The International Journal of Biochemistry & Cell Biology* 43: 504

138. Zagorac GB, Mahmutefendić H, Tomaš MI, Kučić N, Le Bouteiller P, Lučin P. 2012. Early endosomal rerouting of major histocompatibility class I conformers. *Journal of Cellular Physiology* 227: 2953

139. Mahmutefendić H, Zagorac GB, Tomaš MI, Groettrup M, Momburg F, Lučin P. 2013. Endosomal trafficking of open Major Histocompatibility Class I conformers—Implications for presentation of endocytosed antigens. *Molecular Immunology* 55: 149

140. Li Y, Wang Y, Zou L, Tang X, Yang Y, Ma L, Jia Q, Ni Q, Liu S, Tang L, Lin R, Wong E, Sun W, Wang L, Wei Q, Ran H, Zhang L, Lian H, Huang W, Wu Y, Li QJ, Wan Y. 2016. Analysis of the Rab GTPase Interactome in Dendritic Cells Reveals Anti-microbial Functions of the Rab32 Complex in Bacterial Containment. *Immunity* 44: 422-37

141. Bainton DF, Takemura R, Stenberg PE, Werb Z. 1989. Rapid fragmentation and reorganization of Golgi membranes during frustrated phagocytosis of immobile immune complexes by macrophages. *Am J Pathol* 134: 15-26

142. Labrousse AM, Meunier E, Record J, Labernadie A, Beduer A, Vieu C, Ben Safta T, Maridonneau-Parini I. 2011. Frustrated phagocytosis on micro-patterned immune

complexes to characterize lysosome movements in live macrophages. *Front Immunol* 2: 51

143.   Touret N, Paroutis P, Terebiznik M, Harrison RE, Trombetta S, Pypaert M, Chow A, Jiang A, Shaw J, Yip C, Moore HP, van der Wel N, Houben D, Peters PJ, de Chastellier C, Mellman I, Grinstein S. 2005. Quantitative and dynamic assessment of the contribution of the ER to phagosome formation. *Cell* 123: 157-70

144.   Campbell-Valois FX, Trost M, Chemali M, Dill BD, Laplante A, Duclos S, Sadeghi S, Rondeau C, Morrow IC, Bell C, Gagnon E, Hatsuzawa K, Thibault P, Desjardins M. 2012. Quantitative proteomics reveals that only a subset of the endoplasmic reticulum contributes to the phagosome. *Mol Cell Proteomics* 11: M111 016378

145.   Welz T, Wellbourne-Wood J, Kerkhoff E. 2014. Orchestration of cell surface proteins by Rab11. *Trends Cell Biol* 24: 407-15